AD-A099 306 H S S INC BEDFORD MASS F/G 4/1
EVALUATION, FEASIBILITY, AND DESIGN OF A THREE-WAVELENGTH INFRA--ETC(U)
SEP 80 D F HANSEN, H S STEWART, C C PETTY F19628-79-C-0132
UNCLASSIFIED HSS-B-071 AFGL-TR-80-0323 NL

LEVEL II

AFGL-TR-80-0323

EVALUATION, FEASIBILITY, AND DESIGN OF A THREE-WAVELENGTH INFRARED ATMOSPHERIC AEROSOL EXTINCTIOMETER

D. F. Hansen
H. S. Stewart
C. C. Petty
L. B. Woolaver

HSS Inc.
2 Alfred Circle
Bedford, Massachusetts 01730

AD A093836

Final Report
9 July 1979 - 8 June 1980

2 September 1980

Approved for public release; distribution unlimited

This research was supported by the Air Force In-House Laboratory Independent Research Fund

DTIC ELECTE MAY 26 1981

AIR FORCE GEOPHYSICS LABORATORY
AIR FORCE SYSTEMS COMMAND
UNITED STATES AIR FORCE
HANSCOM AFB, MASSACHUSETTS 01731

DTIC FILE COPY

81 5 26 006

UNCLASSIFIED

SECURITY CLASSIFICATION OF THIS PAGE (When Data Entered)

REPORT DOCUMENTATION PAGE	READ INSTRUCTIONS BEFORE COMPLETING FORM
1. REPORT NUMBER (19) (12) AFGL-TR-80-0323 / 2. GOVT ACCESSION NO. AD-A099 306	3. RECIPIENT'S CATALOG NUMBER
4. TITLE (and Subtitle) Evaluation, Feasibility, and Design of a Three-Wavelength Infrared Atmospheric Aerosol Extinctiometer	5. TYPE OF REPORT & PERIOD COVERED (9) Final Rept. 9 July 1979-8 June 1980
	6. PERFORMING ORG. REPORT NUMBER (14) HSS-B-071
7. AUTHOR(s) (10) D. F. Hansen, C. C. Petty, H. S. Stewart, L. B. Woolaver	8. CONTRACT OR GRANT NUMBER(s) (15) F19628-79-C-0132
9. PERFORMING ORGANIZATION NAME AND ADDRESS HSS Inc 2 Alfred Circle Bedford, MA 01730 (12) 190	10. PROGRAM ELEMENT, PROJECT, TASK AREA & WORK UNIT NUMBERS 61101F (16) ILIR9DAA 17 9D
11. CONTROLLING OFFICE NAME AND ADDRESS Air Force Geophysics Laboratory Hanscom AFB, Massachusetts 01731 Monitor/ V. Turner/OPA	12. REPORT DATE 2 September 1980
	13. NUMBER OF PAGES 189
14. MONITORING AGENCY NAME & ADDRESS(if different from Controlling Office)	15. SECURITY CLASS. (of this report) Unclassified
	15a. DECLASSIFICATION/DOWNGRADING SCHEDULE

16. DISTRIBUTION STATEMENT (of this Report)

Approved for public release; distribution unlimited

17. DISTRIBUTION STATEMENT (of the abstract entered in Block 20, if different from Report)

18. SUPPLEMENTARY NOTES

This research was supported by the Air Force In-House Laboratory Independent Research Fund

19. KEY WORDS (Continue on reverse side if necessary and identify by block number)

Extinctiometer; Aerosol Extinctiometer; Atmospheric Aerosols; Aerosol Extinction Coefficients; Infrared; Infrared Extinction

20. ABSTRACT (Continue on reverse side if necessary and identify by block number)

This design study represents the first phase of an AFGL program to develop an instrument for measuring the infrared extinction coefficient of atmospheric aerosols. The performance objectives of the instrument require that the instrument operate in all environments, perform measurements in three wavelength regions (1μm, 3-5μm and 8-12μm), and cover a range defined by 50 kilometer visibility at one extreme and fog at the other extreme. The initial phase of the study was devoted to a review of all known

DD FORM 1 JAN 73 1473 EDITION OF 1 NOV 65 IS OBSOLETE

UNCLASSIFIED

SECURITY CLASSIFICATION OF THIS PAGE (When Data Entered)

20. (Cont.) techniques for determining the extinction coefficient of atmospheric aerosols. The review led to the selection of an extinctiometer concept as the best possible approach to achieve the AFGL objectives, given the present technological state-of-the-art in all alternative candidate techniques. Finally, a conceptual design and an engineering design specification were prepared, based on a unique extinctiometer measurement technique.

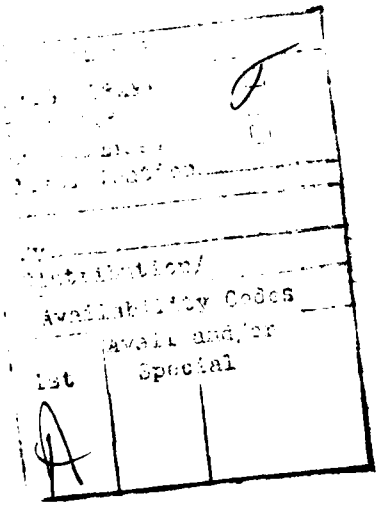

TABLE OF CONTENTS

TABLE OF CONTENTS (Cont.)

LIST OF ILLUSTRATIONS

LIST OF ILLUSTRATIONS (Cont.)

LIST OF ILLUSTRATIONS (Cont.)

LIST OF TABLES

LIST OF TABLES (Cont.)

1. OBJECTIVES OF THE STUDY

1.1 Introduction and Statement of Objectives

The greatest uncertainty in the application of computer models to the on-site calculation of the transmission of infrared radiation over optical paths of military significance in tropospheric situations is in the wavelength dependent attenuation of optical radiation by atmospheric aerosol particles. The attenuations due to the molecular constituents of the atmosphere are known in the case of the uniformly mixed gases (N_2, O_2, CO_2, N_2O, CO, CH_4) or are readily calculable from standard meteorological measurements in the cases of the non-uniformly mixed molecules (H_2O, and O_3). No suitable instrument appears to be available which will measure atmospheric aerosol extinction coefficients over the environmental range required for military requirements. Measurements from such an instrument, if one existed, would provide invaluable inputs for on-site model predictions of infrared atmospheric transmissions.

This study is concerned with a method or methods for determining the component of infrared atmospheric attenuation arising from aerosol extinction using measurements made with equipment located at a single point on or near a transmission path of interest. The single-point constraint rules out conventional transmissometers as well as bi-static or multi-static laser or searchlight measurements. The study program consisted of three basic tasks: (1) a review of existing techniques for measuring aerosol extinction coefficients (2) a study of the sensitivity of several candidate methods for measuring aerosol extinction in the infrared spectral region and (3) the recommendation of a specific technique for such measurements and the conceptual design of an instrument using the recommended technique.

The ultimate instrument is required to be a compact device, operable in outdoor environments from surface levels to 5 km altitude and is to have sufficient dynamic range of sensitivity to cover conditions ranging from fog to 50 km visibility. The preferred technique is a direct measurement of aerosol extinction coefficients although the possibility of separate determinations of aerosol scattering and absorption coefficients is not ruled out. The wavelength region of interest is 1 - 12 micrometers with emphasis on the 1, the 3-5 and the 8-12 micrometer regions. The instrument must sample ambient air which, in the process of sampling, is unperturbed in terms of temperature, relative humidity, number density of aerosol particles and their size distribution. It must be operable unattended for long periods, without frequent operator intervention for calibration or repair.

1.2 Possible Classes of Solutions

It is required that equipment located at one point make measurements from which the component of atmospheric attenuation due to aerosol extinction along a path can be deduced. Solutions to this problem fall into several classes. One class of solutions involves measuring atmospheric transmission. A measurement of atmospheric transmission convolves both the aerosol and molecular components of atmospheric attenuation. The attenuation due only to aerosol extinction is then derivable if the attenuation due to molecular constituents can be estimated or calculated.

Two other classes of solutions are (1) a direct measurement of the optical attenuation parameters of aerosols; i.e. the aerosol extinction coefficient, or separate measurements of the scattering and absorption coefficients, and (2) measurement of the physical parameters of the aerosols with a derivation of the optical extinction.

1.2.1 Atmospheric Transmission Measurements

The simplest method for measurement of atmospheric transmission involves targets of opportunity such as hills, barns, skyscrapers,

lighthouses, cathedrals, ships, islands, and the sea horizon. These are the natural visibility targets which have been used for the rather subjective visibility estimates made at airports, and at sea. Instruments exist with which transmission along the path to such a target can be determined by measuring the contrast of the target against the horizon sky background. In general this is a daytime technique and in practice its use has been limited to the visibile portion of the spectrum. Such observations are passive in that no optical radiations are projected from the measuring point. Passive observations are sometimes desirable because of the security; i.e., they do not expose the location of the measuring equipments.

A second method for determining the transmission of an atmospheric path involves use of single-ended active equipment. The equipment involves both a projector of radiation along the path and a detector of radiation backscattered by the atmosphere. Usually short laser pulses are used and the time history of backscattered radiation is analyzed to deduce the transmission of the path. Such lidar systems can provide values of path transmission which are based on physical measurements and are calculated using some approximations and assumptions. Paths so investigated can be horizontal, vertical, or slant and the results obtained do not depend on a model of the atmosphere. At present lidar systems which might meet some of the requirements of this study are massive and require frequent, if not constant, attention from an operator. In the long term lidar systems will have been developed which satisfy the technical requirements of this study in terms of precision and sensitivity in the several wavelength regions of interest. This will represent a very important advance in technology because with it path transmission per se will be measured without the use of models to extrapolate measurements of atmospheric parameters made at one point to the total path of interest. Early in the study reported here it was decided not to pursue lidar as a solution. Reasons for this decision include (1) lidar

is active, i.e. it is not secure, (2) the present state-of-the-art lidar systems are delicate, expensive, bulky and require almost constant attention, and (3) the several programs related to lidar determinations of atmospheric transmission which are underway or have been completed are sufficient to assess the present day capabilities of this technique.

1.2.2 Atmospheric Aerosol Extinction Measurements

Measurement of atmospheric aerosol extinction can take two different approaches: (1) separate local values of the scattering coefficient and the absorption coefficient can be measured or the local value of the extinction coefficient (which is the sum of the scattering coefficient and the absorption coefficient) at the wavelength or within the wavelength band of interest can be measured. If measurements are made at only one point on the path of interest then an atmospheric model is required to generate values of the extinction coefficient for the other points along the path. Usually such models are based on changes of aerosol characteristics with changes of atmospheric pressure, temperature and relative humidity as well as changes of the aerosol number density, size distribution and complex refractive index and these, in turn, cause changes in values of the extinction coefficient.

1.2.3 Measurement of the Physical Parameters of Aerosols

This method is similar to the one just outlined except that physical parameters rather than optical parameters of the atmosphere are measured at one end of the path in question. The physical parameters are aerosol size distribution, number density and composition. Rather than composition of the aerosols their complex refractive index is usually given since this is the critical aspect of composition if the aerosol particles are treated as homogeneous spheres. Knowledge of the physical parameters results in somewhat better correlations of changes in the calculated extinction coefficients to

changes in the meteorological conditions. The extinction coefficient at any wavelength can be calculated from the data on aerosol size distribution and concentration if only the real and the imaginary indices of refraction are known at each wavelength and for the various sizes of aerosols. Measuring these indices is difficult and it is usual practice to assign index values appropriate to the weather, the season, the history of volcanic action and the region of the world for which the calculations are being made. The changes in size distribution which occur with changes of meteorological parameters (pressure, temperature, relative humidity) can be predicted if the composition of the aerosols is known. The complex index of refraction is also a function of composition. It may be argued that measurement of the physical parameters of the aerosols is more basic than measurements of optical parameters and this is so. However, the real time measurement of aerosol composition which is required to calculate complex refractive index as a function of wavelength is a difficult task. The complex index is very important throughout most of the infrared where values of the single scattering albedo, which is a function of the imaginary index, are significantly less than one.

The four methods outlined above for measuring atmospheric aerosol extinction are summarized here:

(1) Measurement of the contrast of remote objects against the horizon sky.

(2) Lidar techniques for deducing path transmission.

(3) Point measurements of optical parameters of the atmospheric aerosols.

(4) Point measurements of physical parameters of the atmospheric aerosols.

For various reasons the third method, point measurements of optical parameters of the atmosphere, has been chosen. This method is least desirable when evaluated in terms of extrapolation of the measured values to all points on a transmission path or to other wavelengths than that of the measurements. However, the third method seems most practical in the short term.

The next section (Section 2) presents a literature survey of techniques for the measurement of atmospheric infrared aerosol extinction. Section 3 presents calculations of signal-to-noise ratios appropriate to rather idealized devices for point measurements of optical parameters of atmospheric aerosols. The devices are defined in a way appropriate to measurements in the open and unperturbed air. The calculations are made using a mixture of practical values (source radiances, detector responses) and unappraised optimism (perfect lenses, mirrors, filters, beam splitters and electronics). Section 4 describes a series of experiments relating to the extinctiometer design. Section 5 outlines the approach taken for the conceptual design of the extinctiometer.

The extinctiometer approach taken here has its origin in an instrument concept first described in a proposal by HSS Inc to the Air Force Geophysics Laboratory. A portion of that proposal is included as Appendix A for the sake of completeness.

To be seriously considered as a candidate technique for detailed scrutiny and assessment in light of the performance requirements imposed by AFGL, each possible technique was subjected to the test that it be capable of satisfying the sensitivity requirement. This latter requirement, as analyzed in Section 5, dictates a capability of measuring atmospheric aerosol extinction coefficients as low as 0.015 km^{-1} at 1.0 micron and 0.0015 km^{-1} in the 3 to 4 micron and 8 to 12 micron spectral regions.

2. LITERATURE SURVEY: TECHNIQUES FOR THE MEASUREMENT OF ATMOSPHERIC INFRARED AEROSOL EXTINCTION

2.1 Introduction

The literature survey reported here is part of the initial phase of a study with ultimate objective the conceptual engineering design of a field instrument for measuring atmospheric aerosol extinction. This instrument is to make measurements preferably in terms of extinction, although the possibility of separate determinations of scattering and absorption is not ruled out. The wavelength region is 1-12 micrometers with emphasis on the 1, 3-5, and 8-12 micrometer regions. The instrument is to be a compact device, operable in outdoor environments from ground level to 5 km altitude and is to be sensitive under attenuation conditions from fog to 50 km visibility. The device is to be operated unattended for long periods, without frequent operator intervention for calibration or repair.

The above rather stringent instrumentation requirements have been addressed in a preliminary way by HSS, and a concept formulated for an extinctiometer (Appendix A). The term "extinctiometer" is used here in preference to "transmissometer", since the output signal of the proposed instrument is directly relatable to extinction coefficient rather than to transmission, an apparently unique characteristic of this instrument concept. Indeed, the difference between the two output signals of the extinctiometer, with the windowless cell in two alternate positions, is directly proportional to aerosol extinction coefficient. The windowless cell, containing filtered ambient air, is the key element in this design concept, enabling the precise elimination of any biases associated with differences in the two paths alternately

traversed by the light beam.

The HSS extinctiometer concept will in principle satisfy the measurement requirements set forth above but because it is unproven it was felt prudent to conduct the present literature survey in order to insure that there are no competing systems which might better satisfy these requirements, as well as to determine if other workers have already explored this concept.

Early in the literature survey it became apparent that the various possible instruments for fulfilling the extinction measurement requirements could be grouped into five main groups as follows:

1. Extinctiometer
2. Transmissometer
3. Nephelometer
4. Spectrophone
5. Lidar

The first of these has been discussed above, and it can be said here that the literature survey has not found any reference to an equivalent device. The extinctiometer is thus unique both in its approach to the measurements problem and in the fact that no known effort has been made to construct a workable instrument based on this concept. Transmissometers exist in a variety of configurations, commonly employing a light source separated from a receiver by the scattering/absorbing medium being measured. The spectral region covered is determined by the light source/filter combination. Long-path transmissometers violate the requirements for compactness, leaving for consideration only the so-called White cell instruments. These employ multiple reflections to achieve a folded path, which approaches the conditions of the long path devices within the confines of a small instrument.

The combination of both scattering and absorption, i.e. extinction, is measured. In contrast to this, nephelometers measure only the scattering component of extinction. A number of highly sensitive varieties of this instrument have been developed, including the integrating, polar, and fixed angle nephelometers. Some of these enable separation of the aerosol scattering component by reference to filtered ambient air. Most operate in the visible or near IR spectral regions and make use of incoherent light sources. Spectrophones, which measure only the absorption component of extinction, make use of the pressure rise in the absorbing gas due to its being heated by the absorption process. Pressure rise is sensed either with a manometer or microphone, yielding a highly sensitive means of measuring the absorption coefficient. A great variety of spectrophone devices exist, including pulsed and CW types, and these instruments have been operated over a wide spectral region from the visible to the mid IR at 10 μm. Although most spectrophones employ lasers, this is not essential to their operation.

The final instrument type here considered is the lidar, of which there are many varieties. These narrow-beam laser devices measure the backscattered signal from atmospheric scattering and, under proper circumstances, serve to derive the atmospheric transmission for a portion of the laser beam path. In effect, these devices can become single ended transmissometers. Most lidars are short-pulse devices, although one variant is used in CW mode. Some employ Doppler techniques, and some make use of Raman scatter from specific molecules. Lidars have undergone extensive and highly sophisticated development in the course of the past decade, and show promise for a potentially unique capability for application to the aerosol extinction problem. For this reason, these systems have been included in the present literature survey, even though their development at

the present time may not satisfy some of the operational requirements, i.e. those related to compactness, field worthiness, and maintainability.

To summarize the above instrument groupings: The HSS extinctiometer and the various transmissometer instruments, including lidars, provide a direct measurement of atmospheric extinction or transmission. The extinctiometer and some transmissometers provide for separating the aerosol extinction from that of the ambient air, whereas in general, lidars do not provide such a separation. Both nephelometers and spectrophones are highly developed, ultra-sensitive, devices for measuring atmospheric scattering (nephelometers) and absorption (spectrophones). For an extinction determination it would be necessary to employ a combination of these two instrument types. Each individually has the advantage of a high state of development and well-demonstrated sensitivity at the levels required for the present application. Neither instrument type requires the use of a laser, although most spectrophone applications have to date employed laser sources. Both nephelometers and spectrophones have been used in a differential mode which separates the effects of aerosols from those of ambient air. Whereas spectrophones have been extensively exploited over the full spectral range required (1-12 microns), most nephelometer applications have been in the visible and near IR regions.

A final introductory comment should be made with regard to this literature survey: the survey was far from an exhaustive one. It was limited, as are most surveys, by time constraints which force compromises between the desire to avoid overlooking significant work and the inability to be all-inclusive. The basic objective of the survey was to determine if there are instrumentation developments reported in the literature which could lead to an instrument better meeting the AFGL requirements for

measuring aerosol extinction coefficients than the extinctiometer approach. In this respect, it is believed that the present survey has succeeded, in spite of its limitations and lack of exhaustiveness. We are satisfied that the main efforts in the development of the instrument types enumerated above have been surveyed to the extent that the basic limits of each instrument type are understood, as related to the AFGL requirements, and that the achieved sensitivities in each case have been ascertained over the wavelengths of interest. Finally, a special effort has been made to include foreign literature in the survey, particularly that of the U.S.S.R.

One recent information source is particularly worth mentioning in that it included a literature search into visible and infrared measurement devices for aerosol extinction. This was a study by A. J. Nesti, Jr. (Ref 1), published in May 1978 for the Chemical Systems Laboratory of Edgewood Arsenal. The following is taken from Nesti's report:

" A study of published literature on the subject of aerosol extinction measurement techniques has pointed out several facts.

- Relatively little work has been directed toward "in situ" aerosol extinction measurements. That which has been done has been concerned with atmospheric aerosols (haze, fog, pollutants). Typically, general opacity measurements have been made using both forward transmission and laser backscatter (LIDAR) techniques as general pollution indicators.
- The treatment of liquid aerosol absorptions specifically, is very light.
- There is an abundance of literature on aerosol (particulate) sampling systems geared toward the determination of atmospheric aerosol constituents (chemical make-up), mass loading, and particle count and size distribution. None of this is related to extinction per se.

- Therefore, an instrument specific to the Edgewood Arsenal extinction measurement requirements would have to be designed.

The Edgewood Arsenal requirements were related to extinction measurements for artificial aerosols such as smokes, chemical fogs, etc. It is significant that the findings of the literature survey of Reference 1 led to a recommendation that a special instrument would have to be designed for the extinction measurements. (A two station system was proposed).

2.2 Sources for Literature Survey

The primary source of reference material for the present survey was the AFGL Research Library and its computerized facilities for searching a large number of lists containing a variety of journal articles and other reports. Advantage was also taken of the DDC terminal, located upstairs in the AFGL Library, which accesses reports lists relating to Department of Defense sponsored research. Some of the standard literature search aids of the AFGL Library were also found to be useful in this effort, particularly the Science Citations Index, which allows branching from a key report through later references to it, and the various lists of abstracts by subject (e.g., physics, meteorological aerospace, etc.). Of course, the papers and reports ultimately studied during the course of this search themselves contained many additional references to relevant work in this area.

The AFGL Library files accessed for the computerized search were as follows:

NTIS 64-79/1SS 17 (Copr. NTIS)
COMPENDEX 70-79 (Copr. Engineering Index, Inc).
INSPEC 69-77, File 12 (Copr. IEEE)
INSPEC 78-79, File 13 (Copr. IEEE)
Meteorological, Geological, Astronomical Abstracts (MGA)
SPIN 75-79 (Copr. Amer. Inst. of Physics).
Dissertation Abstracts 1861-1979 (Copr. Xerox Corp.)

Searching of the above files was performed based on certain key words, as follows:

Group 1. Aerosol(s) and:
Atmospheric W/transmission
or, Atmospheric W/attenuation

or, Atmospheric W/ scattering

or, Atmospheric W/absorption

Group 2. Atmospher(ic), and
Nephelometer

or, Transmissometer

or, Spectrophon( )

Group 3. Doppler W/Lidar

Table 1 gives the numbers of reports from each of the above three groups contained in the seven collections searched.

Table 1.

No. of Reports Located

Collection	Group 1	Group 2	Group 3
NTIS	175	65	1
COMPENDEX 70-79 (Eng Index)	15	38	2
INSPEC-12 (IEEE)	18	44	2
INSPEC-13 (IEEE)	11	17	2
MGS	39	34	4
SPIN 75-79 (AIP)	4	9	0
Dissertation Abstracts (Xerox)	0	2	0
TOTALS	262	209	11
GRAND TOTAL:		482	

The totals shown in Table 1 do not take into account duplications, of which there were many, both as between key-word groupings and between the various collections. After taking this into account there were still several hundred individual papers located by the computer search.

In addition to the computer search summarized in Table 1 and the DDC search, three published searches of the NTIS, containing titles, authors and abstracts, were obtained and examined. These searches contained a total of 661 abstracts. They were:

Atmospheric Effects on Laser Beams, Vol I
187 abstracts. (1964-1974)

Atmospheric Effects on Laser Beams, Vol 2
210 abstracts. (1975-Sept. 1978)

Light Detection and Ranging (LIDAR), Vol. 2
264 abstracts. (1975-June 1979)

Based on the abstracts contained in the computerized and published searches, orders were placed with NTIS for copies of reports which seemed relevant to the study. These were 48 in number and are listed in the Bibliography.

In addition to the above sources of information on atmospheric aerosol extinction measurement, several specialized summaries, reviews, proceedings, and memoranda were found useful to the survey. These were:

Atmospheric Aerosols: Their Optical Properties and Effects. Digest of papers presented at the topical meeting at Williamsburg, Va., Dec. 1976. (NASA report CP2004 and Supplement).

The EOMET Cruise of the USNS Hayes: May-June 1977, S. G. Gathman and B. G. Julian, eds. (NRL Memorandum Report 3924).

Visual Range: Concepts, Instrumental Determination, and Aviation Applications. C. A. Douglas and R. L. Booker (NBS Monograph 159, June 1977).

Aerosol Particle Size Measurements at San Nicolas Island During CEWCOM-78. Richard K. Jeck. (NRL Memorandum Report 3931, March 1979).

Optical Propagation in the Atmosphere. Proceedings of the AGARD Conference at Lyngby, Denmark, Oct. 1975 (AGARD Proceedings No. 183, May 1976).

Proceedings on a Workshop on Remote Sensing of the Marine Boundary Layer. Vail, Colorado, August 1976. (NRL Memorandum Report 3430, June 1977).

2.3 Approach

From the various sources described above, the references were collected into several lists of report abstracts and/or titles. These were reviewed, and from them a smaller list was prepared containing only papers of potential relevance to the literature survey. (At this point, duplications from the various overlapping lists were eliminated.) The "boiled-down" list contained approximately 150 references. These were then located and studied, either through the reference shelves of the AFGL or HSS libraries, or in the case of reports available from NTIS, purchased. As the reports were studied, a card file was prepared containing author/title/source information and a brief report summary, indicating applicability to the AFGL aerosol extinction measurement requirements. Copies were made of journal articles which were particularly applicable to the study requirements, e.g. those containing details of instrumentation configuration or performance. Finally, these reports and others obtained from NTIS together with the card-file summaries, formed the basis of the conclusions here reported.

Succeeding sections of this report will summarize findings of the literature survey under the main instrument groupings given in the introduction: nephelometers, spectrophones, transmissometers, and lidars.

2.4 Instrumentation

2.4.1. Nephelometers

Nephelometers measure directly the scattering of radiation from a light-beam, and thus are capable of determining only the scattering component of the aerosol extinction coefficient. They nevertheless constitute a highly developed and highly sensitive class of instrument and could be used in conjunction with a separate device, e.g. a spectrophone, to determine extinction.

Nephelometers can be considered in terms of the basic scattering equation

$$b = 2\pi \int_0^{\pi} \beta(\theta) \sin\theta \, d\theta \qquad (2.1)$$

where b is the volume scattering coefficient, β the scattering cross section per unit gas volume, for beams scattered through an angle θ. Equation 2.1 can be used to characterize three different types of nephelometer: The fixed-angle nephelometer receives scattered radiation only from a very narrow range of scattering angles, θ. The polar nephelometer measures scattering at a number of angles, in order to construct the scattering function $\beta(\theta)$. The integrating nephelometer receives scattered radiation integrated over a wide range of angles, typically excluding only small angular regions near zero and 180 degrees, which are inaccessible. All three types of nephelometer are in current use and will be taken up separately.

2.4.1.1 Fixed-Angle Nephelometer

The fixed-angle nephelometer is based on the empirical evidence that a great many scattering media, including many aerosols, molecules, etc. possess a scattering cross-section $\beta(\theta)$ related to the scattering

coefficient b by the relation

$$b = 4\pi \beta(\theta_o) \tag{2.2}$$

where θ_o is a fixed-angle, in the range 30°-60°. Thus a measurement of the scattering at this single angle can serve to characterize the total scattering through all angles. It is this assumption, albeit based on experimental as well as on some theoretical grounds, that constitutes a basic weakness in the fixed-angle nephelometer approach. It is clear, for example, that all types of aerosol distribution need not conform to the assumption of Equation 2.2. As illustrated below, a variety of fixed-angles, θ, have been chosen for these devices.

The classic Loofah device, of World War II vintage, as described by Middleton (Ref 2) employs a fixed scattering angle of 30°. Two recent examples of fixed-angle nephelometers are illustrated in Figure 2.1. These are the HSS Baxicon (Ref 3) and the Point Visibility Meter (PVM)* of Winstanley and Adams (Ref 4). The upper sketch in Figure 2.1 is of the Baxicon instrument, which employs a unique parabolic reflecting optical element to isolate scattered radiation at angles close to 55°. The lower portion of the figure shows the PVM. The latter instrument employs conventional optics and complex baffling (not shown in the figure) to minimize stray light, with a fixed scattering angle of 35°. The PVM is reportedly sensitive (Ref 4) to a range of scattering coefficients, σ, between 2 and 60 km^{-1},

*British Patent 135200

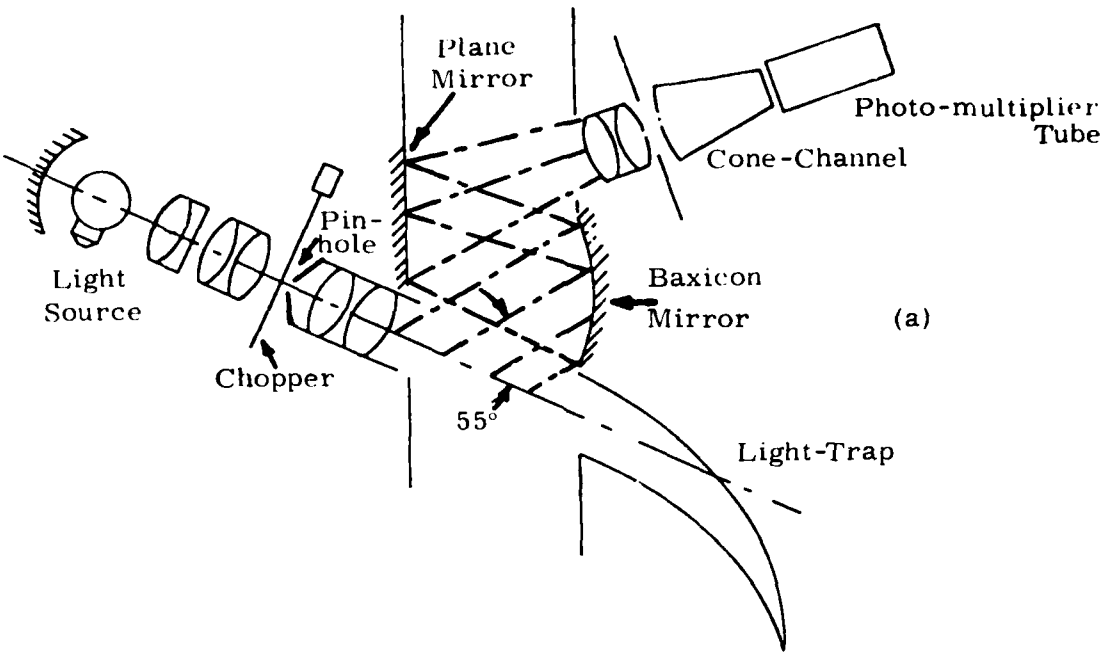

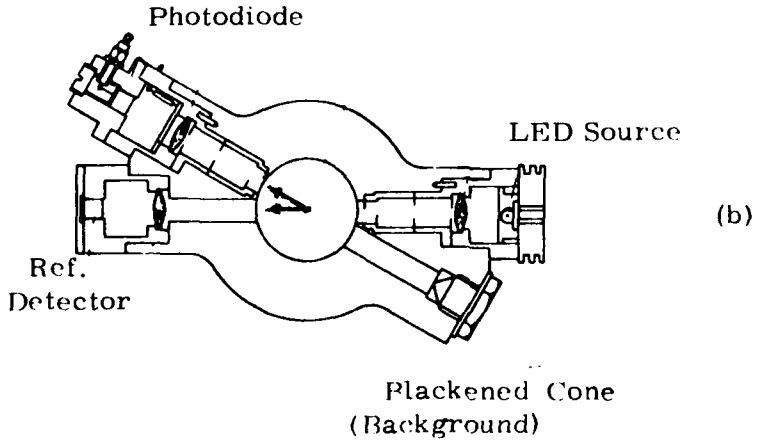

Figure 2.1. Schematic diagrams for two fixed-angle nephelometers: (a) Baxicon (Ref 3) (b) Point Visibility Meter, PVM (Ref 4)

thus being useful primarily for relatively low visibility situations (fogs, etc.). The Baxicon, on the other hand, has sensitivity capable of measuring Rayleigh scattering for nitrogen, i.e. values of σ on the order of .01 km^{-1}. Its ultimate sensitivity is $\sim .002\ km^{-1}$, a level on par with the requirements basic to the present study. Baxicon operates in the visible spectral region, using a tungsten lamp and photomultiplier tube, whereas the point visibility meter employs a Ga As light-emitting diode (904 nm) and silicon photodiode detector.

If the choice were made to satisfy the measurement requirements of the present study through use of nephelometry combined with a separate absorption measurement, a fixed-angle device would have the advantage of relative compactness and simplicity as compared to other types of nephelometer. It is limited, however, by the assumptions of Equation 2.2. Furthermore, a demonstration of its capability over the 1-10 μm spectral region has not been made.

2.4.1.2 Polar Nephelometer

The polar nephelometer is configured so as to measure scattering over a wide range of individual scattering angles, in effect being the equivalent of several fixed-angle nephelometers. This is achieved either by utilizing several detection systems or by changing the relative configuration of detector/light-source/scattering volume. A Soviet device which employs both of these approaches is that reported by Toropova (Ref 5) and shown in Figure 2.2. Three lens/detector combinations are employed in several positions to yield data every two degrees for angles between 2° and 178°, using a He-Ne laser as light-source. The article refers to measurements on "laboratory air, without smoke", thus the device is apparently sensitive close to the Rayleigh limit. As is evident from Figure 2.2, this device is quite large compared for the fixed-angle devices described above.

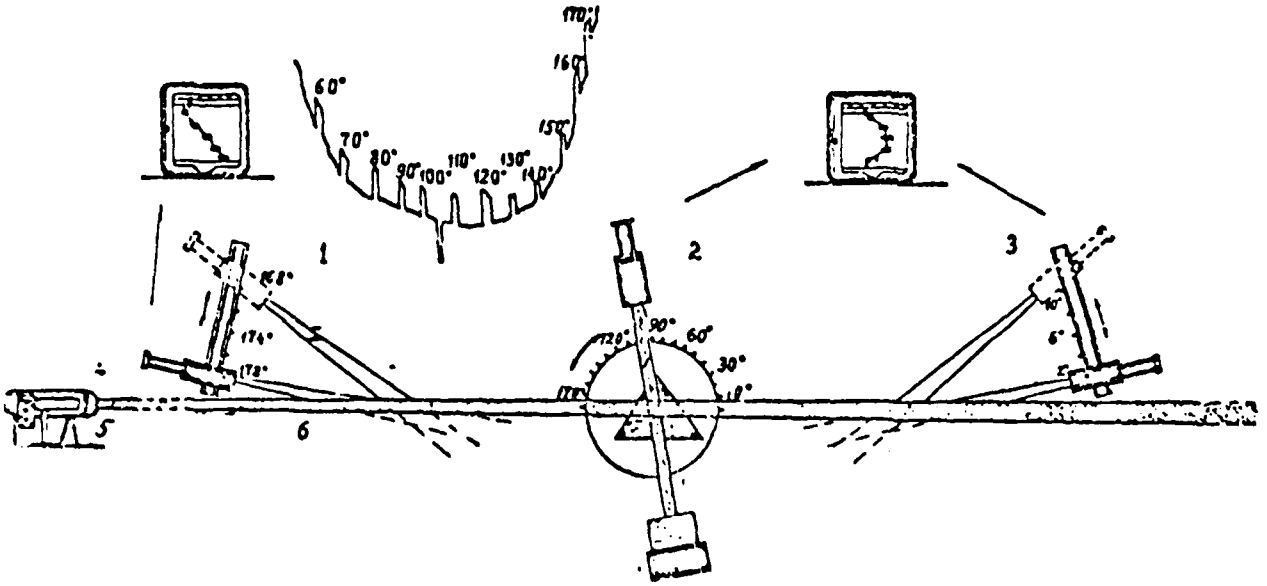

Figure 2. 2. Polar Nephelometer of Toropova (Ref 5)

The polar nephelometer developed at AFGL and reported by Gibson (Ref 6) has been flown on a balloon to 26 km altitude, measuring scattering coefficients of ambient air as small as 10^{-4} km^{-1} sr^{-1}, using a xenon light source and five photomultiplier detectors. Scattering is measured at 15°, 30°, 50°, 100°, and 150° and at four visible wavelengths and two polarizations. Figure 2.3 shows sample data for this device, as taken from Reference 6. The insert shows a schematic of the nephelometer. Overall dimensions of the instrument are approximately 10'x 5' x 2'. Baffled airducts permit unobstructed vertical flow of ambient aerosols into the measurement region, while providing sunlight shielding.

The airborne polar nephelometer developed at NCAR and reported by Grams et al (Ref 7) employs a He Ne laser and single photo-multiplier detector mounted in conjunction with a rotating disc and stepping motor, with capability for varying the measured scattering angle in small increments under control of a mini-computer. An exploded diagram of this device, taken from Ref. 7, is shown in Figure 2.4. An interesting feature of this instrument is the adjustability of laser polarization to yield zero Rayleigh (molecular) scattering at 90°, thus isolating the effects of aerosols. Scattering cross-sections on the order of 10^{-8} - 10^{-9} cm^{-1} are reported in Ref. 7.

If translated to the infrared region of interest by appropriate models, the sensitivity demonstrated in the visible region by the AFGL and NCAR polar nephelometers and by the fixed-angle baxicon would satisfy the requirements imposed on the present study. As will be seen below, the same can be said for integrating nephelometers, where ultra-sensitive devices for the visible spectral region have been highly developed.

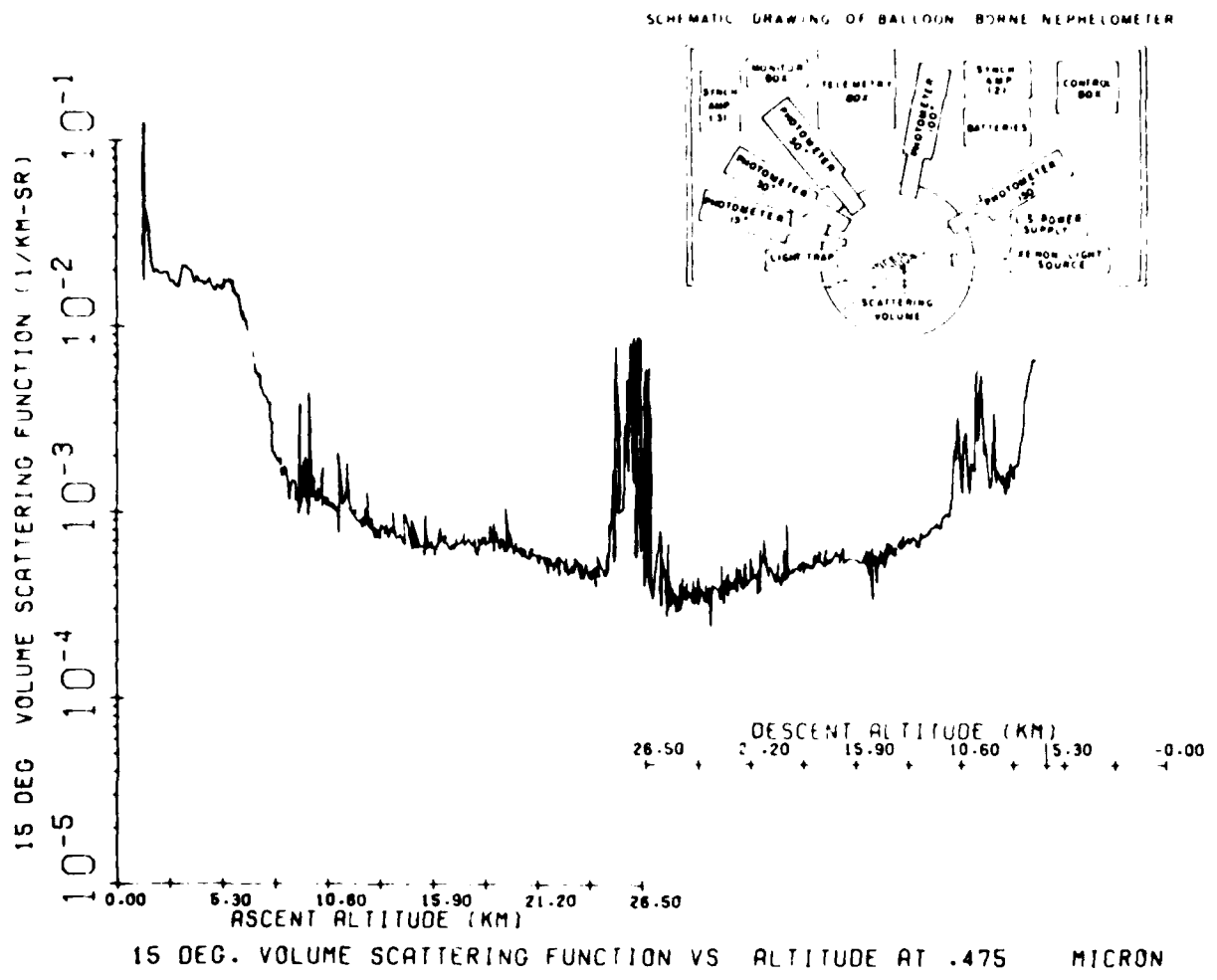

Figure 2.3. Data from AFGL balloon-borne polar nephelometer, reported by Gibson (Ref 6). Insert shows schematic diagram of instrument.

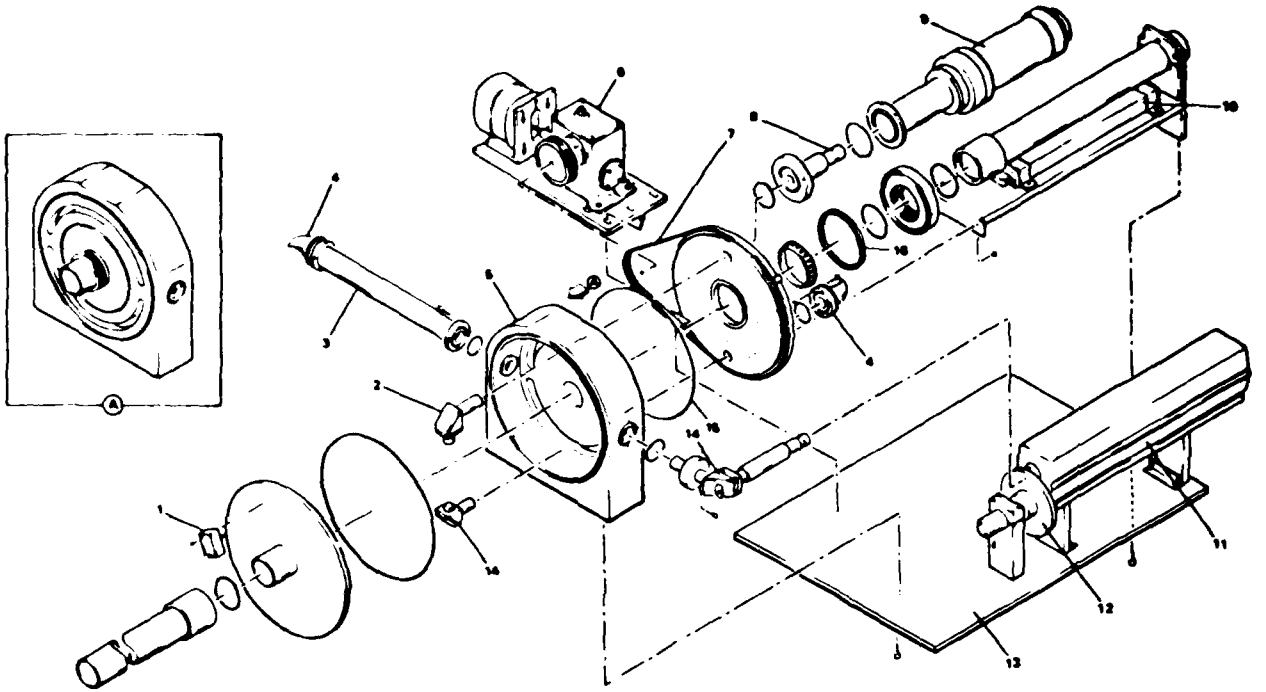

PARTS IDENTIFICATION

1	PRESSURE AND TEMPERATURE SENSOR	9	PHOTOMULTIPLIER
2	MIRROR AND LENS ASSEMBLY	10	PULSE AMPLIFIER AND DISCRIMINATOR
3	TUBE	11	He Ne LASER
4	LIGHT TRAP	12	CHOPPER
5	NEPHELOMETER HOUSING	13	BASE
6	STEPPING MOTOR AND 20 : 1 REDUCER	14	MIRROR ASSEMBLY
7	DRIVE BELT	15	TEFLON 'O' RING
8	BAFFLE ASSEMBLY	16	TEFLON SEAL

Figure 2.4. Exploded diagram of NCAR Polar Nephelometer using He-Ne laser. (From Ref 7)

2.4.1.3 Integrating Nephelometers

As pointed out previously, the integrating nephelometer measures scattering from a volume corresponding to a large span of scattering angles between zero and 180°. This volume is much larger than that measured by the polar or fixed-angle nephelometers, and hence it is to be expected that the achievable sensitivity of the integrating nephelometer will be much greater. This is in fact the case and, as will be seen, the demonstrated sensitivity with some commercial devices operating in the visible spectral region has been as low as one percent of Rayleigh scattering.

Problems of interpretation, similar to those previously discussed for the fixed-angle nephelometer, accompany the very high sensitivity of the integrating nephelometer. This is illustrated by reference to Figure 2.5, which shows the relative scattering function for a heavy aerosol concentration compared to that for the molecular constituents of pure air, i.e. Rayleigh scattering. The areas under these curves are proportional to the total scattering, and the curves are so scaled as to give equal area under each. A marked difference is to be seen at both small and large scattering angles between aerosol and molecular scattering. An ideal integrating nephelometer would encompass all scattering angles between 0-180° and thus yield an output signal proportional to total scattering for all types of scattering medium. However, achievable integrating nephelometers are limited to angles greater than some finite angle near zero and less than some angle near 180°, thus their outputs are somewhat distorted in a manner dependent on the scattering medium. Heintzenberg and Quenzel (Ref 8) have studied this so-called "truncation problem" in detail, and have made estimates,

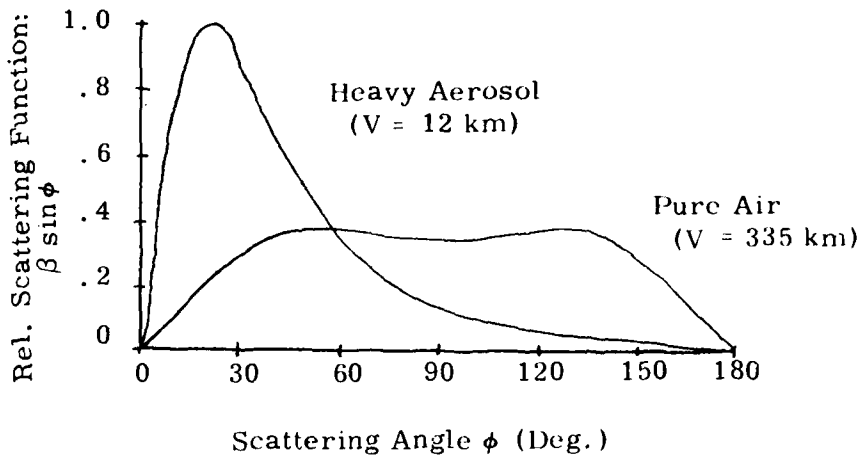

Figure 2.5. Relative scattering functions for aerosol and pure air, normalized to give equal areas under each curve.

using Mie and Rayleigh scattering theory, of the errors introduced by the nephelometers developed by Ruppersberg (Ref 9) and by Charlson (Ref 10) for Rayleigh atmospheres and for several aerosol distributions, including those of Diermendjian (Ref 11). They found that except for cloud and fog distributions, the readings for both nephelometers required less than 20 percent correction. For clouds and fog the required corrections were in the range 40-50 percent. The authors suggest that in practical applications with integrating nephelometers, suitable correction factors should be chosen based on estimates of the particle distributions for the atmospheres being measured. For the present application, such a procedure would be required if this type of nephelometer were to be employed for obtaining the scattering component of extinction.

A highly developed and commercially available integrating nephelometer stems from work done at the University of Washington by R. J. Charlson and his associates (Refs. 10, 12, 13). This instrument is manufactured under license by MRI, Altadena, California. Figure 2.6, taken from Ref 13, shows a schematic diagram of the Charlson nephelometer, which integrates over scattering angles of 7° to 170°. Note that the system is lensless, the field-of-view of the photomultiplier being defined by a series of baffles, a common approach in integrating nephelometers. The tungsten source shown in the figure, which illuminates an opal glass diffuser, is replaced in earlier models by a xenon flash-tube. The detail shown at the bottom of the figure illustrates the use of a partial shutter, which enables measurements of back-scatter only, integrating between 90° and 170°.

Recent use of the MRI integrating nephelometer has employed photon-counting techniques and long integration times, enabling measurement of scattering as low as one percent of Rayleigh scattering. B. Bodhaine

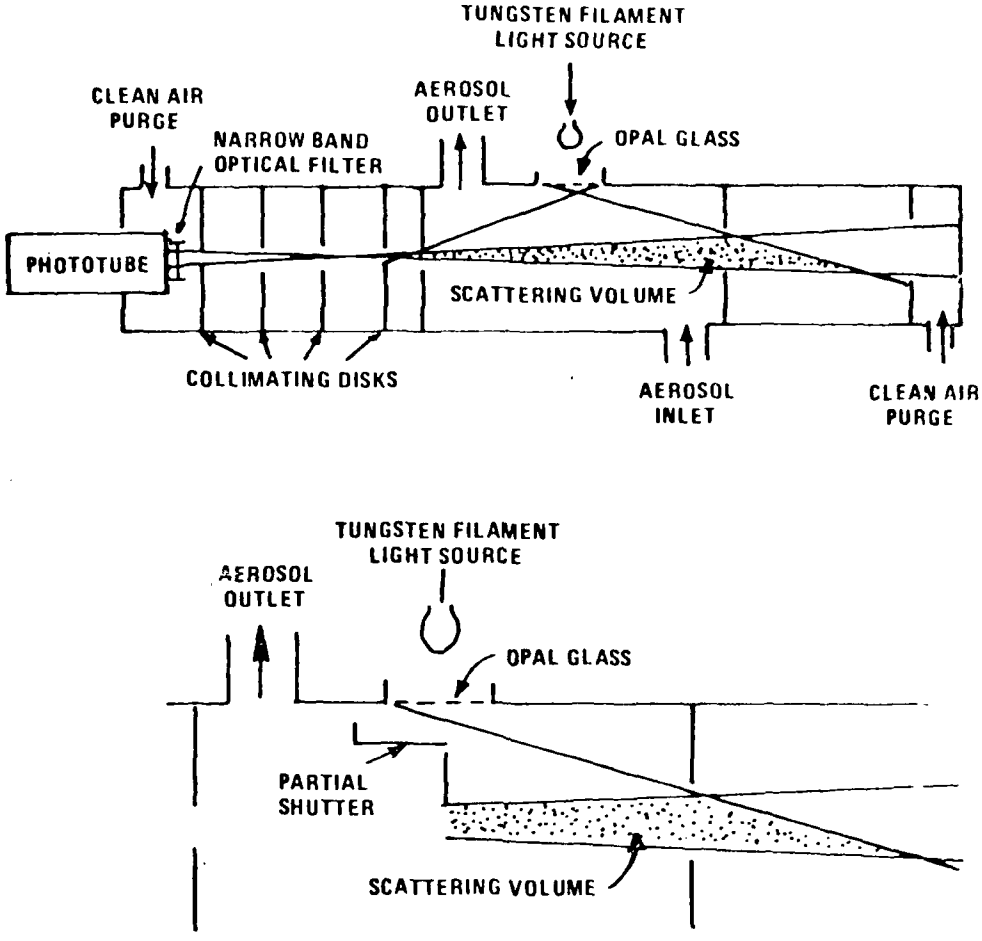

Figure 2.6. Schematic diagram of Charlson's integrating nephelometer (from Ref 13). Top diagram shows operation without the partial shutter, integrating the scattering coefficient over ~7° to 170°. With the shutter in place (bottom diagram) the instrument integrates over ~ 90° to 170°, to obtain back-scattering coefficient.

for example, (Ref. 14) presents summaries of four years of data monitoring aerosol scattering in four wave bands between 450 and 840 nm on the slopes of Mauna Loa, in Hawaii. With 45 minute integration times, Bodhaine reports limiting sensitivity at 2.5×10^{-10} cm^{-1}, consistent with the noise analysis of Waggoner et al (Ref. 12). For very clear conditions, a so-called "air-chop" mode was employed, in which counts are made for equal times on filtered and unfiltered air, the difference being attributed to aerosol scattering. Calibration was achieved using Freon 12 and a white-tipped wire, the latter for the upper end of the scale. Recording was over five decades, from 2.5×10^{-10} cm^{-1} to 2.5×10^{-5} cm^{-1}. Operation over a three year period was with a down time of only five per cent. This field demonstration of the Charlson type MRI instrument is impressive in terms of the requirements of the present study, assuming that such a device could be operated over the IR spectral region of interest, and keeping in mind the limits imposed by truncation errors (which would be less in the IR region).

Some different approaches to integrating nephelometer design have been reported in the literature, with possible applications to the present study. One example is the device reported by Cutten et al (Ref. 15), termed a "visibility meter". This instrument employes a collimating lens used with a tungsten light source, and locates a silicon detector to one side of the beam as shown in Figure 2.7, taken from Ref. 15. This geometry in effect reverses the positions of light source and detector in the Charlson instrument. The truncation angles of 25° and 117.5° shown in Figure 2.7 are empirically chosen to achieve approximately the same percentage of the total scattering for a variety of aerosols and molecular scatterers (see Figure 2.5). Calibration is achieved through use of Freon, CO_2, and pure air, and the detector/filter combination is designed to approximate the photopic response of the human eye. Signal processing employs synchronous rectification and photon counting, requiring approximately one second of counting time for 1 km of visibility (i.e. 5 minutes

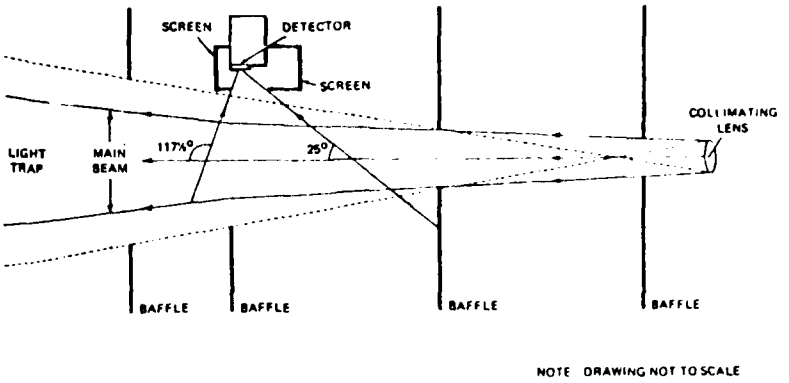

Figure 2.7. Visibility meter of Cutten et al (from Ref 15)

for 300 km visibility). Stray-light is compensated for using helium gas as a reference and the reported resolving capability of the instrument is "at least ten times that for pure air." Reference 15 shows good consistency in comparing results from the visibility meter to integrating nephelometer measurements over a range of visibilities from 10 km to 220 km. Absolute accuracy of 15 per cent is claimed for visibility measurement in the range 5 km - 335 km.

The nephelometer configuration of Cutten, as described above, may have advantages and special applicability to infrared nephelometer design satisfying the requirements of the present study. The silicon detector used is sensitive beyond one micron wavelength, although the system as described filters out all but visible light. Another nephelometer variant, which may also have application to infrared systems, was found in the Soviet literature. Golubitskii (Ref. 16) suggests using an objective lens in front of the detector in a Charlson-type instrument, and provides an analysis to show that this provides an optical gain proportional to the collecting area of the lens. This approach would probably improve the performance of an infrared version of the integrating nephelometer, since the use of small detectors is a likely design choice and the optical gain provided by the lens would improve S/N ratio.

2.4.1.4 Nephelometer Summary

The use of a nephelometer in partial fulfillment of the required extinction measurement is a strategy worth considering, coupled with a separate measurement of the absorption coefficient, e.g. through use of a spectrophone. The present status of nephelometry as related to the requirements of this study may be summarized as follows:

1. Nephelometers measure only the scattering component of extinction.

2. Fixed-angle, polar, and integrating nephelometers have been demonstrated in the measurement of visible-light aerosol scattering coefficients to have the sensitivity and dynamic range appropriate to the requirements of this study.

3. Modifications of these devices to provide scattering measurements over the 1-12 μm spectral region will pose difficulties, due to detector limitations and background problems. The literature contains little work beyond 1 μm.

4. Interpretation of fixed-angle and integrating nephelometer measurements in terms of total scatter requires assumptions as to the characteristics of the scattering medium.

5. The most highly developed and highly sensitive visible-light nephelometers are of the integrating type, capable of measuring scattering coefficients at a level of approximately one per cent of pure air scattering.

6. These ultra-sensitive scattering measurements involve photon counting techniques over periods on the order of 15-45 minutes.

2.4.2 Spectrophones

Although the spectrophone concept was enunciated in the last century by Alexander Graham Bell (Ref. 17), its exploitation and refinement for the measurement of very small molecular and particulate absorptions has taken place largely during the past decade. If coupled with a nephelometer device, the spectrophone-nephelometer combination could yield the desired extinction measurement.

The early work of Kerr and Atwood (Ref. 18) described two spectrophone systems, one using a pulsed ruby laser to measure H_2C absorption in the 694 nm region, the other using a CW CO_2 laser to measure CO_2 absorption at 9.6μm. Pressure rise resulting from heating of the absorbing gas was measured with a capacitance manometer affixed to the short gas sample chamber. (Characteristic of all spectrophones, this pressure rise is independent of absorbing cell length.) Kerr and Atwood give details on the theory of spectrophone operation and demonstrated a sensitivity in measuring absorption coefficient of 10^{-7} cm^{-1} for their system. Linearity of signal vs. absorbing gas concentration was demonstrated over four decades of operation. Problems with spurious signals resulting from window heating were cited as the ultimate limiting factor of their system. This has been a persistent problem in all spectrophone work, with various means employed to circumvent it. Kerr and Atwood suggested lengthening the absorption cell, in situ bake-out of the windows, and purging with dry nitrogen. They felt that the combined use of these measures would improve their sensitivity by a factor of ten (to 10^{-8} cm^{-1}). Later workers have employed accoustic baffling and resonant microphones, as well as differential techniques, to avoid problems associated with window heating. In the pellet spectrophone (References 19 and 20), window heating itself in effect gives rise to the signal, with solid absorbing materials (aerosol, etc.) being pressed into a K Br pellet absorber mounted next to the spectrophone chamber.

Charles Bruce, of the U.S. Army Atmospheric Sciences Laboratory, White Sands Missile Range, published a detailed report in 1976 reviewing the early spectrophone developments at ASL (Ref. 21). This work has given rise to a number of later reports, as discussed below. Reference 21 remains an authoritative general review of spectrophones, and ASL is one of the principal laboratories developing and using these instruments for atmospheric research.

Reference 21 sets forth "required" and "desired" spectrophone characteristics as follows:

Required Characteristics

1. Sensitivity: Measurable absorption coefficients smaller than 10^{-3} km^{-1}.
2. Power linearity of absorption signal.
3. Single measurement precision: 10 per cent of mean at 10^{-3} km^{-1}.
4. Stability: Negligible drift or jitter.

Desired Characteristics

1. Approximately zero passband width, assuring best S/N ratio.
2. Incorporation of acoustic gain (i.e. high Q).
3. Removal of window source signal without sensitive balance procedures.
4. Operational simplicity.
5. Capability of operation in flow-through mode.
6. Potential for pulsed laser use.
7. Linearity with pressure and independence of temperature.

The requirements enumerated above are completely consistent with the extinction measurement requirements of the present study; i.e. they would assure determination of the absorption portion of the extinction coefficient to within the required accuracy, precision, linearity, and stability. (The scattering component would, of course, have to be determined separately.)

The spectrophone requirements of the above list have been found through experience to be entirely reasonable for wavelengths extending from the visible through the near and mid-IR to 10 microns. Furthermore, although most reported spectrophone work makes use of laser sources, this is not a basic requirement to their operation. Indeed, as C. Bruce emphasizes in Ref. 21 , none of the described systems requires a narrow-band radiation source and, "...in fact, a broader band source will simply result in a wavelength integrated absorption measurement." Thus, the spectrophone system is quite flexible as to its spectral coverage, this being determined solely by the radiation source and optical filters used. Optical/IR detectors are, of course, not an essential part of the system.

Reference 21 gives detailed consideration to both CW and pulsed source spectrophones, to balanced (i.e. manometer-type) and acoustic (microphone-type) systems and gives considerable detail on microphone design. Figure 2.8, taken from Reference 21 , shows a typical system for use with an IR laser source. Note the cylindrical microphone which is constructed of thin aluminized mylar and situated within the absorption chamber. The acoustic damping discs shown prevent spurious signals due to the windows from entering the microphone cavity.

Resonant microphones, employing either longitudinal or radial resonances resulting from the cylindrical symmetry, have been found to be most consistent with the "desired" characteristics on the above list from Reference 21 . These are operated in a CW mode and, in effect, phase select the absorption signal due to the gas within the microphone and suppress

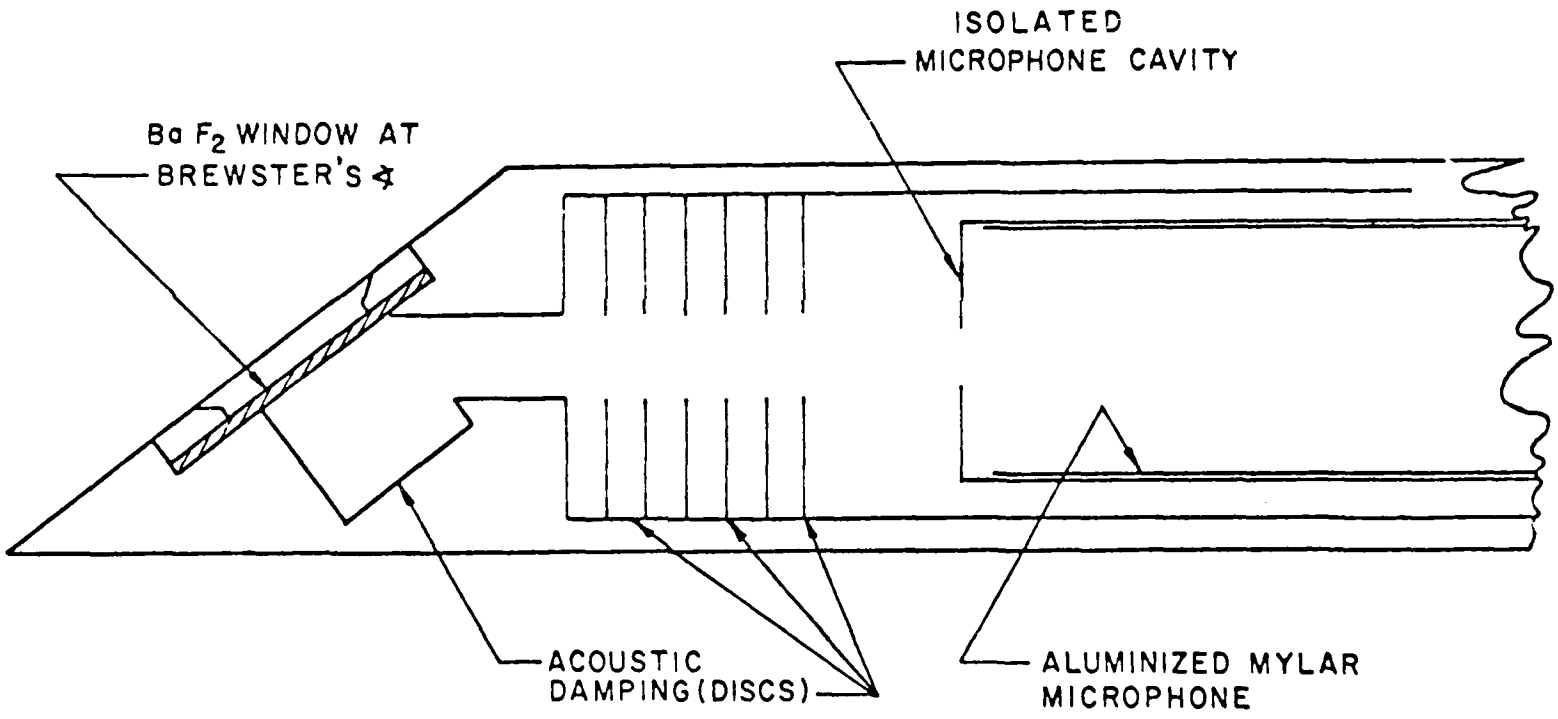

Figure 2.8. General-purpose CW source spectrophone. (From Reference 21)

spurious effects such as those due to window heating. These resonant systems can thus be operated windowless, in a flow-through mode. Figure 2.9, taken from Reference 21, is a schematic of two resonant spectrophones connected for in-situ differential measurements of atmospheric constituents. The flow of the sampled atmosphere is such that the right-hand spectrophone contains aerosols which are filtered out before entering the left hand cavity. Thus the difference in signals from the two resonant cells gives the particulate contribution alone. As pointed out in Reference 21, the end windows in this system can be eliminated. In a later paper (Ref. 22), Bruce and Pinnick employed such a windowless system to measure the absorption of an artificial aerosol consisting of quartz particles, using a CO_2 laser in the 9.2 - 10.8 μm region. The results compared favorable with calculations from Mie theory. Although the system used in Reference 22 is windowless, some kind of induced flow is required through the cylindrical chamber, cross-section of which is on the order of 10 cm^2. Fully "open" resonant spectrophones would pose difficulties.

Terhune and Anderson (Ref. 23) also reported spectrophone measurements of aerosol absorption, which included, among other materials, tobacco smoke. These measurements were criticized by Kerker et al (Ref. 24), who incorrectly claimed that spectrophone measurements are invalid in the presence of aerosols. Crane's spectrophone study (Ref. 25) of explosive vapors indicated a sensitivity of 6×10^{-8} cm^{-1} for a non-flowing system, with degradation to 2×10^{-7} cm^{-1} in a flowing system attributed to turbulence noise. Since this was not a resonance-type acoustic system, the advantages alluded to by Bruce (Ref. 21) of such systems were apparently not available to Crane. Nadov (Ref. 26) gives an optimization analysis of a resonant system with detailed consideration of the acoustic resonances in a cylindrical microphone, and estimates a potential measurement limit as low as 10^{-11} cm^{-1}. He presents measurements taken with a resonant system which show sensitivity to 1.5×10^{-9} cm^{-1} with S/N = 2. Nadov's work

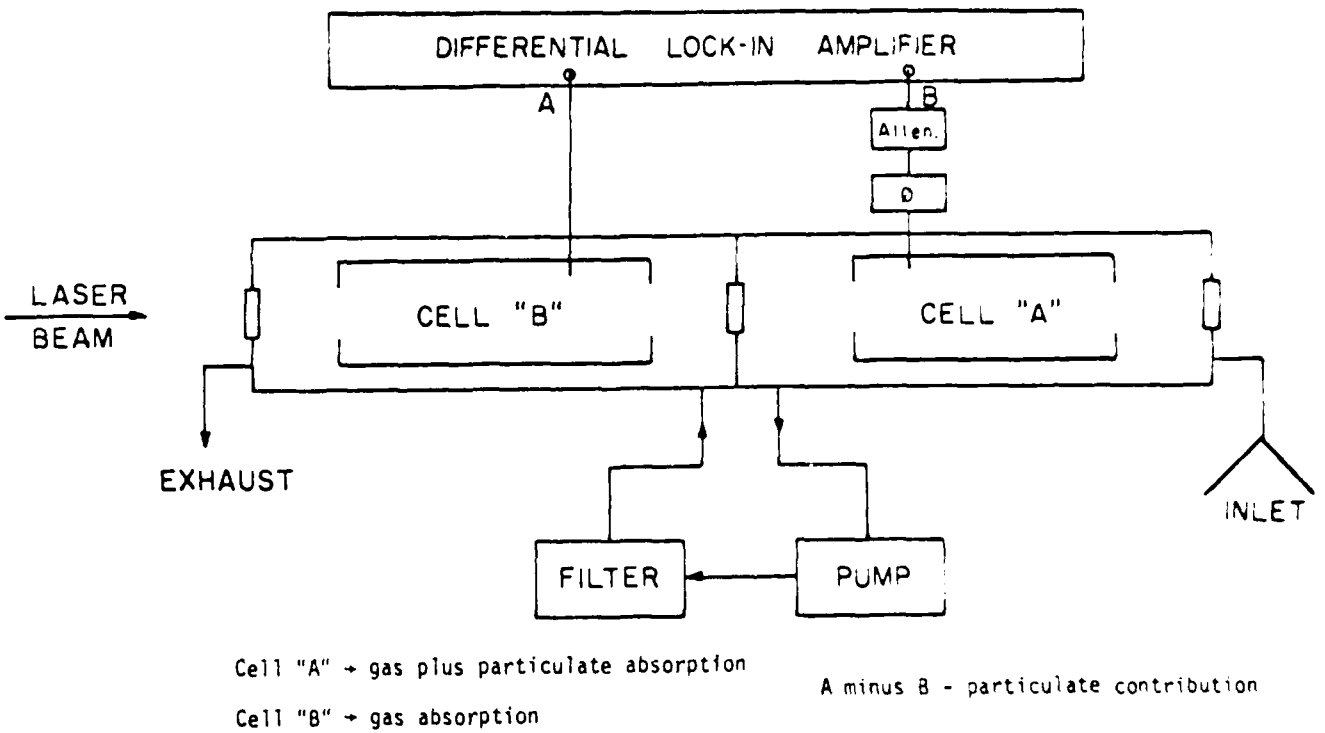

Figure 2.9. Schematic of resonant differential spectrophone for in-situ atmospheric measurements. (From Reference 21)

emphasizes the extreme sensitivity obtainable using resonant spectrophone systems.

A number of other papers have presented data which demonstrate the usefulness of the spectrophone technique for a wide variety of applications for the measurement of absorption coefficients in the visible and IR spectral regions (References 27, 28, 29, 30). For the most part these do not relate to weakly absorbing samples, so they do not show the ultimate sensitivity of these systems. Publication in this field by workers in the USSR has not been extensive, the paper by Antipov and Ponomarev being typical (Ref. 31). Their spectrophone was a pulsed ruby laser system, scanned in wavelength over a water vapor absorption band by temperature cycling of the ruby. Coefficients for H_2O absorption were presented in the range $3\text{-}7 \times 10^{-6}$ cm^{-1}. The authors claimed the ultimate sensitivity of this pulsed system (pulse energy ~ 1 J) to be 10^{-9} cm^{-1}. "Bleaching", i.e. a decrease in absorption coefficient, was noted when the power density was increased from .02 to 0.1 mW cm^{-2}.

2.4.2.1 Spectrophone Summary

The following points may be made in summarizing the work on spectrophones.

1. The state-of-the-art is well developed and demonstrated beyond the sensitivity requirements of this study. Several workers have demonstrated measurement capability to better than 10^{-3} $km.^{-1}$.

2. CW systems with a resonant cylindrical microphone seem to have the best sensitivity and operational characteristics.

3. Spectrophones have been successfully operated throughout the spectrum from the visible to 10 μm IR, requiring no conventional radiation detectors.

4. Lasers have been extensively employed in spectrophones, but are not essential.

5. The likelihood of developing an exposed spectrophone system with high sensitivity is remote.

6. Spectrophones are sensitive only to the absorption component of extinction and cannot discriminate directly between molecular and aerosol absorption. Differential measurements as described in Reference 21 can isolate the aerosol absorption.

7. At present spectrophones can only be calibrated on a relative basis.

2.4.3 Transmissometers

The basic equation for transmission, T, over path length, x, with extinction coefficient, σ, is

$$I/I_o = T = e^{-\sigma x} \qquad (2.3)$$

where I and I_o are the transmitted and initial beam intensities, respectively. This means that an extinction coefficient of 1.5×10^{-3} km^{-1}, one of the measurement goals of the present study, will yield an intensity difference amounting to only .001 of the initial intensity for a 1km path, and 1000 times smaller for a 1 meter path. The instrument designer is thus faced with formidable requirements for instrumental stability and accuracy, even for transmissometers designed for the longer-path measurements, while transmission paths of dimensions corresponding to a compact device become out of the question. We have seen in the previous sections that the extinctiometer, nephelometer, and spectrophone all contain in their designs means for direct measurement of the extinction coefficient, or of its scattering or absorption components. In contrast, any transmissometer must accurately determine the small difference between two separately measured intensities,

leading invariably to the requirement of long paths. In this section the approach will be considered which employs multiple reflections within a confined region, i.e. the White cell. This effectively collapses a long optical path into the confines of a much smaller apparatus. In the next section the alternative approach of lidar will be discussed, which in effect provides a single-ended transmissometer operating over a long atmospheric path outside the instrument.

The principle of the multipath absorption cell was brought forth by J. U. White in an early paper (Ref 32), and recent interest in IR laser attenuation due to various atmospheric constituents and in the monitoring of trace pollutants has brought this device back into use by a number of workers. White's recent paper (Ref 33) shows modifications in the scheme which would permit up to thousands of passes across a cell if reflection losses would permit. The standard White cell employs concave spherical reflection surfaces, although some workers have employed flat mirrors in laser systems. (See, for example, the system of Gerber, Ref 34.) Optical alignment is critical in any of these multipath systems, since a single mirror is used repetitatively to reflect the beam many times. Moreover, thermal expansions can adversely affect overall alignment, and inhomogeneities in the gas sample or in the mirror surfaces can also affect system accuracy as can vibrations. Drifts in the radiation source intensity or in electronic amplification must be carefully controlled in these systems, since the transmission measurement involves a comparison of output signals with and without the absorbing gas in the White-cell. In the case addressed by this study, for example, filtered and unfiltered ambient air would be alternately introduced into the cell.

W. R. Watkins, at the U.S. Army's Atmospheric Sciences Laboratory at White Sands, N.M., has reported a technique for improving White-cell measurement accuracy, termed "path differencing" (Ref 35). Figure 2.10

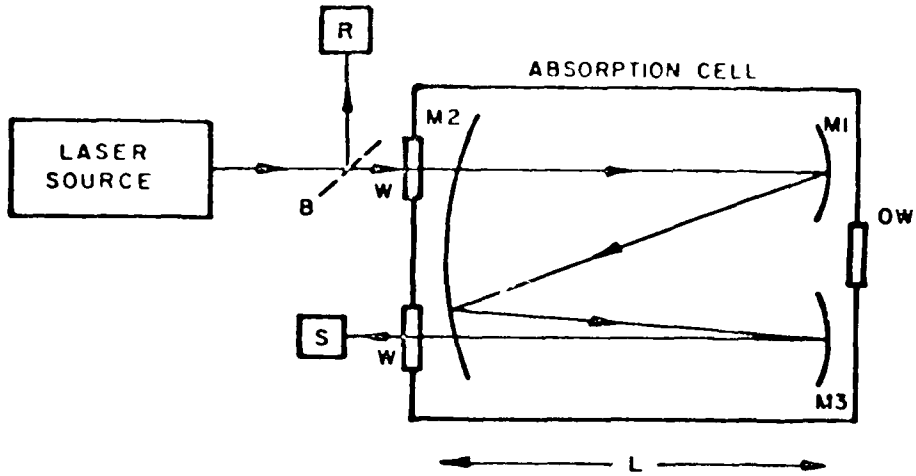

Conventional "White-type" absorption cell experimental setup: B, beam splitter; W, cell windows; OW, observation window; R and S, reference and sample detector systems; M_1, M_2, and M_3, spherically concave cell mirrors; and L, separation distance between cell mirrors.

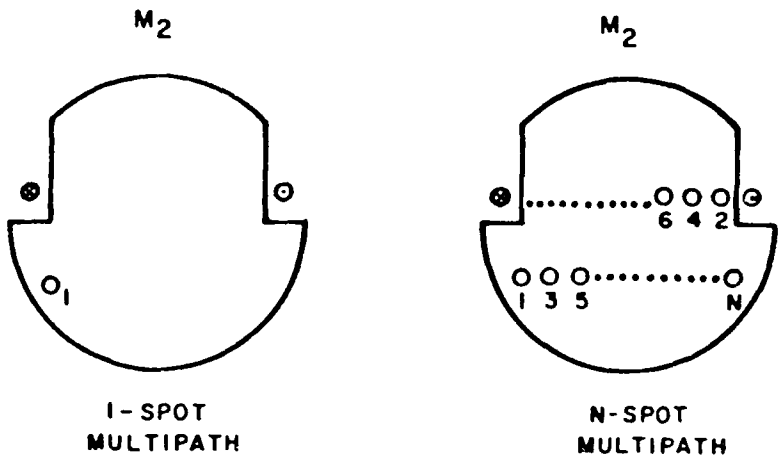

Views of mirror M_2 as seen from the observation window OW for a 1-spot (left) and an N-spot (right) multipath; numbered circles, images of laser source on mirror surface; circle with central dot, laser beam entering cell; and circle with "X," laser beam exiting cell.

Figure 2.10. White-cell system, using path differencing, reported by Watkins (Ref 35). Figure from Ref. 36.

shows schematically how this is used in the ASL 21 meter White-cell system. The system is so constructed that a relatively rapid change-over, taking approximately one minute, can be made from the "1 spot multipath" to the "N-spot multipath" shown in the figure. In this manner, longer-term drifts in the system due to light-source, electronics, etc., are eliminated, and the two measurements determine the combined effect of the longer vs. shorter extinction path and the larger vs. smaller number of mirror reflections. The latter effect is then isolated in a separate path-differencing measuring sequence, with the system flushed and loaded with a zero extinction gas.

A recent Army ASL report, by Watkins and Dixon (Ref 36), discusses methods employed for automating their White-cell measurements and gives elaborate alignment procedures ---"to obtain very accurate absorption coefficient measurements with the path differencing technique". With these reported improvements, the authors claim 1/2 per cent measurement accuracy in transmission for a 1.5 km total path difference, and further mention measuring "absorptions of a few per cent per kilometer". This capability reflects the previously mentioned basic difficulties inherent in any transmission measurement. The goal of the present study; namely, to measure extinction coefficients down to 1.5×10^{-3} km^{-1}, would thus seem to be out of the reach of the ASL White-cell system. Comparable sensitivities have also been reported by Peterson for the 15 meter system at Ohio State University (Ref 37) and by Aerodyne for their DF system (Ref 38). Ref 37 reports H_2O absorption coefficients at CO_2 laser frequencies down to .03 - .04 km^{-1} for their White-cell, whereas coefficients are given down to .01 - .02 km^{-1} for a spectrophone system. Gerber (Ref 34) emphasized portability with his system, and hence was limited to a 20 meter total path and correspondingly less sensitivity. He reported standard deviations in extinction measurements of from ten per cent to several hundred per cent for extinction coefficients in the range 0.1 - 1.0 km^{-1}.

2.4.3.1 Transmissometer Summary

The following points summarize the characteristics and capabilities of transmissometers as related to the requirements of this study.

1. Transmissometers measure the desired quantity, i.e. extinction (combined scattering and absorption).

2. The combined requirements of instrument compactness and capability for measuring very small extinction coefficients ($\sim 1.5 \times 10^{-3} km^{-1}$) leads to a multiple reflection folded path solution, the most common form of which is the White-cell.

3. Typical White-cell systems achieve ~100 reflections giving total optical path length on the order of kilometers in a system 10 - 20 meters in size.

4. Folded-path transmissometers have successfully operated over the desired 1-12 μm spectral region, using either laser sources or non-coherent sources.

5. These systems require great mechanical stability and precise optical alignment, and are subject to vibration and other disturbing factors.

6. Subject to the limitations of systems which take small differences of two separate measurements, current state-of-the-art in folded-path transmissometers yields a limiting sensitivity approximately ten times higher than the goals of this study, i.e. $\sim .01\ km^{-1}$.

7. [illegible] aerosol extinction coefficients are to be calculated from transmissometer measurements, values for molecular extinction coefficients must be provided from models or other measurements.

3. METHODS FOR MEASURING ABSORPTION SCATTERING AND EXTINCTION COEFFICIENTS

3.1 Introduction

Methods for determining the optical parameters of aerosols in the free atmosphere are studied here. Studies are restricted to systems which might meet the given constraints relating to wavelength, sensitivity ruggedness and infrequent calibration and operator intervention. The systems studies include spectrophones, nephelometers and a device called an extinctiometer.

3.2 Signal and Noise of a Spectrophone

The possibility of measuring the absorption coefficient of the ambient atmosphere by using spectrophone techniques is discussed here. Calculations are made assuming that a laser beam is projected along the axis of a long tube and that the detector is embedded in the wall of the tube. This model is chosed for the simplicity it introduces into calculations. The results obtained are essentially correct for a free standing detector operating in a quiet atmosphere without the tube.

It is assumed in this discussion that air heating due to aerosol absorption will produce the same pressure effects as air heating by molecular absorption (Reference 22).

In a generalized sort of way a spectrophone may be treated as an engine and compared to a Carnot Engine having as its piston the sensing element of a microphone. In this model the microphone is sensitive enough to "hear" the Brownian motion of its sensing element. In this case, the work done by the engine, if it is to be detectable, must be equal to or greater

than the energy of the one degree of freedom appropriate to the piston. The efficiency of the spectrophone engine cannot exceed that of the Carnot engine. The calculation made here is for a Carnot engine driving a Brownian-motion limited detector with one degree of freedom. This calculation will set a limit to the signal -to-noise ratio of the spectrophone concept.

For purposes of this discussion consider a spectrophone to be built as shown in Figure 3.1. A pulsed laser beam of cross sectional area, a, is used. Each pulse has duration T and travels along the axis of a long cylinder having radius r. The walls of the cylinder are optically non-reflecting and the wall material has sufficient heat capacity that it may be treated in this calculation as being of constant temperature. Near the midpoint of the cylinder a microphone of active area b is embedded in its wall. The long cylinder is used so that the analysis can be carried out in the two dimensions perpendicular to the laser beam. The atmosphere in which this experiment is conducted has an attenuation coefficient γ, km^{-1}, at the wavelength of the laser. The transmission of a path of length L, km, through the atmosphere is given by

$$T = e^{-\gamma L} \tag{3.1}$$

The attenuation is caused by two processes, absorption and scattering so that

$$\gamma = \sigma + \kappa \tag{3.2}$$

where σ, km^{-1}, is the scattering coefficient and κ, km^{-1}, is the absorption coefficient. The path length, X, from the laser to the far end of the cylinder may be a meter or so. The transmission of this path is

$$T(X) = e^{-\gamma X} \tag{3.3}$$

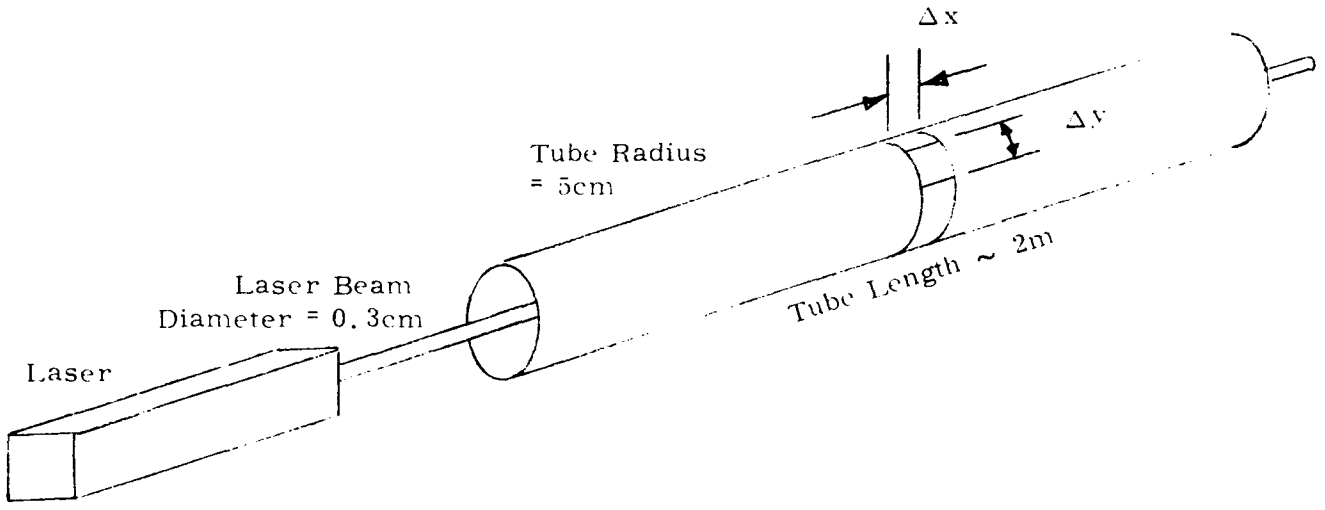

Figure 3.1. Layout Used in Spectrophone Discussion

The environmental conditions of interest to this study involve the following maximum values: a γ no greater than 10 km^{-1}, and path lengths unlikely to exceed 20 meters. Thus the worst case transmission which would occur is:

$$T(X) = e^{-\gamma X} \geq e^{-0.02} \approx (1-\gamma X) = (1 - 0.02) = 0.98 \qquad (3.4)$$

This result supports the assumption which is made here that the laser beam power is essentially constant along the length of the pipe and independent of the value of the attenuation coefficient.

Light is lost from the laser beam by absorption and scattering. It is assumed here that the scattered power travels to the pipe wall without further attenuation and is absorbed there without perceptible heating of the wall material. In the beam the absorbed power heats the air in which it has been absorbed. It is assumed that the conversion of absorbed radiant energy to kinetic energy of the air is instantaneous. If the power in the laser beam is P and the pulse duration is τ then the energy absorbed per pulse in beam length Δx is

$$E(\Delta x) = P \tau \kappa \Delta x \qquad (3.5)$$

It is assumed that the pulse duration is short enough that during the pulse the absorbed energy does not diverge significantly from the region of absorption. The divergency of energy will be via a pressure pulse in the gaseous medium and this pulse will propagate with a velocity about equal to sound velocity, 333 m sec^{-1}. If the laser beam is 3 mm in diameter and expansion of 1 mm is acceptable during a pulse then the pulse duration must be limited to about 3 microseconds. Assuming these or similar conditions are met then ΔT, the temperature rise of the air irradiated by

$$\Delta T = \frac{P_r \kappa \Delta x}{C_a \Delta x} = \frac{P_r \kappa}{C_a} \tag{3.6}$$

where C is the heat capacity of the air per unit volume and a is the cross sectional area of the laser beam.

The efficiency of a Carnot engine is then

$$\frac{\Delta T}{T} = \frac{P_r \kappa}{C_a T} \tag{3.7}$$

where T is ambient temperature in K.

The maximum work per energy pulse that the Carnot engine can do per unit length of pipe, $W(\Delta x)$ is the product of $E(\Delta x)$ the energy absorbed in unit length Δx and the efficiency $\Delta T/T$. To be detectable this must at least equal the energy of one degree of freedom. That is

$$W(\Delta x) = \frac{P^2 r^2 \kappa^2 \Delta x}{C_a T} \geq 1/2\, k\, T \tag{3.8}$$

where k is Boltzmann's constant = 1.38×10^{-23} joules $\deg^{-1}$.

If the radius of the cylinder is r, its circumference is $2\pi r$. A detector might be "wrapped around" the inside of the cylinder and extend for a length Δx along the cylinder. Then all the energy of the pressure pulse from Δx would be incident on the detector. The maximum efficiency of coupling from the sound field to the microphone sensing element is 0.5 when the coupling occurs in finite time. With the wrap around detector, the minimum detectable absorption coefficient, κ_{min}, is

$$\kappa_{min} > \frac{T}{Pr}\sqrt{\frac{C k a}{\Delta x}} \tag{3.9}$$

If a detector is used with sensing element occupying some length, ΔY, around the circumference, then

$$\kappa_{min} \geq \frac{T}{Pr}\sqrt{\frac{2\pi r C k a}{\Delta x \Delta Y}} = \frac{T}{Pr}\sqrt{\frac{2\pi r C k a}{b}} \qquad (3.10)$$

, where $b = \Delta x \Delta Y$, the area of the detector.

To illustrate the application of this result, the following values are used

$$T = 300\,^{\circ}K$$
$$r = 3 \times 10^{-6}\ \text{sec}$$
$$P = 3.3\ \text{watts}$$
$$rP = 10^{-5}\ \text{joules}$$
$$r = 5\ \text{cm}$$
$$C = 1.3 \times 10^{-3}\ \text{joules}\ ^{\circ}C^{-1}\ \text{cm}^{-3}$$
$$k = 1.38 \times 10^{-23}\ \text{joules}\ ^{\circ}C^{-1}$$
$$a = 7 \times 10^{-2}\ \text{cm}^2$$
$$b = 1\ \text{cm}^2$$
$$\kappa_{min} \geq 6.0 \times 10^{-6}\ \text{cm}^{-1}$$

If 10^4 pulses per second are used for an observing time of 100 sec, then

$$\kappa_{min} \geq 6 \times 10^{-9}\ \text{cm}^{-1} \qquad (3.11)$$

The sensitivity (κ_{min}^{-1}) of the system will increase in a linear way with the pulse energy. It increases as the square root of the number of pulses and the area of the detector. The effective detector area can be increased by using acoustical horns, lenses or converging mirrors.

An important conclusion from this exercise is that the sensitivity is inversely proportional to the diameter of the projected laser beam. The maximum pulse duration was set by the beam diameter and in the primitive analysis used here pulse duration was made proportional to beam diameter. By this analysis if the beam diameter is decreased, pulse duration must also be decreased . To keep pulse energy constant the pulse power must be increased. Only when this is done can sensitivity be increased by reducing the laser beam diameter.

Finally, the long tube has been included in the discussion to allow a two-dimensional analysis. It can be removed leaving the detector standing alone without serious modification of the results.

This analysis of a possible spectrophone design has been presented as a study of the roles of various parameters. It is not proposed that such an instrument be built. This brief analysis shows that there is no theoretical reason why a spectrophone cannot be designed and built to meet the requirements of this report. That is, using a laser pulsed 10^4 times per second with individual pulse energy of 10^{-5} joules and duration of 3×10^{-6} sec, absorption coefficients as small as 6×10^{-3} km^{-1} can be measured with signal -to-noise ratios of 10 in 100 seconds. Practical limitations such as the noise of the environment are not included in this evaluation.

3.3 Types of Nephelometers

Nephelometers are devices used to measure light scattered by a sample of the atmosphere. The measuring technique is usually calibrated so that the measured value can be correlated to some aspect of the scattering coefficient of the atmosphere. Integrating nephelometers measure the sum of weighted values of the light scattered at almost all angles (measurements at and near 0° and 180° scattering angle are not included because of difficulty).

The weighting is such that the resulting measurement is proportional to the scattering coefficient of the sample. Polar nephelometers involve a multitude of measurements made at various scattering angles covering the range from close to 0° scattering to close to 180°. Values obtained from a polar nephelometer may be weighted according to the angle of measurement and summed to give a value proportional to the scattering coefficient. The measured values, when divided by the scattering coefficient, can be calibrated to provide values of the normalized phase function for scattering at the angles of the measurements. Fixed angle nephelometers are ones in which the radiant power scattered from a collimated beam is measured within a specific range of scattering angles and the measured amount is taken to be infixed ratio to the total scattering coefficient.

3.4 Signal and Noise of A Baxicon Type Fixed Angle Nephelometer

The baxicon is a fixed angle nephelometer in which the scattering angle is selected to be 55° from the direction of the irradiating beam. In the visible spectrum the normalized phase function at 55° for most aerosol types (urban, maritime, rural) as well as for molecular scattering is about equal to $(4\pi)^{-1} sr^{-1}$. Thus, when viewed at an angle of 55°, the radiance of a beam projected into the atmosphere is in fixed proportion to the scattering coefficient of the atmosphere without regard to the aerosol density or type. Equations for the signal and for the signal-to-noise ratio appropriate to the baxicon concept are developed in terms of design parameters in the following paragraphs.

The principle of the baxicon design is shown in Figure 3.2 which shows the original concept of the baxicon; this is a primitive illustration which allows simple statements to be made about the optical principles involved. It is not the design for which signal and signal-to-noise calculations will be made. In that case an axicon lens is used. An axicon is a glass cone with its

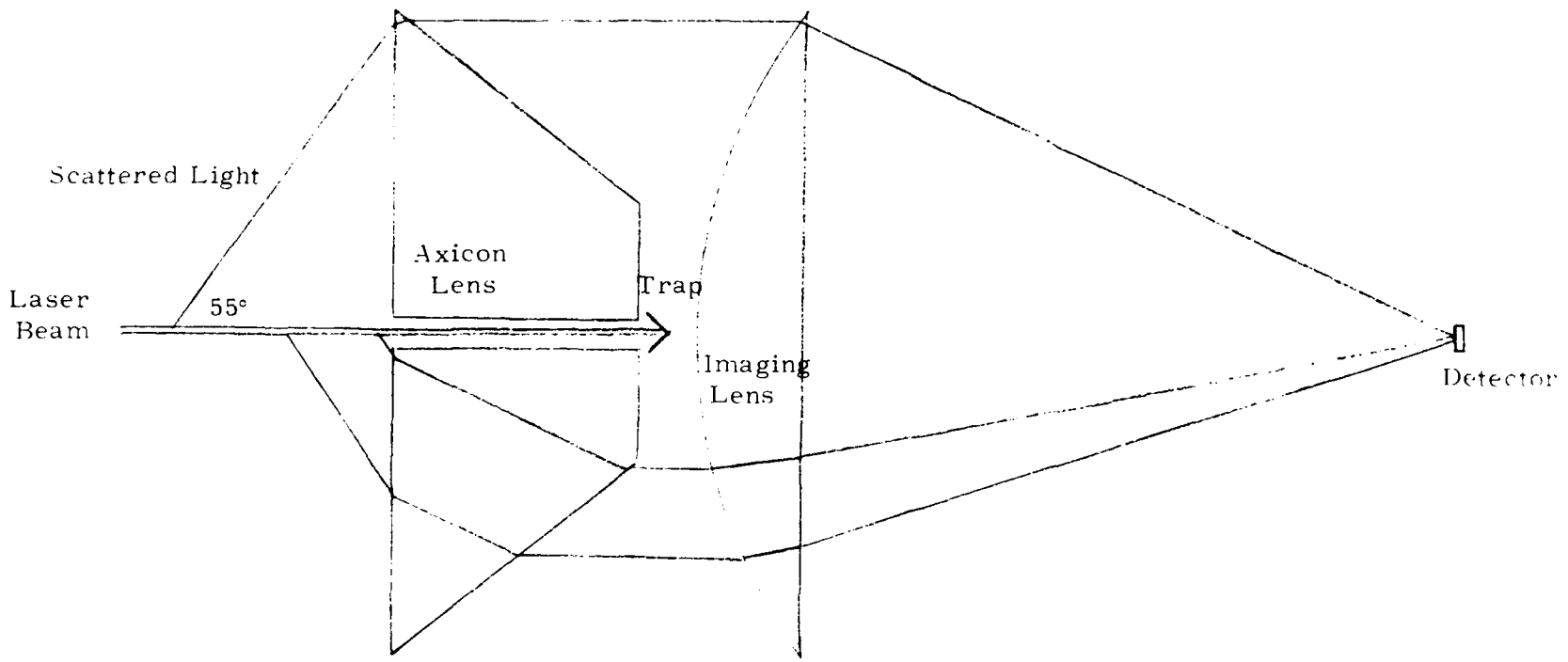

Figure 3.2. Primitive Baxicon.

axis of symmetry coincident with the optical axis. Figure 3.1 is drawn in a plane containing the optical axis and shows a section of the optical system. The projected beam travels along the axis from left to right. If the index of the axicon glass is 1.8 and the apex angle is 77.62° then light which is scattered through an angle of 55° from the projected beam and is incident on the axicon lens will be refracted in its transit of the axicon lens with a total prismatic deviation of 90°. Such a light ray will exit from the axicon in the plane of the figure and parallel to the optical axis. Thus, all rays scattered from the projected beam at 55° and incident on the axicon leave the axicon parallel to each other and to the optical axis. This bundle of parallel rays is collected by a lens and imaged on a detector at its focus. In the sketch of Figure 3.2 there is a hole through the axicon lens along its axis. The projected beam is intended to travel through this hole to a light trap.

A system as shown in Figure 3.2 could be quite heavy because of the amount of glass in the axicon lens and the imaging lens. Further complications arise when any significant range of wavelengths is involved because chromatic effects are then present. For the range of wavelengths to be considered here an all reflecting design seems desirable. One such design concept is presented in Figure 3.3.

In Figure 3.3 a conical mirror takes the place of the conical prism of Figure 3.2. Here, the light from the laser beam which is scattered through 55° and which reaches the conical mirror is reflected so as to be parallel to the optical axis. This parallel light passes through an optical filter and is then focussed onto an off-axis detector by reflection from a parabolic mirror and a tilted plane mirror. The tilted mirror is used so that the detector can be located away from the mechanical axis of the parabolic mirror. This is done because the laser beam must travel along the common axis of the conic mirror and the parabolic mirror. In this design the laser

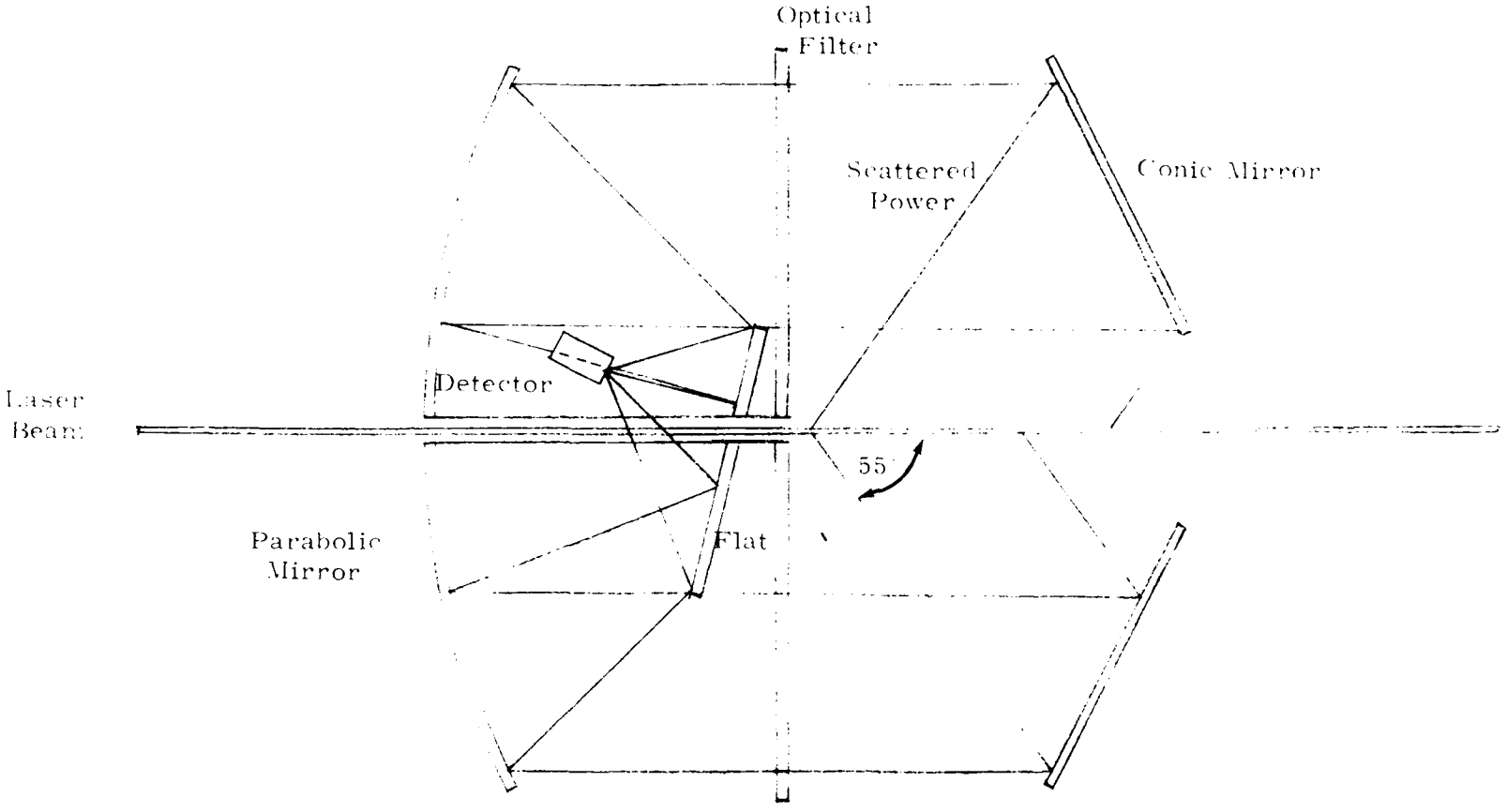

Figure 3.3. VII Reflecting Baxicon

beam travels in a tube from behind the parabolic mirror to a position in front of the filter. Then the beam runs free through the air sample and in this region light scattered from the beam at 55° reaches the conic mirror. The laser beam leaves this region through a large hole in the conic mirror. The size of this hole is somewhat less than the projected size of the tilted flat mirror.

The first calculation made here relates the power scattered from the laser beam to the detector via reflections from the conic mirror, the parabolic mirror and the tilted flat mirror. Figure 3.4 is a simplified sketch of the optical system. Here r is the radius of the circular detector at the focus of the parabola of focal length f_o. The projected source beam travels along the x axis. The radius of the beam is constant and equal to ρ. We consider an element of length of the beam Δx. It is located at a distance x from the apex of the conical mirror. Light scattered at x through an angle ϕ from the laser beam is incident on the conical mirror at radius R. The conical mirror has minimum and maximum radii of R_o and R_m. The combination of conical mirror and parabolic mirror results in the following relationships:

$$\Delta\phi = \frac{2r}{f_o} \tag{3.12}$$

$$\rho_{mx} = \frac{r}{f_o} R_x \cot 55^\circ \tag{3.13}$$

where $\Delta\phi$ is the element of phase function, evaluated from the x axis, which contributes to the signal and ρ_{mx} is the maximum radius about the x axis which can contributed to the signal. When ρ_{mx} of Equation 3.13 is greater than ρ, the beam radius, the power scattered to the detector from Δx, $p_{\Delta x}$, is given by

$$p_{\Delta x} = P_o \sigma \Phi(55^\circ) \left\{ 2\pi \Delta\phi \right\} \Delta x \tag{3.14}$$

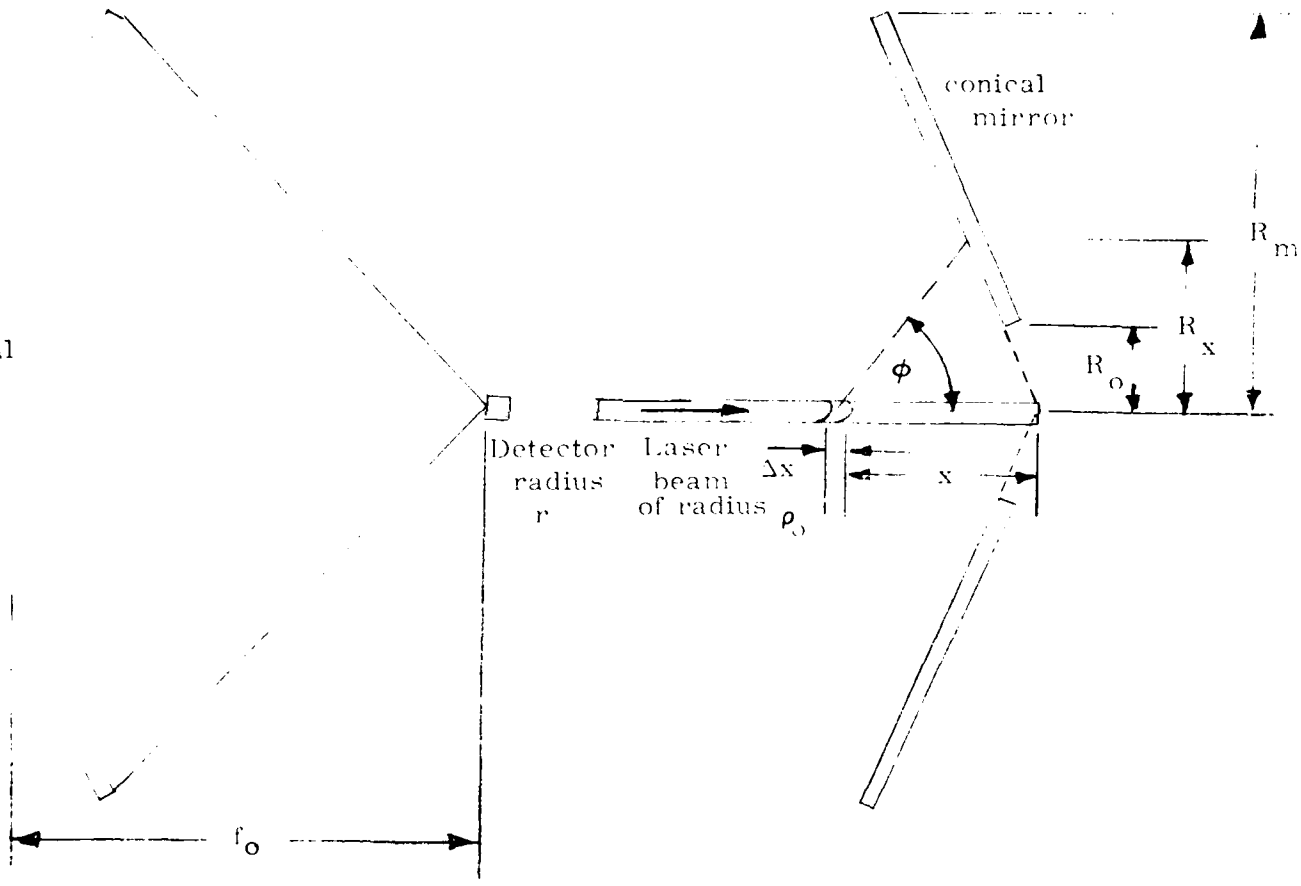

Figure 3.4. Simplified Instrument Layout.

Here $2\pi\,\Delta\varphi$ is the solid angle subtended by the collecting system. Since $\Phi(55°) = 1/4\,\pi$ and, by Equation 3.12 $\Delta\varphi = 2r/f_o$ then

$$p_{\Delta x} = P_o\,\sigma\,\frac{r}{f_o}\,\Delta x \tag{3.15}$$

The total signal p is made up of contributions from $x_o = R_o \cot 55°$ to $x_m = R_m \cot 55°$. If $\rho_{mx} \geq \rho$ at $x = x_o$ the $\rho_{mx} \geq \rho$ for all values of x between x_o and x_m. This requires that

$$\rho_{mx_o} = \frac{r}{f_o}\,R_o \cot 55° \geq \rho \tag{3.16}$$

or

$$r \geq \frac{f_o\,\rho}{R_o}\,\tan 55° \tag{3.17}$$

When this is true

$$p = T_o\,P_o\,\sigma\,\frac{r}{f_o}\,(R - R_o)\cot 55° \tag{3.18}$$

A value for the system transmission, T_o, has been added to cover reflection *losses, etc.*

When Equation 3.17 holds then p, the power to the detector, is proportional to r, the detector radius. The noise equivalent power of the detector and the statistical noise of the background are also proportional to r, so that in most cases the signal to noise ratio is independent of r as long as Equation 3.17 holds. This is not true for the noise due to photon statistics of the signal. For $\rho_{mx_o} > \rho$ such noise is proportional to $\sqrt{r}$ but in all cases considered here the noise due to signal statistics is negligibly small compared to the other noise sources.

In what follows signal to noise ratios will be calculated using a single baxicon optical system and detector with lasers and filters necessary for measurements at or near wavelengths 1μ, 3μ, and 10μ. The characteristics of a pyroelectric detector are used here for calculations. If the observing time is t seconds, then the noise equivalent power, NEP, of a typical pyroelectric detector used in a system involving synchronous rectification at 30 Hz and signal integration time of 100 seconds is

$$NEP = 10^{-9} (2\pi t)^{-1/2} \; r \text{ Watts}$$

$$= 4 \times 10^{-11} \; r \quad \text{Watts} \tag{3.19}$$

At 10μ the detector noise as evaluated with a 300 °K background is dominant so the system NEP ($30,\ 1.6 \times 10^{-3}$) is determined by the detector. The rms value of the fundamental component of the chopped signal is

$$p_{rms} = \frac{\sqrt{2}}{2\pi} \; p$$

where p is given by equation 3.3.6. The signal to noise ratio for a 100 second observation is

$$S/N = 9.8 \times 10^{9} \; P_o \; T_o \; \sigma \; (R-R_o)/f_o \tag{3.20}$$

Reasonable values for T_o and $(R-R_o)/f_o$ are 0.5 and 0.75 respectively. To obtain S/N = 5 the following must hold:

$$P_o = 1.36 \times 10^{-9} \; \sigma^{-1} \tag{3.21}$$

The minimum desired value of σ at 10μ is taken as $\sigma = 5 \times 10^{-9}$ cm^{-1} (AFGL Tropospheric Aerosol Model, Ref. 38, extrapolated to 50 km visual range), thus

$$P_o \approx 1/3 \text{ Watts} \tag{3.22}$$

Similar calculations are made for $\lambda = 3\mu$ and $\lambda = 1\mu$. In these cases it is assumed that an optical filter is used as shown in Figure 3.3. Table 3.1 presents background noise calculations assuming that the system essentially views a white surface irradiated by the sun on its normal. This very conservative calculation shows that the background noise in such a system is less than the inherent pyroelectric detector noise. No additional refinement of background suppression is required. The laser powers required at 3μ and 1μ can be calculated in the same way as above for 10μ. Results are shown in Table 3.2.

Inspection of Table 3.2 indicates that the requirements for measurement of the scattering coefficient can be met using the baxicon concept. Calculations have involved laser sources. Efforts to devise a single baxicon system for the wavelength regions of interest using black bodies or special lamps have failed at 10μ for lack of adequate signal to noise ratio and have been borderline at 3μ.

We conclude that the required sensitivities for measurements of scattering coefficients can be achieved using the baxicon principle and laser sources. The assumption that $\Phi\ (55°) = 1/4\pi$ at the wavelengths 1.3μ to 10μ is weak and should be reviewed if a Baxicon system is given serious consideration.

3.5 The Extinctiometer

The extinctiometer has been designed to measure the extinction coefficient of the aerosols in the free atmosphere. Measurements are to be made in three wavelength bands centering on 1μ, 3μ and 10μ. The design principles discussed in this section involve a single black-body used as source for the three wavelength bands, a single optical system, except for the filters used to isolate the wavelength bands, and a single pair of radiation detectors. It is important to note that the extinction measurement is not to include molecular scattering or absorption.

The following discussion follows the arguments used in the HSS proposal, part of which appears as Appendix A. The minimum values of

Table 3.1. Background Noise Calculations for a Baxicon Nephelometer

Wavelength (μ)	Spectral Radiance of Solar Irradiated Matt Surface ($W\ cm^{-2}\ \mu^{-1} sr^{-1}$)	Filter Band Pass (μ)	No. Photons on 1 sq cm Detector (Note 1)	Noise Equivalent Power (Note 2) (Watts/$\sqrt{Hz}$)
10	7.3×10^{-6}	1.0	6.5×10^{14}	1.27×10^{-12}
3	8.37×10^{-4}	0.05	1.12×10^{15}	5.56×10^{-12}
1	2.36×10^{-2}	0.005	1.05×10^{15}	1.5×10^{-11}

Pyroelectric Detector NEP = 10^{-9} ($\Delta f = 1$, area = 1 cm^2)

Note (1): For an optical system with relative aperture of f/0.5 and a transmittance of 0.50 and one second of chopped observation time.

Note (2): To be compared with the Pyroelectric Detector NEP of 10^{-9} W/$\sqrt{Hz}$ (f = 10 Hz, Area = 1 cm^2)

Table 3.2. Laser Power Requirements in a Baxicon Nephelometer Needed to Measure the Indicated Values of Scattering Coefficients.

Wavelength (μ)	Scattering Coefficient (cm^{-1})	Power Requirement (Note 1) (Watts)
10	5×10^{-9}	3.35×10^{-1}
3	2×10^{-8}	8.3×10^{-2}
1	3×10^{-7}	5.5×10^{-3}

Note 1: An observation time of 100 sec is assumed for measurements at each wavelength; also a S/N ratio of 5 is assumed in the calculation.

extinction coefficient, γ , which are of interest at the three wavelengths are:

$$\gamma_{10} \quad 1.5 \times 10^{-8} \text{ cm}^{-1} \text{ at } \lambda = 10\mu$$
$$\gamma_{3} = 3 \times 10^{-8} \text{ cm}^{-1} \text{ at } \lambda = 3\mu \qquad (3.23)$$
$$\gamma_{1} = 3 \times 10^{-7} \text{ cm}^{-1} \text{ at } \lambda = 1\mu$$

The error in γ , $\Delta\gamma$, is to be less than 20 per cent of γ . That is:

$$\left| \frac{\Delta\gamma}{\gamma} \right| < 0.2 \qquad (3.24)$$

The design principles of the instrument are illustrated in Figure 3.5. In the instrument light travels alternately along two similar paths. Choice of path is determined by the angular position of a rotating sectored-mirror. The two paths are recombined by a beam splitting mirror so that a detector behind the beam splitter receives light alternately from the two paths. Any difference in the power transmitted by the two paths will result in an AC component in the detector output with frequency equal to that of the chopper and amplitude equal to the power difference. With such a set-up the transmission of a sample can be measured by introducing it into one beam and measuring the change in the AC current and the value of the DC current. A more accurate measurement results if the measurement is made with the sample in one beam and again with the sample in the other beam. The ambient air sample is assumed to contain both aerosol and molecular attenuators. In the upper sketch of Figure 3.5 the sample is in path B. Path A, which passes through the open ended container, is free of aerosols because the container is fed filtered air. The molecular composition of the two paths is assumed to be the same. As a second step in the measurement, the open-ended container is moved from path A to path B. A sample path length of 50 cm is assumed.

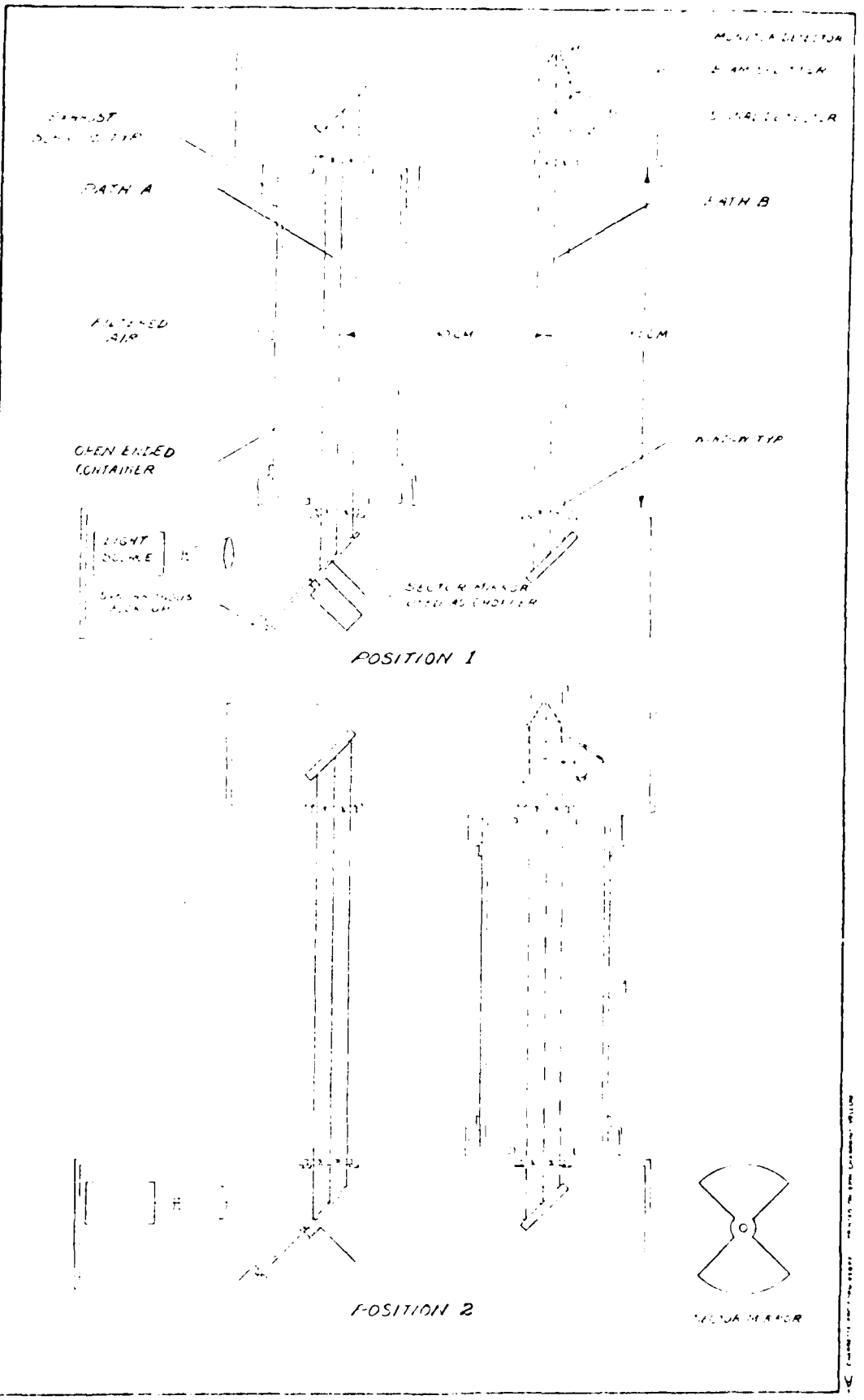

Figure 3.5. Illustration of Design Principles of Instrument.

If P_o is the radiant power projected by a perfect source system, then, when the sector mirror is completely in the projected beam, some fraction of P_o reaches the detector by path A. Let that fraction be AP_o. When the sectored mirror is completely out of the beam then some fraction of P_o, BP_o, reaches the detector. If the mirror sectors and the open sectors are equal in angular extent, then the average power incident on the detector, $\bar{p}$, is

$$\bar{p} = P_o \left(\frac{A + B}{2} \right) \tag{3.25}$$

Then the power p(t) incident on the detector may be written

$$p(t) = \bar{p} \pm \frac{|A-B| P_o}{\pi} \cos(2\pi ft) \tag{3.26}$$

where f is the frequency of chopping.

The term $\frac{|A-B| P_o}{\pi} \cos(2\pi ft)$ is the fundamental component which has an *rms value of*

$$p_{rms} = \frac{\sqrt{2}}{2\pi} (A-B) P_o \tag{3.27}$$

When a sample of length L and extinction coefficient γ is introduced in path A, the power incident on the detector becomes

$$p(t)_A = P_o \left(\frac{A e^{-\gamma L} + B}{2} \right) + \frac{(A e^{-\gamma L} - B) P_o}{\pi} \cos(2\pi ft) \tag{3.28}$$

and

$$P_{rms\,A} = \frac{\sqrt{2}}{2\pi} (A e^{-\gamma L} - B) P_o \tag{3.29}$$

With the sample in path B

$$p_{rms\ B} = \frac{\sqrt{2}}{2\pi} (A - B e^{-\gamma l_s}) P_o \tag{3.30}$$

If the rms detector output signal at frequency f is V_{rms}, then in general

$$V_{rms} = R_f\ p_{rms} \tag{3.31}$$

where R_f is the detector responsivity at frequency f (and at the wavelength of the incident power). The two signals $V_{rms\ A}$ and $V_{rms\ B}$ corresponding to the sample being in path A and again in path B are

$$V_{rms\ A} = R_f \left\{ \frac{\sqrt{2}}{2\pi} (A e^{-\gamma l_s} - B) P_o \right\} \tag{3.32}$$

and

$$V_{rms\ B} = R_f \left\{ \frac{\sqrt{2}}{2\pi} (A - B e^{-\gamma l_s}) P_o \right\} \tag{3.33}$$

The quantity $V_{rms\ B} - B_{rms\ A}$ is just

$$V_{rms\ B} - V_{rms\ A} = \frac{\sqrt{2}}{2\pi} P_o R_f (A+B) (1 - e^{-\gamma l_s}) \tag{3.34}$$

In the cases of interest here $\epsilon l_s << 1$ so

$$\frac{\sqrt{2}\,\pi\ (V_{rms\ B} - V_{rms\ A})}{P_o R_f (A+B)} = \gamma l_s \tag{3.35}$$

The incident DC power is

$$P_o \left(\frac{A e^{-\gamma l_s} + B}{2} \right) \text{or} \quad P_o \left(\frac{A + B e^{-\gamma l_s}}{2} \right)$$

and since $\epsilon l_s << 1$ we take the DC signal, V_{DC}, in either case to be

$$V_{DC} = R_o P_o \left(\frac{A + B}{2} \right) \tag{3.36}$$

where R_o is the DC responsivity of the detector used to measure the DC component of the incident poser.

Finally:

$$= \frac{\sqrt{2\pi}\, R_o}{2\, R_f} \quad \frac{V_{rms\ B} - V_{rms\ A}}{L\, V_{DC}} \tag{3.37}$$

There are two signals given by Equations 3.32 and 3.33 above. In each case the noise is determined by the NEP of the detector added statistically to the statistical variations in photon arrival rate. The NEP of the detector includes 300 °K radiation exchange noise between detector and background so at 10μ only the statistics of the signal photons need attention.

Figure 3.4 will be used to illustrate an idealized aerosol extinciometer operating in the vicinity of 10 microns. The distance between the projection lens near the source, and the collecting lens near the detectors is taken to be 90 cm. The diameter of each of these lenses is assumed to be 5 cm. If the source is black body at 1300 °K and the band pass of the filter is 8 to 12μ then the source radiance N in this wavelength interval is

$$N = 2.57 \times 10^{-1}\ W\ cm^{-2}\ sr^{-1} \tag{3.38}$$

The area of the collecting aperture is 19.6 cm^2 and the projecting aperture. The maximum value of P_o is thus

$$P_o = (2.57 \times 10^{-1}) \times (19.6) \times (2.42 \times 10^{-3})$$

$$P_o = 1.22 \times 10^{-2}\ \text{Watts} \tag{3.39}$$

before accounting for transmission losses.

An efficient way to achieve such projection is to use the projection optics to form an image of the source on the aperture of the collecting optics. If the projection optics have f-number of f/1 and aperture 5 cm and the collecting aperture is 5 cm diameter then the source must have diameter of 2.94 mm or greater. If the collecting optics are f/1 then the detector must have diameter of 2.94 mm or greater. A 3 mm diameter pyroelectric detector working with 30 Hz modulation of the input signal can have a noise equivalent power given by

$$NEP = 10^{-9} \text{ Watts, Hz}^{-1/2} \tag{3.40}$$

The rms noise power of the input signal due to photon statistics is calculated here. The path transmission values A and B are taken to be

$$A \approx B \approx 0.15 \tag{3.41}$$

Provision is to be made to balance the two paths so that

$$\left| A - B \right| \leq 10^{-3} \left(\frac{A + B}{2} \right) \tag{3.42}$$

Under these conditions the DC term of the input power is

$$P_o = \left(\frac{A + B}{2} \right) P_o = 0.15 P_o = 1.83 \times 10^{-3} \text{ Watts} \tag{3.43}$$

The associated noise power Δp_{rms} is 1.5×10^{-11} Watts, Hz^{-1} (3.44)

This is small compared to the detector NEP (Equation 3.40) so the signal to noise ratio may be calculated using the detector NEP.

For purposes of calculating signal-to-noise ratios we take the rms power incident at the modulation frequency to be

$$S = \frac{\sqrt{2}}{2\pi}(.15\ P_o)\left(\frac{A+B}{2}\right)\gamma L \tag{3.45}$$

and with $\gamma = 1.5 \times 10^{-8}$ cm^{-1} and $L = 50$ cm

$$S = 3 \times 10^{-10} \text{ Watts} \tag{3.46}$$

If the observing time is 5 minutes the effective band pass of a synchronous rectifier is 5.3×10^{-4} Hz and the system NEP becomes 2.3×10^{-11} Watts. The resulting signal to noise ratio is

$$S/N = 13 \tag{3.47}$$

Similar calculations have been made for wavelength pass bands at 3μ and $1\ \mu$. The results are summarized in Table 3.3. It is evident that the extinctiometer can meet the requirements of this study.

3.6 Conclusions

The spectrophone described here might measure absorption coefficients of interest to this study. It requires a different pulsed laser for each wavelength investigated. Methods for separation of aerosol absorption from molecular absorption have not been investigated.

The required scattering coefficient measurements can be made with the baxicon. It uses three different modulated lasers. There is no problem in separating out the molecular scattering. Several baxicons have been built and operated. The instrument described here is feasible.

Table 3.3 System Characteristics with 1300 °K Black Body and 3mm Diameter Pyroelectric Detector. Observing Time at Each Wavelength is Five Minutes.

Wavelength, microns	γ, km^{-1}	p_o, Watts	Δp_{rms} W, Hz^{-1}	S, Watts	S/N (5 min)
8-12	1.5×10^{-3}	1.83×10^{-3}	1.5×10^{-11}	3×10^{-10}	13
3-4	3×10^{-3}	7.12×10^{-3}	5.4×10^{-11}	2.3×10^{-9}	100
1-1.1	3×10^{-2}	1.76×10^{-4}	1.48×10^{-11}	5.8×10^{-10}	25

Where:

γ = Extinction coefficient assigned to band

p_o = average power incident on detector

Δp_{rms} = rms photon noise (note Detector NEP = 10^{-9} W $Hz^{-1/2}$

S = rms value of fundamental component of modulated input power to detector

S/N = signal to noise ratio anticipated with 5 min observing time.

The extinctiometer performs a measurement of the aerosol which is the most direct of all the measurement approaches discussed here. It uses a single black or gray body as source. The HSS extinctiometer design also separates aerosol extinction from molecular extinction. Signal-to-noise calculations suggest that such a machine might work. The design requires that a change in path transmission of one part in a million be measurable with signal-to-noise of 10 or so. This places exacting requirements on the design and fabrication of the instrument.

The contract supporting this work calls for recommendation of a technique for measuring extinction or for measuring scattering and absorption. We recommend the extinctiometer as a technique for measuring extinction.

4. EXPERIMENTAL PROGRAM

4.1 Introduction

In the preceding sections of this report investigations are described in which all candidate methods for determining infrared atmospheric aerosol exinction coefficients were reviewed. These investigations reached the conclusion that an extinctiometer was the most promising of the candidate instruments for satisfying the AFGL performance objectives at this time, having assessed the current technological state-of-the-art in the alternate approaches.

Upon completion of the investigations by HSS Inc AFGL was advised of the conclusions which had been reached. While recommending the extinctiometer approach HSS Inc advised that certain feasibility experiments be performed prior to entering into the design phase of an extinctiometer. Experiments were envisioned which would resolve whether there were any fundamental physical limitations to the extinctiometer approach.

An extinctiometer measures the amount of power extracted from a beam of radiation (as distinct from a transmissometer which measures the amount of power remaining in the beam). The AFGL performance objectives require that atmospheric aerosol extinction be measured at the extreme conditions of 50 kilometer visibility and 5 kilometer altitude. This requirement translates into an extinction (in two of the spectral regions of interest) of 15 parts per 10^8 of beam power for a measurement pathlength of 10 centimeters; or 15 parts per 10^7 for a one meter pathlength. These requirements are analogous to the measurement of one mile to an accuracy of 0.01 inch or 0.1 inch respectively for the two situations just described. Such requirements are extremely severe when considered in terms of conventional radiometric measurements.

The particular extinctiometer approach recommended by HSS Inc is believed to be a unique combination of four features which together provide necessary capability to perform aerosol extinction measurements over the extreme range of conditions specified by AFGL. The four features which are married in the HSS Inc extinctiometer approach are: (1) a dual-path radiometer with a single detector in which ambient aerosols and filtered air are interchanged periodically between sample volumes in the two paths; (2) a differential detector which responds only to differences in the radiation received from the two paths; (3) a method for balancing the radiative power in the two paths to a high degree of precision; and (4) the manner in which measurements are processed to give a direct readout of ambient aerosol extinction while simultaneously eliminating any dependence on the internal transmission function of the instrument.

The first and last of these four features are analytic instrument practices about which no serious doubts arise and their incorporation into the design is straight forward (although filtering of the aerosols from ambient air without changing the molecular constituents in any way appears to be a challenging engineering task). However similar positive feelings could not be expressed regarding the second and the third basic features of the extinct-iometer. It was recognized by both AFGL & HSS Inc personnel that fundamental physical limitations may hide in these two features and that it was essential to conduct requirements to prove otherwise.

The issues which were to be addressed experimentally were reduced to the following two questions: (1) Can a balance of high precision be achieved between the radiant power in the two beams of the extinctiometer and (2) Will a differential detector (in this case a pyroelectric detector) maintain its weak-signal response characteristics in the presence of a strong DC-beam of radiation?

If the radiation in the two beams can be balanced to say 1 part

in 10^3 then the problem of measuring an AC signal of 15 parts in 10^7 (i.e. relative to the average DC power in the combined beams) is reduced to a problem of measuring a signal of 15 parts in 10^4, i.e.

$$\frac{15}{10^7} \times 10^3 = \frac{15}{10^4}$$

which places a much more reasonable requirement on a radiometric measurement system.

It was the intent of the experimental effort to investigate only the two questions stated above. However in the process of investigating these questions many unforeseen problem areas were uncovered. In solving each of these additional problems invaluable information was obtained, and techniques were evolved, all of which aided greatly in arriving at the final design of the extinctiometer.

4.2 Ideal Instrument Simulation

The first question to be addressed experimentally was that of the weak-signal response of a pyroelectric detector in the presence of a strong DC beam of radiation. To address this question required, in effect, that the ideal behavior of the extinctiometer be simulated. That simulation was achieved by the experimental set-up shown in Figure 4.1.

In this experimental set-up a tungsten ribbon-filament lamp and optical system were used to obtain a strong DC beam of radiation as shown in the figure. This beam was rendered incident on the pyroelectric detector by field lens L6 which images the aperture stop L3 onto the sensing element.

A weak square-wave unbalance-signal was generated by extracting a portion of the DC beam with a beam-splitter BS-1, passing it through a

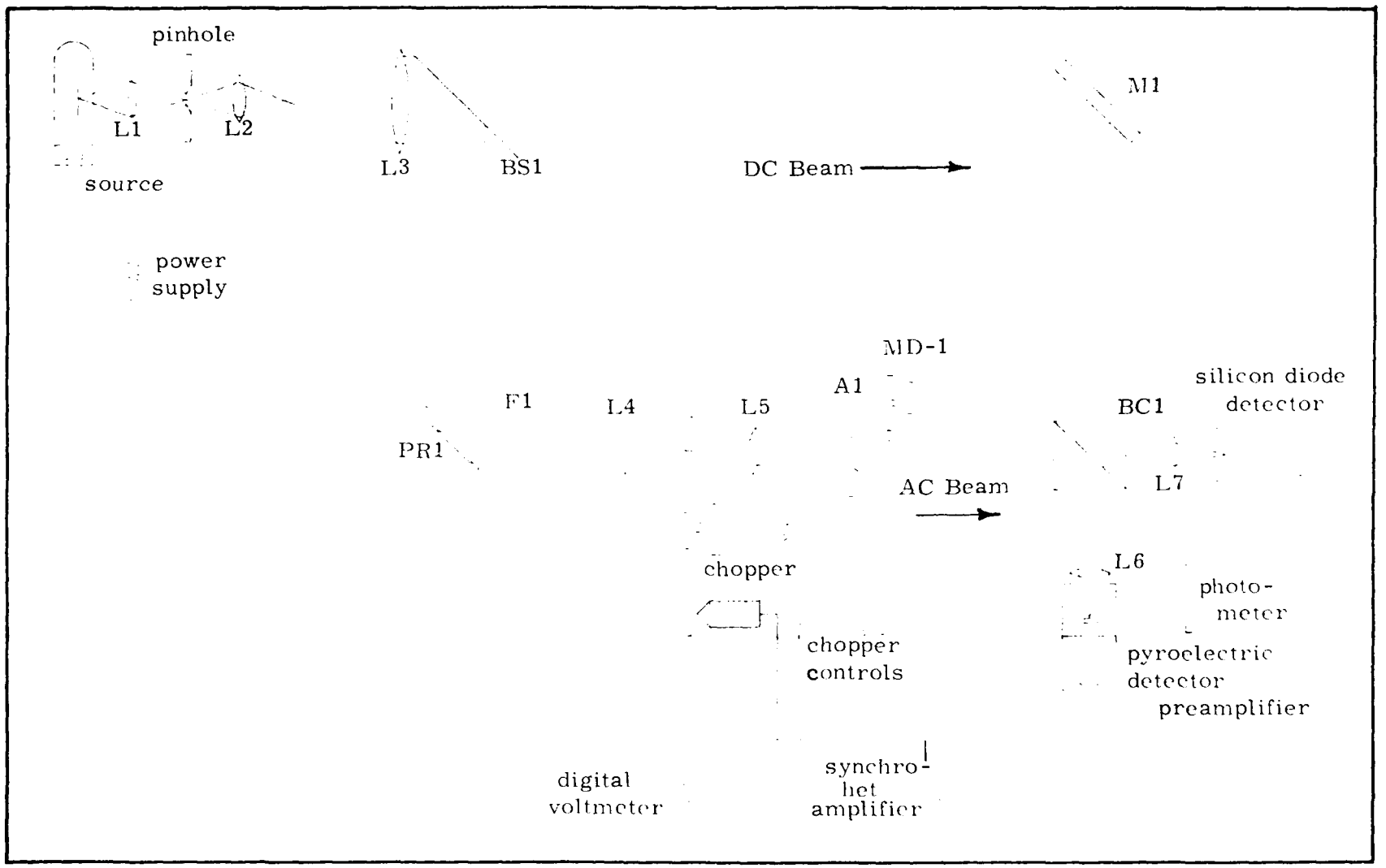

Figure 4.1. Experimental set-up to simulate an almost balanced, perfect-chopping reflective two-beam radiometer.

chopper wheel and recombining it with the DC beam by means of a beam-combiner cube BC1. The combination of the beam-splitter and choice of ND filters inserted at position F1 could provide fractional AC unbalance signal levels of 10^{-2}, 10^{-3}, 10^{-4} of the power in the DC beam.

The use of an interrupt-type of chopper wheel in the above manner simulated the performance of an essentially perfect reflective-chopper in a two-beam radiometer---in which latter case when the beams are re-combined any slight imbalance of power between the two beams is manifest as a weak square wave superimposed on a strong DC beam of radiation.

The pyroelectric detector and pre-amplifier were enclosed in a special housing constructed so as to minimize thermal drifts, microphonic coupling and EMI pick-up. The output of this unit was coupled to a Princeton Applied Research (PAR) Model 186 Synchro-Het Lock-In Amplifier.

The average power in the DC beam was monitored by a silicon detector coupled to a Tektronix Model J-16 Digital Photometer Readout Unit. Further details of the components used in the experimental set-up may be found in Table 4.1.

The AC imbalance signal which was generated in the manner described represents just what its name implies -- a simulation of the residual difference in power levels which remains after the splitting of a single beam of radiation by a reflective chopper wheel, passing the two beams along separate paths of differing transmission, and then the recombining of the two beams.

The actual weak-signal response to be investigated in the experimental set-up was the simulation of slight differences in transmission of the two paths of the extinctiometer. Differences in path transmission were simulated by inserting a fine wire into the AC beam (at MD-1 in Figure 4.1). The wire was mounted on the end of a micrometer screw so that more or

Table 4.1. Description of components used in Almost Balanced, Perfect Chopping Experimental Set-up.

ILLUMINATION SOURCE

SOURCE	G.E. type CG-101-AX Ribbon Filament Lamp, 2mm wide ribbon, rated 18 amperes at 6 volts
POWER SUPPLY	Trygon DC Power Supply, Model S36-20, continuously variable output to 20 amperes

OPTICAL SYSTEM

SYMBOL	COMPONENT	CHARACTERISTICS
L1	CONDENSING LENS	Melles Griot Model 01-CMP-009, 25 mm focal length, 25mm diameter, operated 1:1 conjugates.
P1	PINHOLE	1.5 mm diameter aperture
L2	RELAY LENS	B&F Enterprises, 1/2" focal length, 9/16" diameter aperture, operated at 1:2 conjugates
L3	PROJECTION LENS	Nikon, (f/n) = 2.8, 35 mm focal length, operated at conjugates s:s' = 167:700
BS1	BEAM SPLITTER	Eastman Kodak spectroscopic plateglass without emulsion 0.030" thick, 65 mm by 65 mm, uncoated
M1	MIRROR	100 mm by 100 mm by 12 mm thick front surface mirror, aluminum coated, no overcoat
BS2	BEAM SPLITTER CUBE	Two cemented 50 mm by 50 mm by 55 mm tall right angle prisms, 30 percent transmission, 30 percent reflectance, 40 percent absorption

Table 4.1 (Cont.) Description of Components used in Almost Balanced, Perfect Chopping Experimental Set-up.

SYMBOL	COMPONENT	CHARACTERISTICS
F1	FILTER	Metalic coated neutral density filters: ND-1, ND-2
PR1	MIRROR PRISM	Aluminized 25 mm by 25 mm right angle prism
L4	IMAGING LENS	Technor Projection Lens, f/1.5, 20 mm focal length
L5	PROJECTION LENS	Eastman Kodak Projection Lens, f/1.6, 32 mm focal length
A1	APERTURE	10 mm diameter
MD1	BEAM MODULATOR	1mm diameter rod supported on a micrometer screw and inserted into the AC beam a measured amount
L6	FIELD LENS	Canon, (f/n) = 1.4, 25 mm focal length
L7	FIELD LENS	Cooke Speed Panchro Lens, f/2., 35 mm focal length

ELECTRONIC MEASUREMENT SYSTEMS

BEAM CHOPPER	Laser Precision Corp., Model CTX-534, Radiation Chopper, mirror finish 2 blade chopper, or equivalent
PYROELECTRIC DETECTOR/ PREAMPLIFIER	HSS Inc design and manufacture, sensor 2 mm diameter pyroelectric, Eltec Model 404 VM-4
SYNCHRO-HET AMPLIFIER	Princeton Applied Research, Model 186, Synchro-Het Lock-in amplifier or equivalent

Table 4.1 (Cont.) Description of Components used in Almost Balanced, Perfect Chopping Experimental Set-up.

DIGITAL VOLTMETER	3 1/2 digit; Fluke 8020A, 4 1/2 digit; Model 2480 R(or equivalent) 5 1/2 digit; Fluke Model 8052 or equivalent
SILICON DIODE DETECTOR	HSS Inc design and manufacture; Silicon Photoconductive Cell UTC Model PIN-100, operated in photovoltaic mode.
PHOTOMETER	Tektronix, Model J16 Digital Photometer; 3 1/2 digit readout

less of the wire could be inserted into the beam. By using various size wires of known diameter, and using the fine motion provided by the micrometer screw, precise amounts of attenuation of the AC unbalance signal could be achieved. An attenuation as small as 10^{-3} of the AC beam power could be provided in this manner.

The first tests with the idealized instrument set-up were conducted with a randomly-polarized TEM_{oo}, 2 milliwatt, HeNe laser as the source of radiation. That source was quickly abandoned because of the poor stability in its power output and the inordinate amount of random power fluctuations in its output.

The second source which was tried was a G. E. ribbon-filament microscope illuminator lamp operated slightly under its ratings. This lamp also proved to have inherent noise characteristics associated with its radiant output, but was less noisy than the laser. Of all the lamp types which were investigated none were less noisy than this microscope illuminator lamp. Seven of the microscope illuminator lamps were tested in order to select the least noisy lamp. One lamp, initially quieter by a factor of ten than the other six, abruptly became equally as noisy after a short period of usage.

Several noise characteristics inherent in the microscope illuminator lamps were isolated and their possible origins identified, these are:

(1) A very large amplitide low-frequency (~1 Hz) periodic variation of the lamp output. Its origin is still a mystery after much effort to identify its source.

(2) Very low frequency drifts in the output of the lamp. The source of these drifts is believed to be ambient air motion near the lamp which cools the envelope; the envelope in turn cools the fill-gas of the lamp which in turn induces temperature and radiant output changes in the filament.

(3) Microphonic noise. Noise in the radiant power output could be induced by acoustic noise sources coupling both through the air and through the mount support structure.

(4) An underlying random noise present at all frequencies. This noise is believed to be generated at the contact points between the tungsten filament and its supports (tungsten filaments are invariably attached by a crimping process).

Noise from tungsten lamps was not unexpected. However, the magnitude of that noise was far more than anticipated.

Another problem which arose in the experimental set-up shown in Figure 4.1 was the presence of a false-signal which was 180 degrees out of phase with the true AC signal. The false-signal led to nonsensical outputs from the PAR Synchro-Het Amplifier at low AC signal levels.

The false signal had its origin in that portion of the DC beam which, through a combination of reflecting in the beam-combiner cube BC-1, was directed into the path of the AC beam but in a direction reverse from which the true AC signal was traveling. The spurious DC radiation was then reflected from the backside of the chopper blades, redirected to the beam-combiner cube, and thence to the detector. The false-signal problem was minimized by tilting of the chopper wheel so that the DC radiation impinging on the backside of the blades was not retro-reflected.

The Measurements performed with the idealized instrument set-up demonstrated a capability of detecting an AC-signal approximately equal to 10^{-6} of the DC power level. It was however concluded, without proof, that if a radiant source with a noise level equal to or less than the NEP of the detector had been used in the set-up, the goal of measuring an AC signal equivalent to 10^{-7} of the DC power level could have been reached.

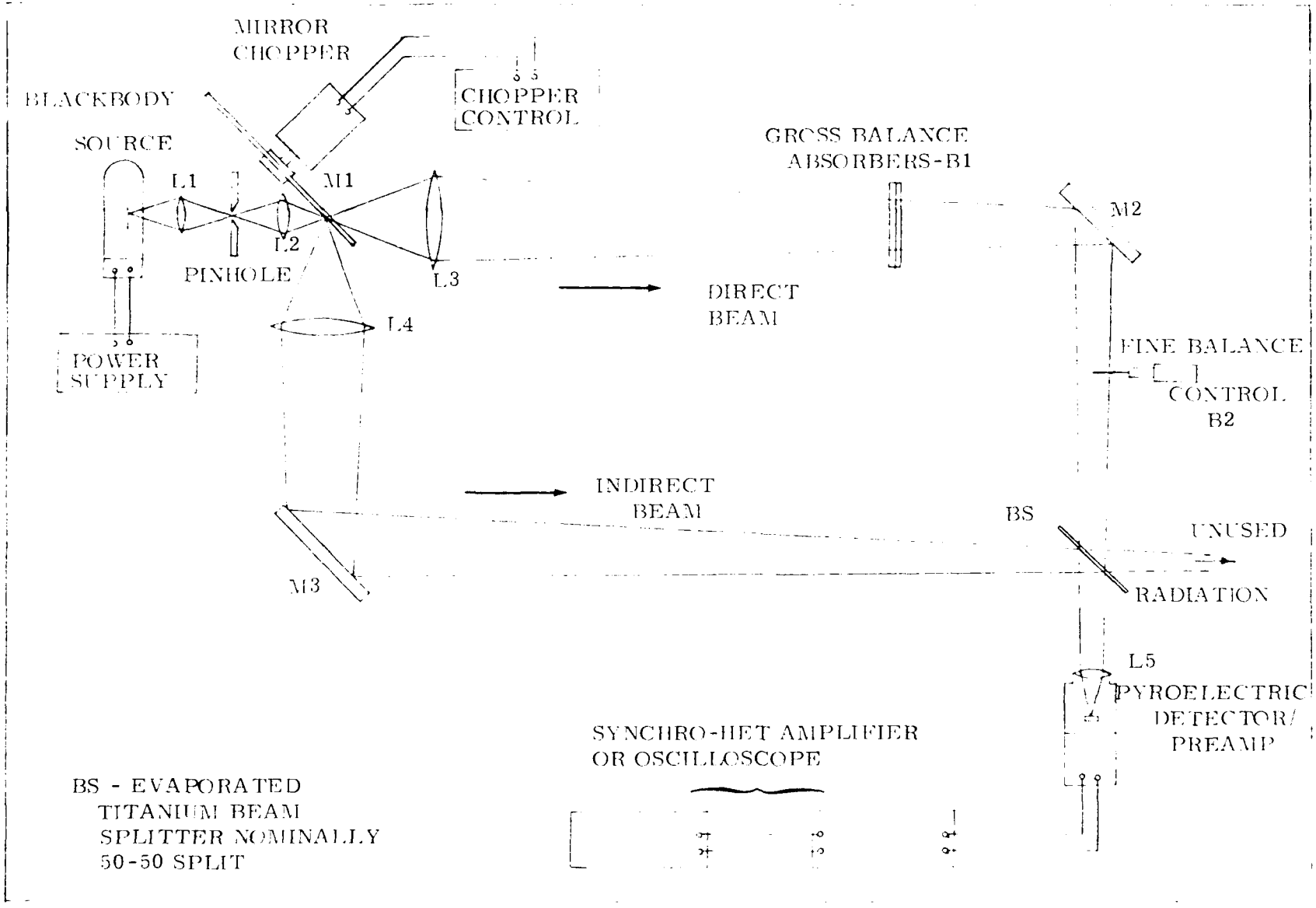

Figure 4.2. Schematic layout of the two-beam balance system with focal point chopping

4.3 A Two-Beam Balanced System

4.3.1 Focal Point Chopping

The second basic question to be addressed experimentally concerned the balancing of a two-beam radiometer system. In this system the second of the two beams originates at a reflective chopper wheel, the two beams are then directed along separate paths, recombined into a single beam and then imaged onto a pyroelectric detector. Figure 4.2 illustrates the experimental arrangement used to simulate the two-beam radiometer. In this arrangement the chopping occurs at a focal point of the system. Figure 4.3 shows two photographic views of the set-up and Table 4.2 provides a list of all the optical components used in the experiments. The source, detectors and electronic readout units were the same as those indicated in Table 4.1.

First attempts at achieving a balanced beam system utilized an interrupter-type chopper wheel which was hand-polished to a mirror finish. The wheel proved completely inadequate to the task. The best balance which could be achieved was such that the residual AC signal-power was one-tenth of the average power level. Invaluable experience was gained, however, since the deficiencies of the blade served to dictate the requirements for an improved chopper wheel.

All tests described here were preceded by a careful alignment of the optical components to insure both the sample and reference beams were imaged to the same point on the sensing surface of the detector, and that both images were of the same size. This precaution proved to be necessary since image-motion, or an alternation in image size between the chopped or direct beam on the pyroelectric sensing element, appeared to induce a second order signal effect in addition to the signal caused by the major defects of the chopper wheel.

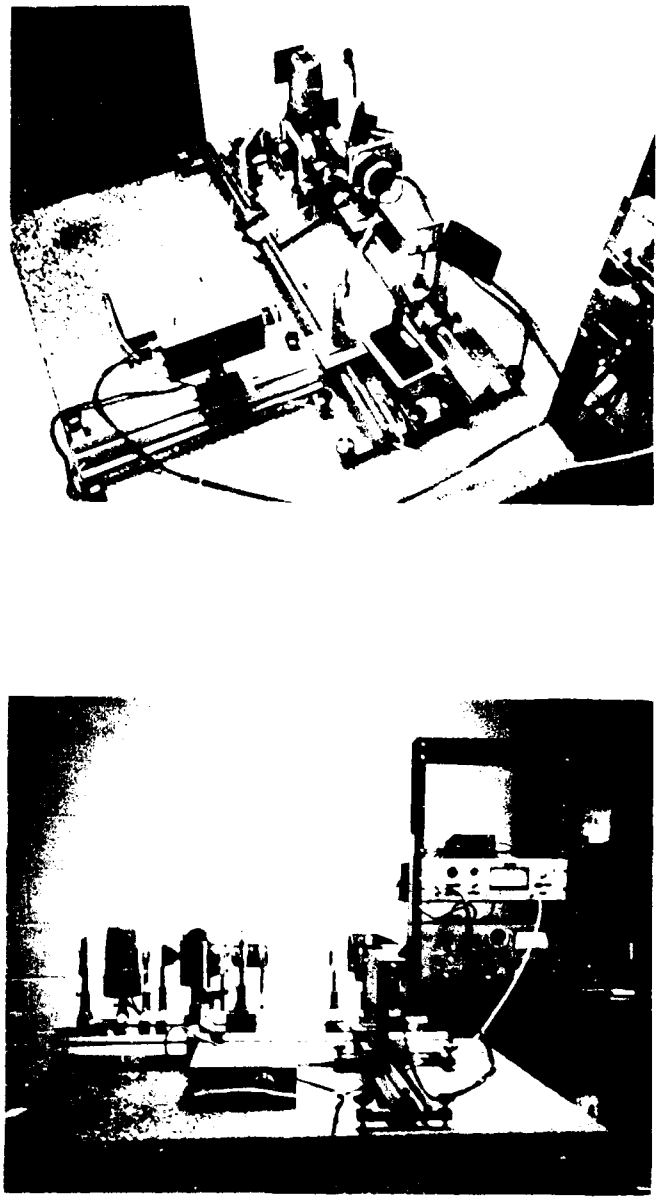

Figure 4.3. Two views of the two-beam balanced system with focal point chopping.

AD-A099 306 H S S INC BEDFORD MASS F/G 4/1
EVALUATION, FEASIBILITY, AND DESIGN OF A THREE-WAVELENGTH INFRA--ETC(U)
SEP 80 D F HANSEN, H S STEWART, C C PETTY F19628-79-C-0132
UNCLASSIFIED HSS-B-071 AFGL-TR-80-0323 NL

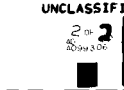

END
DATE FILMED
4-81
DTIC

Table 4.2. Description of Optical Components Used in the Balanced Two-Beam System.

OPTICAL SYSTEM

SYMBOL	COMPONENT	CHARACTERISTICS
L1	CONDENSING LENS	Melles Griot Model 01-CMP-009, 25mm focal length, 25 mm diameter, operated 1:1 conjugates.
P1	PINHOLE	1.5mm diameter aperture
L2	RELAY LENS	Eastman Kodak, 32mm focal length, f/1.6 projector lens.
L3, L4	PROJECTION LENS	Nikon, (f/n) = 2.8, 135mm focal length, operated at conjugates s:s' = 165:700
M1, M2	MIRROR	100mm by 100mm by 12mm thick front surface mirror, aluminum coated, no over-coat.
BS	BEAM SPLITTER	Evaporated titanium on 0.030" thick glass, 65mm x 65mm, nominally 0.5:0.5 split.
B1	GROSS BALANCE ABSORBERS	Several pieces uncoated glass.
B2	FINE BALANCE CONTROL	1.0mm diameter wire on micrometer screw.

The reflective chopper wheel which had been improvised from an interrupt-type of blade was replaced with a high quality reflective two-blade chopper wheel. An improvement by a factor ten in performance resulted from the use of this precision reflective chopper wheel. But despite all attempts the imbalance factor could not be improved beyond 10^{-2} when the beam was chopped at a focal point of the system. The results to that point gave some insights as to the primary and secondary causes of imbalance signals in a dual-beam radiometer system using a reflective chopper and a pyroelectric detector. These are as follows:

A. Primary Causes of Imbalance

1. Energy lost from the beam due to scattering by imperfect knife-edges on the chopper blades.

2. Non-uniform reflectance of the chopper blade.

B. Secondary Causes of Imbalance

1. Motion of the image from the reflected beam due to misalignment of optics.

2. Differences in image sizes on the detector between reflected and direct beams of radiation.

3. Motion of the image from the reflected beam due to wobble in the chopper wheel caused by an imperfect motor-shaft, shaft bearings, or hub seat.

4. Change in source-temperature/spectral-characteristics: This effect was significant in the test set-up because no spectral isolation was used and plane-glass attenuators were used to obtain gross adjustments of beam balance thus creating slightly different spectral transmission properties between the two beams.

4.3.2 Non-Focal Point Chopping

After the above series of beam-balance tests were performed it was concluded that chopping the beam where it has a significantly larger diameter than at a focal point might improve the performance. The rationale being somewhat obvious: if the primary cause of beam imbalance is the loss of radiation due to imperfect knife edges on the chopper blades then the effect may be reduced by simply chopping at a larger beam size. The effects of the blade edges should diminish inversely with the increase in beam diameter at the chopping point. The revised experimental set-up is shown in Figure 4.4 and in the accompanying photographs (Figure 4.5). In the set-up shown in these illustrations beam-chopping occurs at a point where the radiation bundle is only slightly less than the maximum bundle diameter.

This second beam-chopping arrangement improved the balance only slightly (a question would be a factor-of-two). As a result of this latter experiment we were forced to conclude that one or more of the secondary effects described in the preceding section had become a dominant signal-imbalance generating mechanism. In approaching the beam-balance problem it must at all times be remembered that a pyroelectric detector senses any change in the radiant power incident on it. It therefore is not a sufficient condition for a "balance" that equal amounts of energy arrive at the detector during each half of a chop cycle. If the rate at which the equal amounts of energy arrive were to change in any way during the cycle a signal will be induced. Further, a difference in position of the two images on the sensing element causes an imbalance signal to occur since the radiation is alternating between the two beams.

The conclusion reached from the two-beam balancing experiments

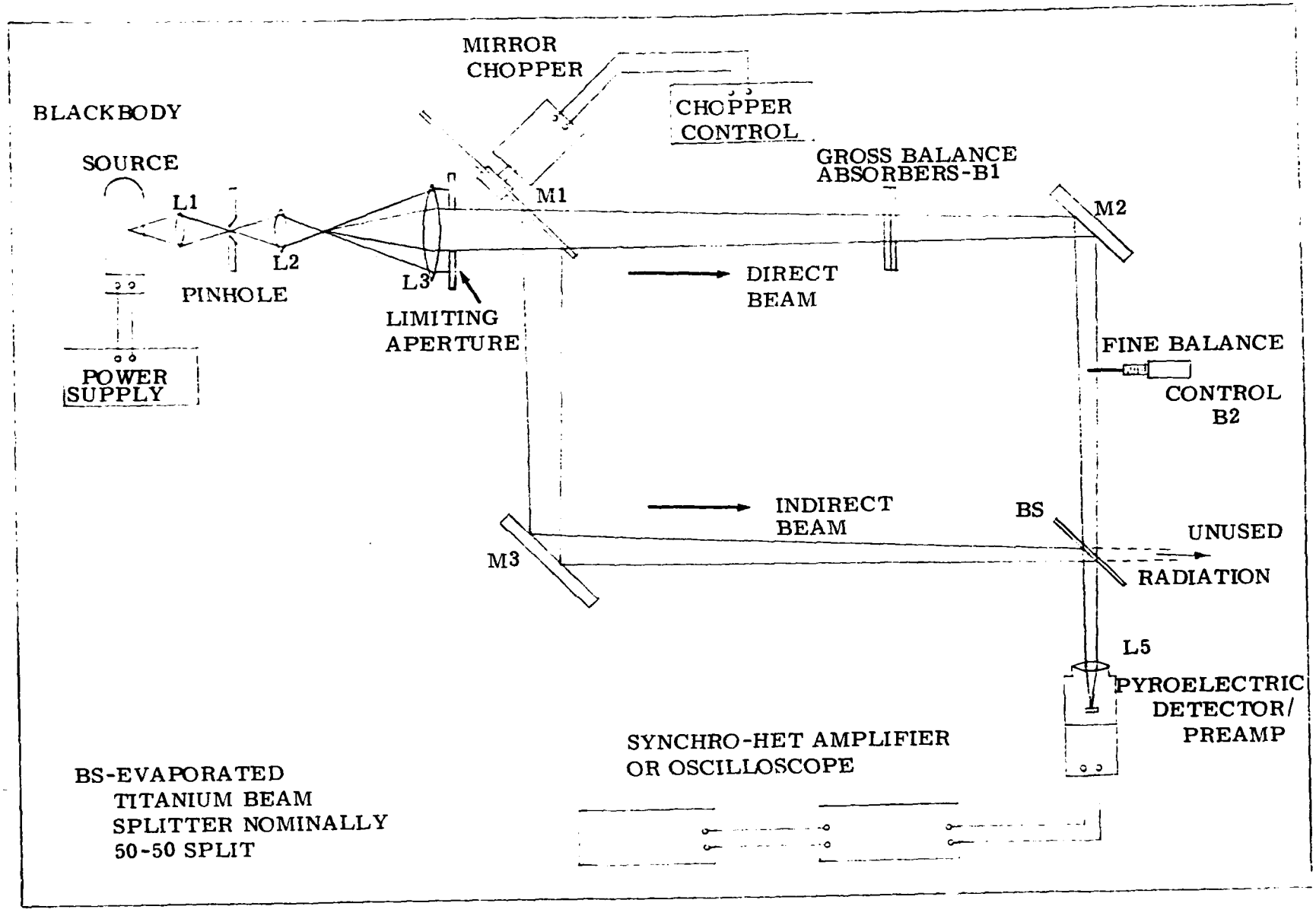

Figure 4.4. Schematic layout of the two-beam balanced system with non-focal point chopping.

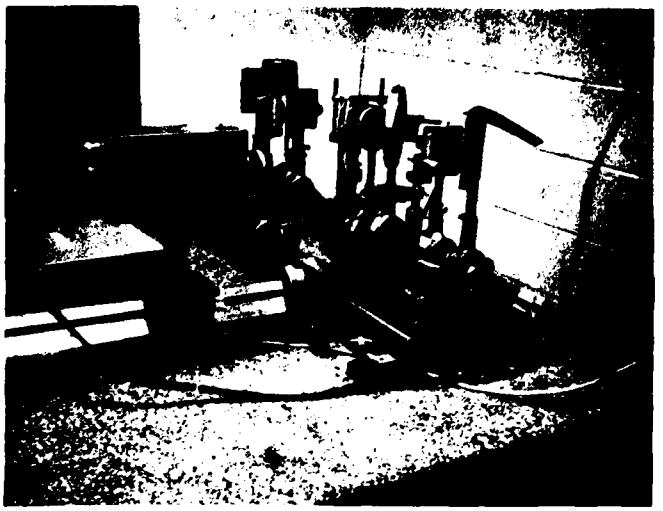

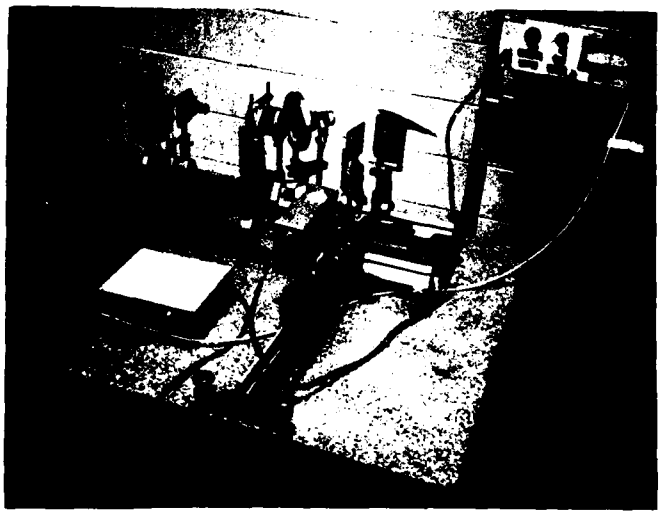

Figure 4.5. Two views of the two-beam balanced system with non-focal point chopping.

was the following: An imbalance signal as small as 10^{-3} of the average beam power is probably achievable provided the entire mechanism responsible for the beam chopping is engineered with sufficient precision to reduce the primary and secondary causes of beam-imbalance by exacting specifications. Again, this is not a proven conclusion, but results from the learning experience gained during the preceding sequence of experiments. It is also felt that an imbalance signal as small as 10^{-4} is probably beyond the present state-of-the-arts in reflective chopper wheels.

4.3.3 Reduction-To-Practice

While the two-beam experimental set-up shown in Figure 4.2 was still intact measurements were performed which were intended to fully demonstrate the principles involved in the HSS Inc extinctiometer concept and thus to constitute a reduction-to-practice for patent purposes. A black-body source was substituted for the microscope illuminator lamp.

Aerosol extinction was simulated first by placing a fine wire of known diameter first in one beam and then the other beam. Measurements were taken with the PAR Synchro-Het Amplifier. Recording times up to two minutes were employed. Applying the extinctiometer algorithm to these measurements (as outlined in Appendix A) the simulated extinction σL was determined. The measured extinction was shown to be in reasonable agreement with the value obtained by calculating the cross-sectional area of the beam removed by the wire.

As a further demonstration of the principle open cylinders were installed in each of the two beams. Cigarette smoke was introduced first into one beam then the other. The measurements which were then made were illustrative of the kind of extinction which might occur in a fog situation.

4.4 Noise Power Measurements

The ideal instrument simulation described in Section 4.2 was intended to address the question of whether weak signals could be detected by a pyroelectric detector in the presence of a strong DC beam of radiation. In the process of conducting that experiment it was found that standard sources of radiant power can be very noisy --- tungsten lamps and lasers in particular. In fact, source generated noise proved to be the ultimate limitation on the ability to measure weak signals in the presence of a strong DC beam of radiation. It thus became necessary to prove that a low-noise source of radiant power covering the spectral range from 1 to 12 microns was attainable in order to demonstrate that the extinctiometer approach was feasible.

The experimental set-up shown in Figure 4.2 was modified by replacing the microscope illuminator lamp by a blackbody cavity as the source of radiation and substituting a Nikkor-S, 50mm, f/1-4 lens for lens L1 in order to maximize the throughput of the new optical arrangement. The blackbody cavity was operated at a temperature of 1200 °C. The chopper was removed from the set-up and operated solely as a means to obtain a reference frequency for the PAR 186 Synchro-Het Amplifier. The "Noise Power" measurement feature of the PAR 186 was enabled, so that the RMS noise voltage in a 1 Hz band centered on the reference frequency could be measured. Measurements were then performed for a variety of frequency and DC radiant power levels.

DC radiant power levels were measured with a Laser Precision Radiometer Model RK-5100 using an RKP-545 pyroelectric detector probe. Power levels were varied by metallic neutral-density filters. The detector noise power output (NEP), for each combination of reference frequency and DC beam power incident on the detector, were determined from the customary

expression

$$NEP = \frac{V_{RMS}}{R} \tag{4.1}$$

where V_{RMS} is the measured noise voltage and R is the voltage responsivity of the detector. The voltage responsivity vs frequency of the particular pyroelectric detector used in these experiments was determined by an independent set of measurements and shown to be in close agreement with the published results of the manufacturer (ELTEC).

Table 4.3 presents the significant results of the noise power measurements. The results indicate that the optimum operating frequency is in the vicinity of 30 Hz. At that frequency the blackbody added very little noise power to the NEP of the detector.

Table 4.3. Noise Power Measurements Using a Blackbody Source and Pyroelectric Detector

Reference Frequency (Hz)	Unattenuated Blackbody		Blackbody +ND-1 Filter		Detector Capped-Off	
	Beam Power (mw)	NEP $W/\sqrt{Hz}$	Beam Power (mw)	NEP $W/\sqrt{Hz}$	Beam Power (mw)	NEP $W/\sqrt{Hz}$
10	0.76	6.7×10^{-10}	0.081	4.8×10^{-10}	0	4.5×10^{-10}
30	0.76	5.9×10^{-10}	0.081	5.3×10^{-10}	0	5.0×10^{-10}
90	0.76	4.0×10^{-9}	0.081	8.4×10^{-10}	0	7.6×10^{-10}

5. THE EXTINCTIOMETER DESIGN

5.1 Instrument Concept

Upon completion of the experiments described in the previous section (Section 4) the conceptual design of the extinctiometer was initiated. The design relied heavily on the results of those experiments and on previous applications' experience with pyroelectric detectors. Results of the foregoing experiments were also instrumental in setting the performance specifications for those components which are critical to the proper operation of the instrument.

The basic form of the instrument is that of a two beam-radiometer where the two beams alternate in passing through a sample volume of ambient air and a filtered volume of air. The two beams are created from a single beam by means of a reflective mirror-chopper-wheel. All-mirror imaging optics are required to accommodate the broad spectral range from 1 to 12 microns over which the instrument operates. A complete measurement cycle was taken to be 15 minutes in duration. Each cycle is devoted to measurements in three wavelength intervals; each of these intervals being of five minutes duration. A filter wheel is used to isolate the spectral region of interest. Calibration cycles are periodically interspersed with the measurement cycles.

A beam-recombiner is not used in the actual system because of the severe penalty which would be paid in the form of radiant power loss to the system if such a component were utilized, (combined with the severe polarization effects introduced from the use of high-index IR transmitting material which would be employed). Instead the beams are recombined in a manner which departs from conventional methods as shown in Figure 5.1. This figure is a schematic layout of the instrument and also serves to illustrate the principle features of the instrument. Details of the instrument design and the

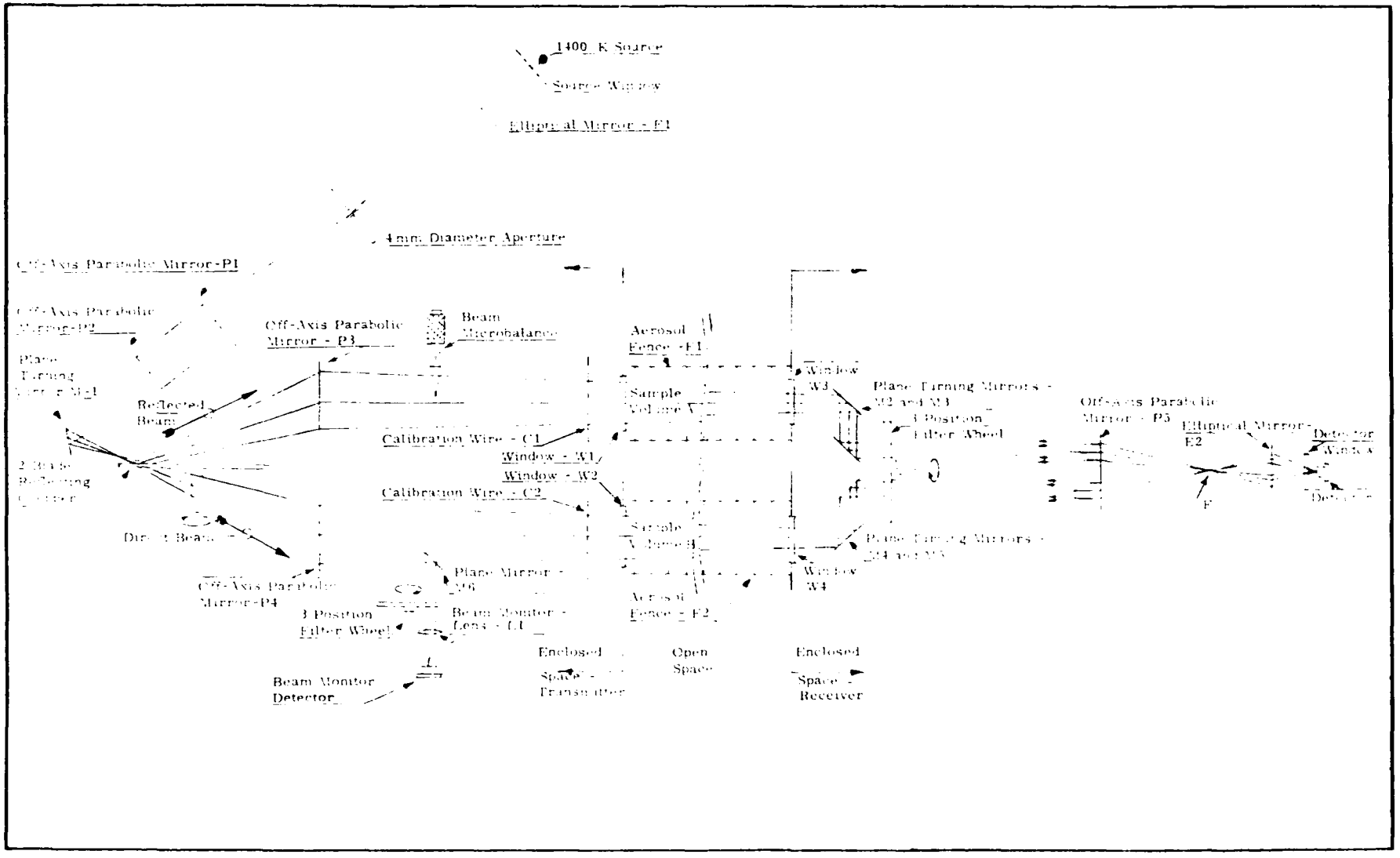

Figure 5.1. Schematic diagram of the optical system for the atmospheric aerosol extinctiometer.

specifications of all critical components are provided in Appendix B to this report. The design is treated in such detail in the appendix that only a brief outline of the design is given here.

5.2 Optical Layout

To achieve the performance objectives of the instrument requires a highly efficient optical system covering the wavelength region from 1 to 12 microns. Mirror optics are essential to achieving that goal. Coupled with the need for high efficiency is the need for the maximum possible relative aperture. A relative aperture of f/2 is believed to be realistically achievable and was chosen as a design goal for the optical system.

Transmitting optics (e.g. windows, beam-splitters and beam combiners) were held to a minimum. Operation over the wavelength range from 1 to 12 micron prohibits use of transmission-enhancement coatings on optical components. The use of transmission components would therefore, severely reduce the throughput of the system, especially since most broad-band infrared transmitting materials have high indices of refraction. Severe polarization effects can also be introduced by high index materials operating in situations where radiation is not normal to their surfaces.

A description of the optical system shown in Figure 5.1 is as follows: Radiation from a high temperature graybody source is imaged by elliptical mirror E1 onto a 4 millimeter diameter field stop at 2:1 conjugates transforming the f/2 collecting aperture into an f/4 bundle. A pair of off-axis parabolic mirrors P1 and P2 re-image the field stop at a point ahead of a rotating reflective chopper wheel. Radiation is alternately transmitted and reflected by the chopper wheel to a second pair of off-axis parabolic mirrors P3 and P4 which relay the (now two) images of the field stop onto a parabolic field mirror P5. In passing from mirror P3 and P4 to P5 the two beams

are required to transit the sample volumes A and B. Turning mirrors M2 - M5 lessen the separation between the two beams and by slight tilts direct the beams to P5 such that principal rays from the centers of the two mirrors P3 and P4 become axial rays allowing P5 to form coincident images of the two aperture stops P4 and P5 at image point F. A second elliptical mirror E2 then reimages the image point F onto the pyroelectric detector. The relative aperture of each bundle of radiation reaching the detector is f/2 and the geometric image is a circle 2 millimeters in diameter.

Reducing the separation between beams with mirrors M2 - M5 permits the use of a single field mirror P5 and permits the use of a single filter wheel for both beams. The filter wheel is located immediately after mirrors M3 and M5 in radiation bundles having minimum amounts of divergence.

Four windows W1 - W4 are necessary to provide environmental protection for the optical and electronic components housed in the transmitting and receiving enclosures. The windows must transmit radiation from 1 to 12 microns and be capable of withstanding environmental effects for a reasonably long period of time before resurfacing or replacing. ZnSe has been selected as the material most suitable for fulfilling these two requirements.

An optimization of the first-order optical system design given in Appendix B, using a computer optical design program, is required. Merit function, spot diagram and knife edge analysis must be used to provide: (1) component focal lengths and tolerances (2) the surface accuracy (figure) of each component (3) optimum conjugate distance relationships (4) additive effects of tolerances and surface accuracies on the overall system performance, and (5) chief ray behavior to prescribe sufficient clear apertures for each component and thus avoid any vignetting in the system.

5.3 Performance Analysis

The analysis of the measurement capability of the extinctiometer design shown in Figure 5.1 utilizes the extinction coefficient values given in Table 5.1. These values were deduced from the range of measurement parameters specified by AFGL. A performance objective of AFGL is that the instrument be capable of measuring the extinction coefficient to an accuracy of $\pm$ 20 percent or better over this entire range of values.

The error analysis developed in Appendix B derived an expression for the average thermal power M required at the detector in order to fulfill the AFGL accuracy requirement. That expression is

$$M = \frac{10^{-1}\,NEP}{\sqrt{2}\;\sigma(cm^{-1})} \quad \text{Watts} \qquad (5.1)$$

where the NEP of the detector is specified in watts/$\sqrt{Hz}$ and the units of the extinction coefficient are cm^{-1}.

A measurement pathlength of 50 centimeters was assumed in this derivation. For a pyroelectric detector whose NEP is 10^{-9} watts/$\sqrt{Hz}$ the flux values which must be achieved in each of the three channels in order meet the performance objective are given in Table 5.2.

Choosing realistic values for the instrument parameters as shown in Table 5.3, and for the efficiency of the optical system components as given in Table 5.4, the power incident on the detector for the extinctiometer design of Figure 5.1 may be calculated as outlined in Appendix B. These predicted values are given in Table 5.5 for each of the three wavelength channels; they are to be compared with the required flux levels as specified in Table 5.2.

TABLE 5.1. Wavelength Bands and Extreme Values of Atmospheric Attenuation Coefficients.

Wavelength Region (microns)	Wavelength Bandwidth (microns)	Largest Extinction Coefficient[1] (km^{-1})	Smallest Extinction Coefficient[2] (km^{-1})
0.98 - 1.08	0.1	20	.015
3-4	1	20	.0015
8-12	4	20	.0015

Note (1): The extinction coefficient for fog is taken to be that of Shettle and Fenn Advection Fog Model 2 for light to moderate advection fog; E. P. Shettle and R. W. Fenn, "Models for the Aerosols of the Lower Atmosphere and Effects of Humidity Variations on their Optical Properties", AFGL-TR-79-0214, 20 September 1979.

Note (2): The extinction coefficient for 50 kilometer visibility at 5 kilometer altitude was obtained by scaling of the AFGL Tropospheric Aerosol Model to these parameters.

Table 5.2. Flux Required at the Detector to Measure the Limiting Extinction Coefficients to an Accuracy of 20 percent

Channel No.	Mean Wavelength (μ)	Maximum Extinction Coefficient		Minimum Extinction Coefficient	
		σ (km^{-1})	Flux (μW)	σ (km^{-1})	Flux (μW)
1	1	20	.036	0.015	47
2	3.5	20	.036	0.0015	470
3	0.6	20	.036	0.0015	470

TABLE 5.3. Instrument Design Parameters.

GRAYBODY SOURCE:	
Temperature	1400 °K
Emissivity (1-12 μ)	0.9
PYROELECTRIC DETECTOR	
Diameter (Actual)	3 mm
Diameter (Effective)	**2 mm**
NEP (1-12 μ; 34 Hz; 1 Hz)	10^{-9} Watts/$\sqrt{\text{Hz}}$
OPTICAL SYSTEM	
Transmission (Each Beam)	0.21
Relative Aperture	f/2
CHOPPER WHEEL	
Chopping Frequency	34 Hz
Beam Imbalance	10^{-3}
MEASUREMENT TIME	
A-Beam (Ambient); B-Beam (Reference)	100 sec
A-Beam (Reference); B-Beam (Ambient)	100 sec
OPTICAL BANDWIDTHS	
Channel 1	0.98 - 1.08μ
Channel 2	3-4 μ
Channel 3	8-12μ
SAMPLE VOLUMES	
Pathlength	50 cm

Table 5.4. Efficiency of Optical System Components

	System Component	Material	Transmission or Reflectance	Percent Radiation Remaining
TRANSMITTER	Source Window	Unknown	1.00	1.00
	Ellipse No. 1	Air Coated	0.98	0.98
	Parabola No. 1	Air Coated	0.98	0.96
	Parabola No. 2	Air Coated	0.98	0.94
	Turning Mirror No. 1	Air Coated	0.98	0.92
	Beam Chopper	Air Coated	0.98	0.90
	Parabola No. 3	Air Coated	0.98	0.89
	Window No. 1	Zn Se	0.68	0.60
RECEIVER	Window No. 2	Zn Se	0.68	0.41
	Turning Mirror No. 2	Air Coated	0.98	0.40
	Turning Mirror No. 3	Air Coated	0.98	0.39
	Channel Filter	Various	0.70	0.28
	Parabola No. 4	Air Coated	0.98	0.27
	Ellipse No. 2	Air Coated	0.98	0.26
	Window No. 3	BaF_2	0.90	0.24
	Detector Window	BaF_2	0.90	0.21

This window may not be required

Table 5.5. Calculated Flux Available at the Detector in the Three Wavelength Intervals Using a 1400 °K Graybody Source.

Channel No.	Mean Wavelength λ (microns)	Band-width $\Delta\lambda$ (microns)	Spectral Radiance at λ ($W/cm^2.\mu.ster$)	Instrument Trans-mission	Flux at detector (λ) (μ Watts)
1	1	0.1	0.417	0.21	41
2	3.5	1.0	1.275	0.21	1240
3	10	4.0	0.0664	0.21	259

It can be concluded on the basis of a comparison of required and predicted flux levels that the average power requirements may be met in the case of the 1 micron and the 3-4 micron channels but not for the 8-12 micron channel. The thermal power falls short by a factor of 1.8 for the latter channel.

The failure to achieve the necessary thermal power in Channel 3 introduces a 36 percent error into the measurement of σ at the extreme limit of σ (i.e. .0015 km^{-1}) instead of the required 20 percent error.

Changes in the instrument design in order to achieve a 20 percent accuracy at the extreme limit for Channel 3 are considered impractical. Gross changes in the instrument design would have to be effected. For example, a graybody source temperature of 2100 °K could give the necessary thermal power, or an improved relative aperture of f/1.5 vs f/2.0 could also result in the necessary increase in power. But either of these options has size, weight or electrical power implications which should be avoided. Increasing the measurement time for Channel 3 by a factor of 3 could achieve the desired accuracy but would result in a violation of the requirement for performing the measurements in all three channels within a 15 minute time period.

5.4 Critical Components

If the performance goals of the extinctiometer are to be reached then particular attention must be given to those components and features of the instrument which are the limiting technological factors toward achieving those goals. We list here six areas where we believe that the specifications must be especially demanding, in some instances bordering on the state-of-the-art:

Optical System Design

Graybody Source

Primary Detector and Amplifiers

Reflective Chopper Wheel

Filter Wheel Assembly

Air Filter System

Each of these critical areas is discussed in Appendix B. In some instances detailed specifications of the components are provided. In the case of the Air Filter System an independent error analysis was required to determine how the measurements would be effected if the air filtering process were to change the amount of water vapor in the reference beam from the amount present in the ambient-air-sample beam. The results of that investigation are given in Appendix C.

REFERENCES

1. Nesti, A.J., Jr., "Instrumentation of Edgewood Arsenel Smoke Test Chamber", Final Report, General Electric Co., Ordnance Systems, Pittsfield, Mass., DDC Report AD B028002, (May, 1978).

2. Middleton, W.E.K., "Vision Through the Atmosphere", Univ. of Toronto Press (1952).

3. Stewart, H.S., Brouwer, W., Shuler, M.P., "Baxicon: An Efficient Fixed-Angle Nephelometer", Final Report, HSS Inc, Bedford, Mass (1974).

4. Winstanley, J.V., Adams, M.J., "Point Visibility Meter: A Forward Scatter Instrument for the Measurement of Aerosol Extinction Coefficient", Appl. Optics 14, (9), 2151, (1975).

5. Toropova, T.P., "Spectral Transparency and Scattering Indicatrices of Certain Turbid Media", Akademiya Nauk Kazakhskoy SSSR, Alma-Ata Trudy Astrophysicheskogo Instituta, Vol 18, In "Scattering and Absorption of Light in the Atmosphere", translated by U.S. Army Foreign Service and Technology Center (1973) DDC Report AD781013.

6. Gibson, F.W., "In-Situ Photometric Observations of Angular Scattering from Atmospheric Aerosols", Appl. Optics 15 (10), 2520 (1976).

7. Grams, G.W., Dascher, A.J., and Wyman, C.M., "Laser Polar Nephelometer for Airborne Measurements of Aerosol Optical Properties", Opt. Engineering 14 (1), 85 (1975).

8. Heintzenberg, J., and Quenzel, H., "Calculations on the Determination of the Scattering Coefficient of Turbid Air with Integrating Nephelometers", Atmos. Environ. 7 (5), 509 (1973).

9. Ruppersberg, G.H., "Ein Sichtmesser fur Luftfahrzeuge", Jahrbuch der Wissenschaftlichen Gesellschaft fur Luftfahrt, 321 (1954).

10. Ahlquist, N.C., and Charlson, R.J., "Measurement of the Wavelength Dependence of Atmospheric Extinction Due to Scatter", Atmos. Environ. 3, 551 (1969).

11. Diermendjian, D., "Electromagnetic Scattering on Spherical Polydispersions", Elsevier, N.Y. (1969).

12. Waggoner, A.P., Ahlquist, N.C., and Charlson, R.J., "Recent Developments in Nephelometers", in Proceedings of the Topical Meeting on Atmospheric Aerosols, Williamsburg, VA, Dec. 1976, NASA Report CP 2004.

13. Waggoner, A.P., and Charlson, R.J., "Aerosol Characteristics and Visibility", EPA Ecological Research Series, NTIS Report PB 269944 (1977).

14. Bodhaine, B., "The Mauna Loa Four Wavelength Nephelometer: Instrument Details and Three Years of Observation", NOAA Technical Report ERL 296 ARL-5, NTIS PB 284020 (1978).

15. Cutten, D.R., et al, "A Visibility Meter for Monitoring Atmospheric Aerosol Parameters", Atmos. Environ. 9, 253 (1975).

16. Golubitskii, B.M., "On Modifying an Integrating Nephelometer for Measuring Atmospheric Transmission", Soc. J. Opt. Technol. 43, (1976).

17. Bell, A.G., Proc. Am. Assoc. Adv. Sci. 29, 115 (1880).

18. Kerr, E.L. and Attwood, J. G., "The Laser Illuminated Spectrophone: A Method for Measurement of Weak Absorptivity in Gases at Laser Wavelengths", Appl. Optics 7, 915 (1968).

19. Schleusener, S.A., et al, "Differential Spectrophone Measurements of the Absorption of Laser Energy by Atmospheric Dust", Appl. Opt. 14 (11), 2564 (1975).

20. Schleusener, S.A., et al, "Spectrophone Measurements of IR Laser Energy Absorption by Atmospheric Dust", Appl. Opt. 15(10), 2546 (1976).

21. Bruce, C.W., "Development of Spectrophones for CW and Pulsed Radiation Sources", U. S. Army Electronics Command Technical Report 5802, DDC No. AD A025594 (1976).

22. Bruce, C.W., and Pinnick, R.B., "In-Situ Measurements of Aerosol Absorption with a Resonant CW Laser Spectrophone", Appl. Opt. 16 (7), 1762 (1977).

23. Terhune, R.W., and Anderson, J.E., "Spectrophone Measurements of the Absorption of Visible Light by Aerosols in the Atmosphere", Optics Letters 1(2), 70 (1977).

24. Kerker, M., et al, "Optical Properties of Cigarette Smoke Aerosols", Appl. Opt. 17 (19), 3030 (1978).

25. Crane, R. A., "Laser Optoacoustic Absorption for Various Explosive Vapors", Appl. Opt. 17 (13), 2097, (1978).

26. Nodov, E., "Optimization of Resonant Cell Design for Optoacoustic Gas Spectroscopy", Appl. Opt. 17(7), 1110 (1978).

27. Brewer, R.J., and Bruce, C.W., "Photoacoustic Spectroscopy of NH_z at the 9μm and 10μm CO_2 Laser Wavelengths", Appl. Opt. 17(23), 3746 (1978).

28. White, et al, "Water Vapor Continuum Absorption in the 3.5-4.0 μm Region", Appl. Opt. 17(17), 2718 (1978).

29. Peterson, J.C., et al, "Water Vapor-Nitrogen Absorption at CO_2 Laser Frequencies", Appl. Opt. 18(6), 834 (1979).

30. Schumate, et al, "Water Vapor Absorption of CO_2 Laser Radiation", Appl. Opt. 15(10), 2480 (1976).

31. Antipov, A.B., and Ponomarev, Y.N., "Investigation of Weak Absorption Lines of Gases with a Laser Spectrophone", Soc. Journ. Quantum Electron. 4(6), 740 (1974).

32. White, J.V., "Long Optical Paths of Large Aperture", Journ. Opt. Soc. Am. 32, 285 (1942).

33. White, J.V., "Very Long Optical Paths in Air", Journ. Opt. Soc. Am. 66(5), 411 (1976).

34. Gerber, H., "Feasibility of Shipboard Laser-Attenuation Measurements With a Portable Transmissometer", NRL Report 8290, Naval Research Lab., Washington, D.C., ADA067665, 26 February 1979.

35. Watkins, W.R., "Path Differencing: An Improvement to Multipath Absorption Cell Measurements", Appl. Opt. 15(1), 16 (1976).

36. Watkins, W.R., and Dixon, Richard G., "Automation of Long-Path Absorption Cell Measurements", U.S. Army R&D Technical Report: ECOM 5821, DDC No. AD041858.

37. Peterson, J.C., et al, Thomas, M.E., Nordstrom, R.J., Damon, E.K., and Long, R.K., "Water Vapor-Nitrogen Absorption at CO_2 Laser Frequencies", Appl. Optics 18(6), 834 (1979).

38. Shettle, E.P., and Fenn, R.W., "Models of the Atmospheric Aerosols and Their Optical Properties", Proceedings No. 183 on Optical Propagation in the Atmosphere, U.S. Dept. of Commerce, NTIS AD-A028 615, May 1976.

APPENDIX A

Excerpts from HSS Inc Proposal HSS-P-103;
4 April 1979; "Design Study of a Technique
for Measurement of Atmospheric Infrared
Aerosol Extinction"

APPENDIX A.

2. TECHNICAL APPROACH

2.1 The aerosol parameters used here to quantify the requirements of the Solicitation have been derived using "Models of the Atmospheric Aerosols and their Optical Properties" by E. P. Shettle and Robert W. Fenn.[A1] We have searched for a solution of the stated problem in the 8-12μm region of the spectrum believing this to be the most difficult. We have found an interesting possible solution for the 8-12μm region which seems to survive tests in the 3-5μm and the 1μm region. In addition, there seems to be some promise that the solution can meet the more stringent requirements imposed by battlefield conditions.

2.2 Here, then, in the Technical Approach, we outline a particular solution which meets analytic test but may challenge engineering state-of-the-art. What follows is a discussion of a specialized transmissometer.

2.3 The worst case is represented by the tropospheric model[1] (characteristic of 5 km altitude) and visibility of 50 km. At 10.6μm this predicts an aerosol extinction coefficient, σ, of about $1.5 \times 10^{-3} km^{-1}$. Accuracy of 20% implies an ability to measure to values of σ corresponding to $3 \times 10^{-4} km^{-1}$. The transmissometer to be described may have a measuring path of 0.5 meters, or optical depths of 7.5×10^{-7}. The accurace requirement implies an ability to read optical depth difference of 1.5×10^{-7}.

2.4 In discussions at Air Force Geophysical Laboratory on October 13, 1978 Vernon Turner, of that organization, addressed the problem of measuring aerosol extinction per se and described a possible measurement system of invariant geometrical parameters in which the path length through the aerosols in question could be varied. Honoring his concept but, we believe, making more practical the design principles involved, we have developed the following measurement plans:

2.4.1 The aerosol transmissometer involves two similar but not necessarily identical light paths, one through the ambient air and the other through ambient air from which the aerosols have been filtered. The container for the filtered air has open ends (as opposed to windowed) Figure A.1 is a sketch of such a transmissometer. At the top of the figure the first of two measuring positions is shown. In this position reasonably parallel light from the source is alternately directed along path A, through the filtered air container, or path B, through ambient air. Mirrors direct the light in the two paths to a beam-splitter so located that one-half of the light in both paths proceeds in the direction of beam A to the signal detector and one-half of the light in both paths goes in the direction of beam B to the monitor. The signal detector and its circuits are designed to measure the magnitude of the modulation of the incident radiation and the monitor is used to measure the magnitude of the carrier.

2.4.2 If P_o is the power projected by the light source then, in the absence of aerosol extinction, some fraction α would arrive at the detector via path A and some fraction β would arrive via B. If L is the length of the open ended container and σ is the aerosol extinction coefficient then the peak to peak modulation S_1 is given by

$$S_1 = \alpha P_o - \beta P_o e^{-\sigma L} \qquad (1)$$

When the container is moved to Position 2, as shown at the bottom of Figure 1 the peak to peak modulation S_2 is given by

$$S_2 = \alpha P_o e^{-\sigma L} - \beta P_o \qquad (2)$$

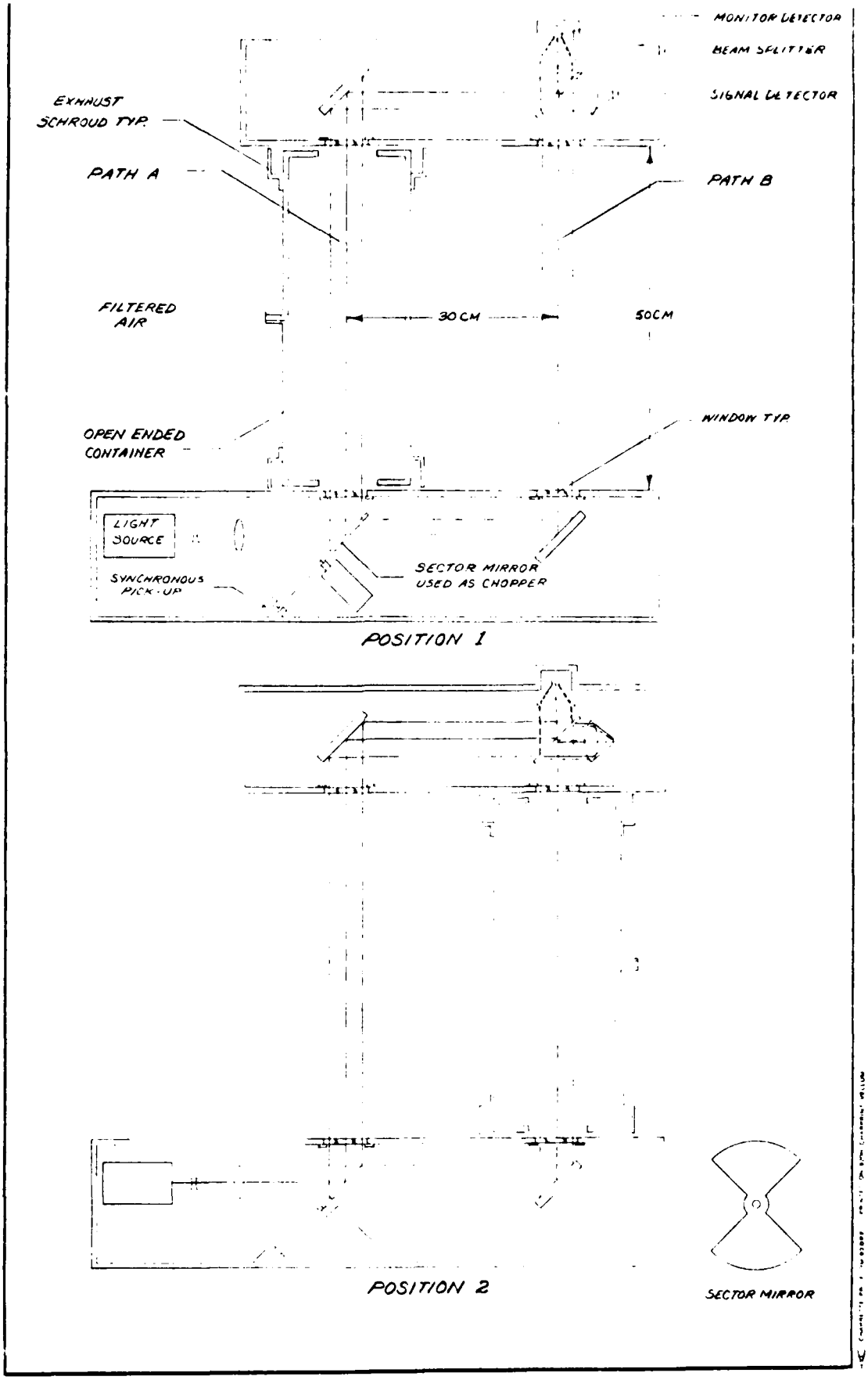

Figure A.1. Aerosol extinctiometer

It is assumed here that synchronous rectification is used in the modulation detector so that the signs (+ or -) of S_1 and S_2 are preserved. Now

$$S_2 - S_1 = (\alpha + \beta) P_o e^{-\sigma L} - P_o(\alpha+\beta) \tag{3}$$

If a good beam splitter is used (reflection equals transmission at 45° incidence) then the monitor signal M is

$$M = P_o \frac{(\alpha+\beta)}{2} \tag{4}$$

except for a correction of $e^{-\sigma L}$ in one or the other beam. Since $1-e^{-\sigma L} < 10^{-4}$ for all cases of interest this correction may be neglected and

$$\sigma L \approx 1 - e^{-\sigma L} = \frac{S_1 - S_2}{2M}$$

or

$$\sigma = \frac{S_1 - S_2}{2\,LM} \tag{5}$$

2.5 We consider this to be a significant result in that values of $1-e^{-\sigma L} = 10^{-6}$ or so can be measured with reasonable (± 20 %) accuracy even though source power, monitor detector sensitivity and signal detector sensitivity all wander between measurement sequences as much as ± 5 % or so. In addition the optical efficiencies of path A and path B need not be known and can change from one set up to another or, indeed, from one measurement sequence to the next, without introducing errors in the values obtained of σL.

REFERENCES

A 1. E. P. Shettle & R. W. Fenn, "Models of the Atmospheric Aerosols and Their Optical Properties", Proceedings No. 183 on Optical Propagation In the Atmosphere, U.S. Dept. of Commerce, NTIS AD-A028 615, May 1976

APPENDIX B

ENGINEERING DESIGN SPECIFICATIONS FOR A THREE WAVELENGTH INFRARED ATMOSPHERIC AEROSOL EXTINCTIOMETER

1. OBJECTIVES

1.1 Quantity to be Measured

This is an engineering design specification for a prototype instrument which will measure the extinction coefficient of atmospheric aerosols in three infrared spectral regions. The quantity to be measured, i.e. the aerosol extinction coefficient, is defined here as the sum of the scattering and absorption coefficients of ambient atmospheric aerosols.

1.2 Range of Measurement Parameters

The instrument shall measure the ambient aerosol extinction coefficient under the following range of conditions:

Visibility Range:	Fog conditions to 50 km.
Altitude Range:	Ground level to 5 km.
Time of Measurement:	All hours, all seasons.
Location:	All outdoor environments.
Ambient Temperature Range:	-25°C to +50°C
Spectral Regions:	1μ, 3-4μ and 8-12μ.

1.3 Performance Criteria

The instrument shall be designed and fabricated to meet the following performance criteria:

Accuracy: The extinction coefficient shall be measured to an accuracy of $\pm$ 20 percent.

Sample Rate: One set of measurements shall be made in the three spectral regions within a 15 minute period.

Sample Volume: The sample volume shall be large enough to give a representative signal from all aerosol particles present in the ambient atmosphere over the sample time period including those of the largest size of importance at all wavelengths. The aerosol sample must be left undisturbed by the instrument or any of its components and the sample volume must be left open to the atmosphere.

Reliability: The instrument will be operated unattended for long periods of time. It should not require frequent operator attendance for either calibration, performance of measurements, repair or servicing.

Size and Weight: The size and weight should be kept to the minimum possible consistent with the accuracy and reliability requirements. Attention should be given in the design to the portability of the instrument for moving it between station locations.

2. DESCRIPTION OF INSTRUMENT

2.1 Measurement Technique

The basis of the measurement technique is the use of a double-beam filtered radiometer with a sample volume residing in one beam and a reference volume in the other beam. Infrared radiation, provided by a high-temperature gray-body source, is alternately sent by a reflective chopper down one or the other of the two paths to a pyroelectric detector. Suitable wavelength isolation filters define the spectral regions of the measurement.

During one half of the measurement period that is devoted to a given wavelength interval the air in one path is filtered to remove all ambient aerosols while the other path remains exposed to the prevaling atmospheric conditions. During the other half of the same measurement period the conditions in the paths are reversed. The process is then repeated for each of the remaining bandwidth isolating filters.

The passage of radiation along paths which are not optically equivalent (i.e. due to slight differences in reflections and transmissions from the optical components) implies that the flux arriving at the detector differs for each of the two paths. If the paths are assigned the labels A & B then the flux arriving at the detector from the two paths is symbolized by ϕ_A and ϕ_B, in the absence of ambient aerosols. The pyroelectric detector responds only to changes in flux levels hence it measures only the difference in the two flux levels ϕ_A and ϕ_B.

When ambient aerosols are introduced into the sample volume of beam A, and the air in the sample volume of beam B is filtered to remove the aerosols, a signal voltage S_1 is produced by the pyroelectric detector which is given by

$$S_1 = R (\phi_A T_a - \phi_B) \qquad 2.1$$

Where R is the responsivity of the detector and T_a is the transmittance of the aerosols in the sample volume of path A. Similarly when the ambient atmosphere is introduced into the sample volume of path B and the air in the sample volume of path A is filtered the signal S_2 produced by the pyroelectric detector is given by

$$S_2 = R (\phi_A - \phi_B T_a) \qquad 2.2$$

An independent detector is used to monitor the average power in the two beams. This signal M is given by

$$M = R' (\phi_A + \phi_B)/2 \qquad 2.3$$

where R' is the responsivity of the beam monitor detector.

Assuming that the amplifier gains of the two systems are adjusted to compensate for unequal responsivities of the two detectors the following signal treatment can be performed.

$$\frac{S_2 - S_1}{M} = \frac{(\phi_A - \phi_B T_a) - (\phi_A T_a - \phi_B)}{(\phi_A + \phi_B)/2} \qquad 2.4$$

$$= 2(1 - T_a)$$

Attenuation of radiation in the beams due to the aerosols is very small so that the transmission of the aerosols may be expressed as

$$T_a = \epsilon^{-\sigma L} = 1 - \sigma L \qquad 2.5$$

where σ is the aerosol extinction coefficient and L is the path length through the sample volume. Upon substitution into Equation 2.4 this gives

$$\frac{S_2 - S_1}{M} = 2\sigma L \qquad 2.6$$

Thus the aerosol extinction coefficient is given by the relation

$$\sigma = \frac{1}{2L}\left[\frac{S_2 - S_1}{M}\right] \qquad 2.7$$

Equation 2.7 is the fundamental relation applying to the instrument described in this specification. In actual practice the instruments must measure the average power at the time of each signal measurement to compensate for any changes in the output power of the source during the course of the measurement. Equation 2.7 for computational purposes is then written as

$$\sigma = \frac{1}{2L}\left[\frac{S_2}{M} - \frac{S_1}{M}\right] \qquad 2.8$$

To achieve the measurement accuracy desired it is necessary to perform the ensemble average of many individual measurements. Again, for computational reasons, Equation 2.8 is rewritten as

$$\sigma = \frac{1}{2L}\left(\overline{\frac{S_2}{M}}\right) - \left(\overline{\frac{S_1}{M}}\right) \qquad 2.9$$

where the bars indicate an ensemble average of many measurements.

The signal processing equations illustrate a most important feature of this unique extinctiometer design. Any differences in optical efficiency between the two paths cancels out in the process of subtracting S_1 from S_2.

2.2 Principal Features of the Instrument

2.2.1 Optical Layout

A schematic diagram of the optical system housed within the instrument is shown in Figure **B2.1.** The performance objectives require a highly efficient optical system covering the wavelength region from 1 to 12 microns. Mirror optics are essential to achieving that goal. Coupled with the need for high efficiency is the need for the maximum possible relative aperture. A relative aperture of f/2 is believed to be realistically achievable and has been chosen as a design goal for the optical system.

Transmitting optics (e.g. windows, beam splitters and beam combiners) must be held to a minimum if the necessary efficiency is to be achieved. Operation over the wavelength range from 1 to 12 micron prohibits use of transmission enhancement coatings on optical components. Transmission components will,in most instances, severely reduce the throughput of the system, especially if high index of refraction materials are used. Severe polarization effects can also be introduced by high index materials operating in situations where radiation is not normal to their surfaces.

A description of the optical system is as follows: Radiation from a high temperature gray body source is imaged by elliptical mirror E1 onto a 4 millimeter diameter field stop at 2:1 conjugates transforming the f/2 collecting aperture into an f/4 bundle. A pair of off-axis parabolic mirrors P1 and P2 re-image the field stop at a point ahead of a rotating reflective chopper wheel. Radiation is alternately transmitted and reflected by the chopper wheel to a second pair of off-axis parabolic mirrors P3 and P4 which relay the now two) images of the field stop onto a parabolic field mirror P5. In passing from mirror P3 and P4 to P5 the two beams are required to transit the sample volumes A and B. Turning mirrors M2 - M5 decrease the separation between the two beams and by slight tilts direct the beams to P5 such that

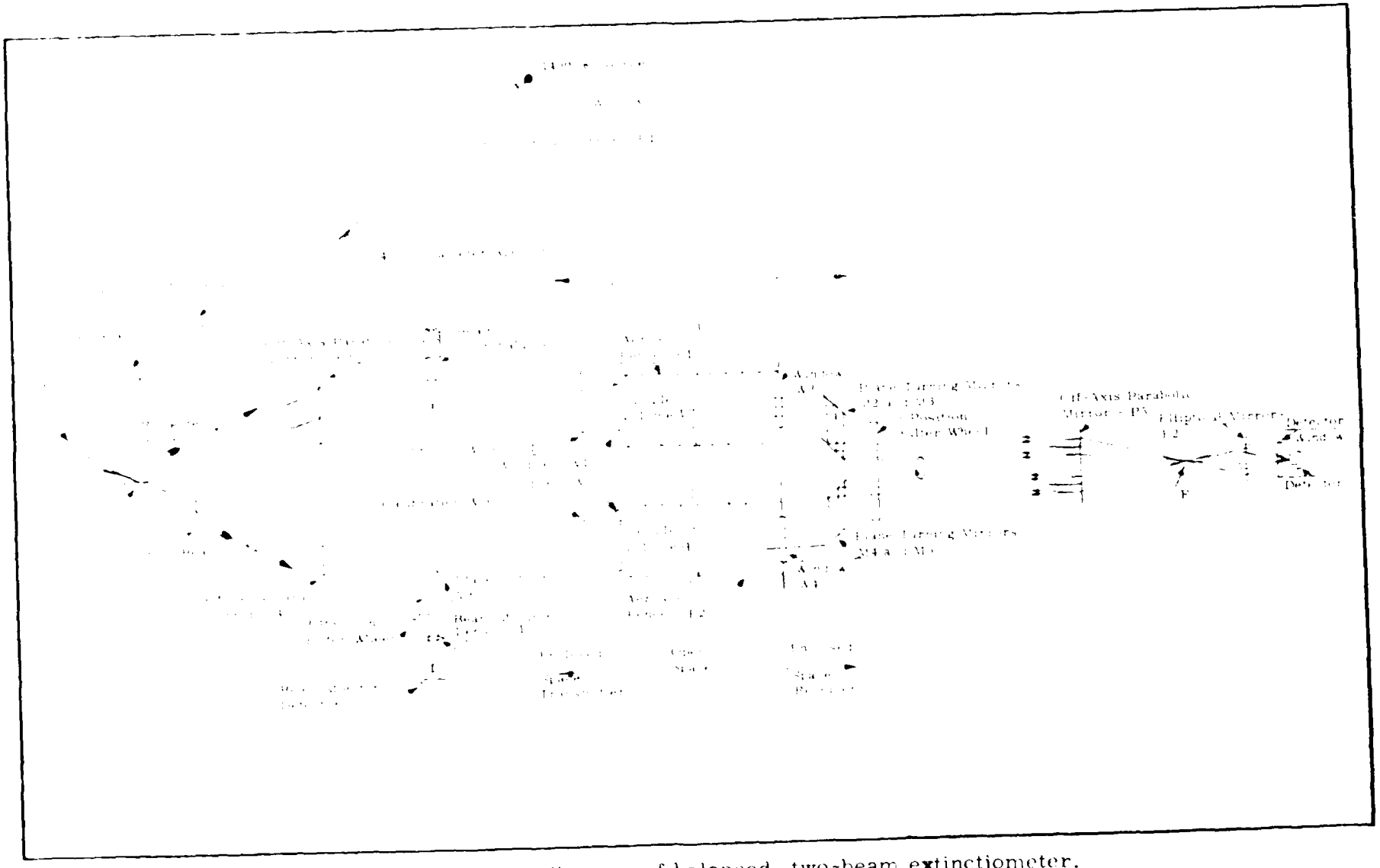

Figure B2.1. Schematic diagram of balanced, two-beam extinctiometer.

principal rays from the centers of the two mirrors P3 and P4 become axial rays allowing P5 to form coincident images of the two aperture stops P4 and P5 at image point F. A second elliptical mirror E2 then reimages the image point F onto the pyroelectric detector. The relative aperture of each bundle of radiation reaching the detector is f/2 and the geometric image is a circle 2 millimeters in diameter.

Reducing the separation between beams with mirrors M2 - M5 permits the use of a single field mirror P5 and permits the use ot a single filter wheel for both beams. The filter wheel is located immediately after mirrors M3 and M5 in radiation bundles having minimum amounts of divergence.

Four windows W1 - W4 are necessary to provide environmental protection for the optical and electronic components housed in the transmitting and receiving enclosures. The windows must transmit radiation from 1 to 12 microns and be capable of withstanding environmental effects for a reasonably long period of time before resurfacing or replacing. ZnSe has been selected as the material most suitable for fulfilling these two requirements.

2.2.2 Detectors

The primary detector is of the pyroelectric type having a 3 millimeter diameter sensing element. The detector is housed in an enclosure which is sealed with a BaF_2 window to prevent air motion around the detector. The detector also has a BaF_2 window to further reduce air motion from reaching the sensing element. The detector is mounted inside the detector enclosure in a manner which will minimize thermal convection and conduction, secure acoustic and vibration isolation, and provide maximum EMI protection.

The radiation incident on the primary detector is essentially [illegible] (modulated) radiation. The slight differences in the transmittance

of optical components in Path A vs Path B plus the very small attenuation due to the aerosols present in one beam or the other create small radiation imbalances at the frequency of the chopper. The signal treatment (see Section 2.1) provides for extraction of the aerosol extinction coefficient from the small difference voltage signals created by the radiation imbalance at the primary detector.

A second pyroelectric detector is utilized to monitor source power. An ideal location for monitoring the average power in both beams might seem to be at the end of the optical train using a beam splitter to extract a fraction of the total power and either a thermopile or thermistor bolometer to perform the average power measurement in each of the three wavelength intervals. An average power detector at this location would, however, have to perform a DC measurement and hence be extremely susceptible to ambient temperature drifts and changes in the ambient radiation levels entering through Windows W3 and W4. An appropriate compromise location is in the transmitter enclosure monitoring the average power in Beam B. A measurement of the average power in one beam suffices to determine exactly one-half the average power in both beams since the power in each beam is closely balanced. The accuracy required for the monitoring of the source power is not stringent hence some liberties may be taken with this measurement.

Only a fraction of the power in Beam B is required for the monitoring of source power. A pick-off mirror is used to extract approximately one percent of the radiation in Beam B. A mirror (or possibly a lens) is used to image the radiation onto the sensing element of the pyroelectric detector. The precautions previously indicated to prevent the generation of spurious signals and to eliminate noise sources within the primary detector housing also apply to the source monitor detector.

A separate three position filter wheel must be utilized with the

source monitor system if it is placed at this location. The wavelength isolation filters should be a close match to those used in the primary filter wheel. The two filter wheels are always moved in tandem, never separately controlled.

A possible (and more attractive) location for the source monitor system is in Beam B immediately after the primary filter wheel. This location would eliminiate the need for a second filter wheel. However, a protrusion into the beam at this location could create false signals. Radiation that is reflected back toward the source from the window of the detector enclosure, the detector window and from the sensing element of the detector can be scattered from the rear of the pick-off mirror and find its way back to the sensor. In this manner radiation from Beam A can appear in Beam B even when Beam B is fully occulted. (Obviously, the primary filter wheel and all ZnSe windows must be tilted a slight amount to prevent this retro-reflected signal from being reintroduced back onto the primary detector).

2.2.3 Chopper Wheel

Many of the design features incorporated into the instrument are critical to its proper operation. Perhaps none is more critical than the performance of the chopper wheel. In all situations except heavy fog the residual unbalance in the two beams can be reduced to the minimum permitted by the performance of the chopper wheel. A maximum of 0.1 percent radiant power imbalance between the two beams is vital to achieving the performance objective of the instrument as outlined in this design specification. If a maximum imbalance of 0.1 percent is not achieved the performance objectives cannot be met without serious modification to the instrument design.

A pyroelectric detector senses any changes in the radiant power

incident on it. It therefore is not a sufficient condition for a 'balance' that equal amounts of energy arrive at the detector during each half of a chop cycle. If the rate at which the equal amounts of energy arrive were to change in any way during the cycle a signal will be induced. Further, a difference in position of the two images on the sensing element causes an imbalance signal to occur since the radiation is alternating between the two beams.

Imbalance signals can thus be introduced by the chopper wheel in many ways: misalignment of the optical beams, non-parallel chopper blades, non-uniform reflectance to the chopper blades, etc. The most serious of all imbalance signals is created by flux lost to either or both beams because of imperfections and roll-off at the edges of the chopper blades. Roll-off and imperfections must be held to the minimum possible. State-of-the-art knife edges must be specified for the chopper blades. A high degree of flatness and uniformity of surface quality for each of the blades must also be achieved. Tolerances on the chopper wheel hub, the hub seat, drive shaft and bearings must be exacting.

The instrument design outlined herein makes an allowance for the possibility that a significantly better balance may be achieved with one blade over the other of a two-blade chopper. Signals from one or the other of the two blades may be processed independently to derive the extinction coefficient. If comparable balances are achieved with both blades then the data processing can proceed with both sets of data and achieve the same accuracy in half the time required if data from only one blade is used.

The ability to select the data acquired from one chopper blade or the other requires that the blades be coded in such a manner that an interrupter or reflecting sensor can distinguish between the two blades.

Position of the chopper wheel in the optical train is also a critical matter. Perfect knife-edge blades are not physically realizable.

Hence, it is important that the cross-section of the beam to be chopped be as large as possible at the point of chopping. Chopping at a focal point is the least desirable situation. However, chopping at the largest possible beam diameter would require an inordinately large chopper wheel. The present design compromises between these two extremes by chopping at a point displaced several centimeters from a focal point in a divergent bundle of radiation.

The chopper wheel is located as close to the source as possible so that only source radiation is chopped. If the chopper were located near the detector chopped ambient radiation would be indistinguishable from the source radiation.

2.2.4 Beam Balance System

Differences in transmission between the two paths must be compensated if a balance of 0.1 per cent or better is to be achieved. A small polished steel rod on the end of a stepper-motor-driven micrometer screw is used to achieve the balance. The diameter and length of penetration of the rod must be determined by experiment during fabrication of the instrument.

The optimum balance for one wavelength interval may not be the optimum for another wavelength interval. Hence, prior to the measurement period allotted to each wavelength interval the instrument must automatically adjust its balance for that particular wavelength interval.

Furthermore, because the filter wheel may not seat in precisely the same position each time, and because source temperature changes can change the spectral characteristics of the radiation, it is necessary that the instrument perform its automatic balancing function each time the filter wheel is moved to a new position.

2.2.5 Graybody Source

Laboratory experiments have demonstrated that when D.C. radiation from a true blackbody source is incident on a pyroelectric detector the noise voltage at the output of the detector is increased above that of the detector with no radiation on it for certain frequencies and flux levels. A chopping frequency of 34 Hz has been selected as the best compromise for minimizing source-induced noise components for the instrument.

Ribbon-filament tungsten lamps were demonstrated to produce prohibitive amounts of source-induced noise. A HeNe laser also gave a prohibitive amount of source noise. An alternative instrument design which would utilize two radiation sources, one being a tungsten lamp, to produce greater amounts of radiation at the 1 micron wavelength was therefore ruled out.

The assumption has been made in this design specification, without verification, that a graybody source (e.g. a globar or ceramic rod) operating at 1400 °K will produce no greater noise than a blackbody operating at that same temperature.

In keeping with the reliability and size and weight constraints on the instrument a large blackbody with attendant problems of large electrical power demands and heat dissipation problems has been avoided in the design. Small blackbody cavities are virtually eliminated as candidate sources because of their limited apertures and constrained fields-of-view.

The source must be housed in an enclosure to prevent rapid changes in source temperature due to air motion around the source. A window may be required on the enclosure if experience shows that an enclosure (with a necessary wide aperture) is not sufficient to reduce the rapid changes in temperature.

The source is imaged on a field-stop by relay optics. This feature is essential to restrict the area of the source which contributes to the radiation and to eliminate all contaminant radiation (e.g. from the source supports and the source enclosure).

2.2.6 Air Filter System

Two possible air filter systems must be investigated in the course of the engineering design. These are: (1) The Electrostatic Fence, and (2) The Alternating Cylinder.

An electrostatic fence is constructed of coarse wire screening with needles attached at periodic intervals. A high voltage ($\sim$12,000 volts, with non-lethal current capacity) is applied to the fence to create a corona discharge. The resultant electronic charge transfer processes result in a charge being deposited on any particles trying to penetrate the fence; and the particles are then repelled by the fence. (Reference: S. A. Hoenig, Applied Optics; Vol. 19, No. 5; 1 March 1980). It is contended by Hoenig that a cylindrical electrostatic fence surrounding a sample volume 50 centimeters long should exclude all dust, aerosol or fog particles, of the sizes of interest in the extinctiometer, in a matter of seconds.

If the electrostatic fence approach proves feasible the air filtering process should prove to be uncomplicated because there would be no moving parts. Two cylindrical fences would be used, one surrounding each of the sample volumes which are exposed to ambient air. Filtering of the air in one path or the other is then accomplished by simply turning on one fence or the other. Both fences can be turned on for self-calibration of the instrument. A very-wide-mesh screen would surround the entire sampling area to prevent inquisitive persons from receiving the mild shock that would result from touching a live screen.

The electrostatic fence approach for filtering the air can only be utilized if its potential problems are resolved. The potential problems which have been recognized are as follows:

(a) Ozone and dimer molecules are created by molecular recombination processes after bombardment of air molecules by electrons. The infrared absorption by these molecules could perturb the measurement of aerosol extinction because the molecular absorption would attenuate the beam passing through only the filtered air thereby inducing an imbalance signal.

(b) Electrostatic fences will not function properly when wind velocities exceed 15-18 mph.

(c) Corona discharge from the electrostatic fences could result in EMI pick-up in the detector/amplifier electronics.

Each of these three problem areas must be dealt with in the engineering design of the instrument. Possible approaches are as follows: (1) Hoenig states that the production of ozone can be reduced significantly by using a pulsed power supply to energize the fence, (2) At a given stage in the development of the instrument a mock-up using actual components could be used to test the electrostatic fence filtering approach, (3) At high wind velocities a wind baffling system could be used to slow the air motion prior to entering the sampling volumes. A properly designed baffling system must include isokinetic air flow design principles, (4) The use of insulating stand-offs for the electrostatic fences and good EMI shielding practice should prevent EMI pick-up by the detector/amplifier electronics.

If the electrostatic fence approach should prove to be incompatible with the extinctiometer design the Alternating Cylinder appraoch must be used to achieve filtered air for the reference beam. Although this approach at first glance seems straightforward it is not without problems. Its greatest drawback is the complications it adds to the instrument: (1) an efficient system for filtering aerosols having diameters greater than 0.1 micron must be added to the instrument, (2) a cylinder for containing the filtered air must surround the reference beam, and (3) when the reference beam is changed from path B to path A or vice versa, the cylinder must be made to move from the one location to the other without loss of the filtered air (loss of the filtered air would require repurging of the cylinder with filtered air and the addition of a significant time-delay before the measurements can proceed).

Several problems attendant to the alternating cylinder approach have been recognized and must be treated in the engineering design of the instrument: (1) the wall of the cylinder offers a means for introducing stray chopped-radiation into the reference beam which could seriously impair the measurement since it introduces an imbalance signal which does not cancel out (in the electrostatic fence approach the two fences are stationary and any effects due to reflected or scattered radiation cancel out in the final computation), (2) the cylinder cannot be sealed by windows at its ends since its transmission is required to be 100 percent, (3) the lips of the cylinder must provide a circumferential small air leak where they approach the housings of the transmitting and receiving sections of the instrument. (This controlled air leak will prevent any aerosols and dust from entering the cylinder and will require a slight positive pressure of air from the air filtering system) and (4) the air filtering process must not change the water vapor content of the filtered air in the reference volume from that of the ambient air in the sample volume by more than an amount set by the performance objective on accuracy of the measurement.

The last problem mentioned has greatest implications for the 8-12 micron channel where the infrared water-vapor continuum-absorptions is severest. An error analysis of the effects of water-vapor continuum-absorption on a measurement at 10 microns reached the conclusions outlined below.

A model atmosphere for a mid-latitude summer was assumed, with: T = 294°K, a relative humidity of 76 percent and a barometric pressure of 1013 mb. The water vapor continuum absorption coefficient was taken to be $0.23\,km^{-1}$ at a wavelength of 10.6 microns. The meteorological expression for the water vapor density ρ_v of moist air is

$$\rho_v = \frac{r}{(1 + r/\epsilon)} \left(\frac{P}{RT}\right) \qquad (2.10)$$

where:

- r = mixing ratio of water vapor to dry air.
- ϵ = ratio of molecular weight of water vapor to that of dry air.
- P = barometric pressure
- T = absolute temperature
- R = gas constant for dry air.

Any change in P, T or r produces essentially a linear change in ρ_v. An error analysis using Equation 2.10 can be used to arrive at the permissable amount of difference in any of these three quantities between the sample and reference volumes.

Assuming that the full error budget of 20 percent for measurement of the aerosol extinction coefficient is given to the air filtering process the maximum allowable difference in pressure, temperature or mixing ratio between the sample and reference volume for various values of the atmospheric aerosol extinction coefficient is as follows:

Aerosol Extinction Coefficient (10μ) σ (km^{-1})	Maximum Allowable Difference in P, T or r $\frac{\Delta P}{P}$, $\frac{\Delta T}{T}$, $\frac{\Delta r}{r}$
0.0015	0.0013
0.003	0.0026
0.01	0.0078
0.03	0.026
0.10	0.086

The difference values quoted in the table are for any one of the three atmospheric parameters assuming no change in the other two. If there are changes in all three parameters, then the allowable difference is a limit on the linear sum of all three changes in relative values.

The requirements placed on the air filtering process by the above analysis are severe. Obviously the full error budget cannot be given to the air filtering process. If the Alternating Cylinder approach must be used, and if the above design constraints cannot be met there may arise situations where the 8-12 micron measurement is perturbed by the effects of water vapor continuum absorption.

2.2.7 Instrument Calibration

If the instrument somehow utilized the same detector to measure the imbalance signals S_1 and S_2 and also the average power M, no calibration would be required. The use of two detectors, having different responses, amplifiers, etc. implies that a calibration must be performed. The calibration is here assumed to be an operation performed on the measured value M' of the average power which is a small fraction of the average power M incident on the primary detector, i.e.

$$M = KM' \qquad (2.11)$$

During the calibration a known amount of attenuation $\Sigma = \sigma L$ is placed first in one beam and then the other. Processing the resultant data gives the calibration constant for the instrument

$$K = \frac{1}{2\Sigma} \left\{ \left(\frac{S_2}{M'} \right)_{cal} - \left(\frac{S_1}{M'} \right)_{cal} \right\} \qquad (2.12)$$

If electrostatic fences are used for obtaining filtered air the calibration may be performed periodically during the normal operation of the instrument. Both fences may be turned on and a fine wire (0.001 inch diameter or less) automatically inserted across one beam and then the other. The attenuation of the beam by the fine wire is determined by the ratio of the geometric area of the beam excluded by the wire to the cross-sectional area of the beam at the point of insertion of the wire.

If the Alternating Cylinder method for filtering air is employed the instrument calibration becomes more involved. The calibration constant must be determined by use of two cylinders containing gases of known extinction (or absorption properties) which are interchanged between the two beams.

In this latter situation the fine wires may be used to periodically monitor any changes in the calibration constant of the instrument. The monitoring of the calibration constant in this manner is only reliable when the ambient aerosol extinction is a small fraction of the extinction provided by the fine wire. In fog situations, for example, a reference check on the calibration constant by this technique would not be possible.

2.2.8 Configuration and Environmental

The instrument is required to perform the aerosol extinction coefficient measurement over a wide range of situations and environments (Section 1.2).

In certain environments (e.g. rain, sleet, hail, and snow) the instrument cannot be expected to perform properly unless adequate covers or a shelter is provided. Coverings or a shelter however perturb the ambient aerosol content. A determination has yet to be made whether protection from severe weather will be made, and if so what form it will take, or if the instrument will be considered non-operational under such conditions. This determination will be made by AFGL at the outset of the program and the engineering design will incorporate any features which are necessary to implement that decision.

It is essential that the air flowing through the sample volume be truly representative of the ambient air. Aerosols may be lost from the sampled air because of non-isokinetic air flow around the instrument. The optimum instrument orientation to prevent non-isokinetic air flow through the sample volume would appear to have the two beams passing horizontally between the source and receiver sections of the instrument with the beams always normal to the direction of the prevailing wind.

3. PERFORMANCE ANALYSIS

3.1 Range of Aerosol Attenuation Coefficients

The performance analysis outlined in this engineering design specification is intended to demonstrate the performance objectives as stated in Section I of the specification. A performance analysis of the instrument requires that the range of atmospheric aerosol attenuation coefficients be specified. Table B3.1 presents the values and ranges of aerosol attenuation coefficients used for this analysis and for the design of the instrument. Sources of information for the aerosol extinction coefficients are identified in footnotes to the table.

3.2 Signal and Thermal Power Requirements

The performance analysis outlined herein is devoted to the requirements for measuring the aerosol extinction coefficient to an accuracy of 20 percent under 50 kilometer visibility conditions at an altitude of 5 kilometers. Performance under fog conditions places the least demands on the instrument and is handled in the customary manner of providing sufficient dynamic range for the instrument.

Equation 2.7 states that three measurements can be combined to give the aerosol extinction coefficient in the following manner:

$$\sigma = \frac{1}{2L}\left\{\frac{S_2 \quad S_1}{M}\right\} \qquad 2.7$$

Treating the three measurements S_1, S_2 and M as having independent errors and performing an error analysis wherein the total error is assumed to propagate as the **square root** of the sum of the squares of the individual errors, the following relationship may be derived.

$$\frac{\Delta S_1}{S_1} = \left\{\left(\frac{S_2}{S_1}\right)^2\left(\frac{\Delta S_2}{S_2}\right)^2 + \left(\frac{2L\sigma M}{S_1}\right)^2\left[\left(\frac{\Delta \sigma}{\sigma}\right)^2 + \left(\frac{\Delta M}{M}\right)^2\right]\right\}^{1/2} \qquad (3.1)$$

TABLE B3.1. Wavelength Bands and Extreme Values of Atmospheric Attenuation Coefficients.

Wavelength Region (microns)	Wavelength Bandwidth (microns)	Largest Extinction Coefficient[1] ($km.^{-1}$)	Smallest Extinction Coefficient[2] ($km.^{-1}$)
0.98 - 1.08	0.1	20	.015
3 - 4	1	20	.0015
8 - 12	4	20	.001

Note (1): The extinction coefficient for fog is taken to be that of Shettle and Fenn, Advection Fog Model 2 for light to moderate advection fog; E.P. Shettle and R.W. Fenn, "Models for the Aerosols of the Lower Atmosphere and Effects of Humidity Variations on their Optical Properties," AFGL-TR 79-0214, 20 September 1979.

Note (2): The extinction coefficient for 50 kilometer visibility at 5 kilometer altitude was obtained by scaling of the AFGL Tropospheric Aerosol Model to these parameters.

This equation expresses the relative error demand placed on the measurement of S_1 (i.e. $\Delta S_1/S_1$) in terms of the relative errors in the measurement of S_2 and M, and the relative error requirement placed on σ by the performance objectives. But the signal S_1 and S_2 are almost identical in strength so that Equation 3.1 can be rewritten as

$$\frac{\Delta S}{S} = \sqrt{2}\,\sigma L \left(\frac{M}{S}\right)\left\{\left(\frac{\Delta\sigma}{\sigma}\right)^2 + \left(\frac{\Delta M}{M}\right)^2\right\}^{1/2} \qquad (3.2)$$

where for convenience, S, is substituted for either S_1 or S_2.

Because most of the signal strength of S_1 or S_2 arises from imbalance due to the chopper wheel the bracketed term (M/S) can be viewed as a statement of the residual imbalance resulting from the chopper. The present design specifications require the imbalance to be 10^{-3} or better, so that $M/S \geq 10^3$.

The performance objectives require that σ be measured to an accuracy of 20 percent (i.e. $\Delta\sigma/\sigma = 0.2$). A reasonable accuracy requirement for the measurement of the average power M is 5 percent. An examination of Equation 3.2 then indicates that the error term $(\Delta M/M)$ can be neglected with respect to $(\Delta\sigma/\sigma)$.

If the sample pathlength L = 50 centimeters, Equation 3.2 now reduces to the reciprocal of the signal-to-noise ratio

$$\frac{\Delta S}{S} = \sqrt{2} \times 10^4\, \sigma\ (\mathrm{cm}^{-1}) \qquad (3.3)$$

A fundamental limitation placed on the measurement of either S_1 or S_2 is the combined noise power of the pyroelectric detector and the graybody source. Assuming that the noise power of the source can

be reduced to a value below the NEP of the detector and substituting NEP for S in Equation 3.3 gives as a minimum requirement for S

$$S = \frac{10^{-4}\ NEP}{\sqrt{2}\ \sigma\ (cm^{-1})} \tag{3.4}$$

But $M/S \geq 10^{3}$; therefore, we also have as a requirement for the average thermal power on the detector

$$M \geq \frac{10^{-1}\ NEP}{\sqrt{2}\ \sigma\ (cm^{-1})} \tag{3.5}$$

The average power M incident on the pyroelectric detector is given by

$$M = \frac{\phi_A + \phi_B}{2} \tag{3.6}$$

But $\phi_A \simeq \phi_B$; thus $M \simeq \phi$ where

$$\phi(\lambda) = \frac{\pi A_d\ \epsilon(\lambda)\ \bar{B}_\lambda\ \Delta\lambda\ T_o(\lambda)}{[1 + 4\ (f/n)^2]} \tag{3.7}$$

In Equation 3.7 $\bar{B}_\lambda$ is the average source radiance over the spectral bandwidth $\Delta\lambda$, $\epsilon(\lambda)$ is the spectral emissivity of the source, $T_o(\lambda)$ is the transmittance of the optical system, A_d is the effective area of the detector and f/n is the relative aperture of the optical system. The throughput of the optical system, $E(\lambda)$, can of course be written as

$$E(\lambda) = \frac{\pi A_d T_o(\lambda)}{[1 + 4(f/n)^2]} \qquad (3.8)$$

in which case Equation 3.7 can be expressed as

$$\phi\lambda = E(\lambda) \quad \epsilon(\lambda) \quad \overline{B}_\lambda \quad \Delta\lambda \qquad (3.9)$$

The pertinent design parameters for the instrument specified herein are listed in Table B3.2. Given these parameters, it may be concluded that the average power requirements for each channel, as specified by Equation 3.5, may be met in the case of the 1 micron and the 3-4 micron channels but not for the 8-12 micron channel. The thermal power falls short by a factor of 1.8 for the latter channel.

The failure to achieve the necessary thermal power in Channel 3 introduces a 36 percent error into the measurement of σ at the extreme limit of σ(i.e. .0015 km^{-1}) instead of the required 20 percent error.

Changes in the instrument design in order to achieve a 20 percent accuracy at the extreme limit for Channel 3 are considered impractical. Gross changes in the instrument design would have to be effected. For example, a graybody source temperature of 2100 °K could give the necessary thermal power, or an improved relative aperture of f/1.5 vs f/2.0 could also result in the necessary increase in power. But either of these options has size, weight or electrical power implications which should be avoided. Increasing the measurement time for Channel 3 by a factor of 3 could achieve the desired accuracy but would result in a violation of the requirement for performing the measurements in all three channels within a 15 minute time period.

Equations 3.2 and 3.7 place fundamental limitations on many of the instrument parameters. These equations must therefore be viewed as the tradeoff equations when any changes in instrument parameters affecting signal strength and thermal power are contemplated.

TABLE B3.2. Instrument Design Parameters.

GRAYBODY SOURCE:

Temperature	1400 °K
Emissivity (1-12 μ)	0.9

PYROELECTRIC DETECTOR

Diameter (Actual)	3 mm
Diameter (Effective)	2 mm
NEP (1-12 μ; 34 Hz; 1 Hz)	10^{-9} Watts/$\sqrt{\text{Hz}}$

OPTICAL SYSTEM

Transmission (Each Beam)	0.21
Relative Aperture	f/2

CHOPPER WHEEL

Chopping Frequency	34 Hz
Beam Imbalance	10^{-3}

MEASUREMENT TIME

A-Beam (Ambient); B-Beam (Reference)	100 sec
A-Beam (Reference); B-Beam (Ambient)	100 sec

OPTICAL BANDWIDTHS

Channel 1	0.98 - 1.08μ
Channel 2	3-4 μ
Channel 3	8-12μ

SAMPLE VOLUMES

Pathlength	50 cm

4. OPERATIONAL FUNCTIONS AND CONTROLS

4.1 General

The operational functions and controls of the instrument as described herein are based on the assumption that electrostatic fences are employed to filter the ambient air. If the Alternating Cylinder approach for filtering air is employed the functions and controls of the instrument must be modified appropriately. It is also assumed that an ensemble averaging over a 100 second time period is required for each S_1 and S_2 measurement in order to achieve a 20 percent accuracy of measurement for σ.

A block diagram of the electronic control and data processing functions is given in Figure B4.1. A microcomputer is required to perform all necessary sequencing of operations and to handle the data processing.

There are two modes for operating the instrument, manual and automatic. In the manual mode the instrument is under full control of the operator who may select any mode of operation within the capability of the function selections of the control panel. In the automatic mode the instrument performs a sequence of calibration and measurement cycles with the number of measurement cycles per calibration cycle selectable within limits. Figure B4.2. illustrates an example with the selection set at 3. The warm-up time is not specified; it will depend mainly on the time for the graybody source to come up to temperature and must be empirically determined during the fabrication of the instrument.

Each calibration or measurement cycle is allotted 15 minutes of time. During that 15 minute period the instrument will cycle through the three filters and perform measurements in each of the three channels; a total of 5 minutes being devoted to each wavelength channel and the necessary housekeeping functions whenever a filter change is made.

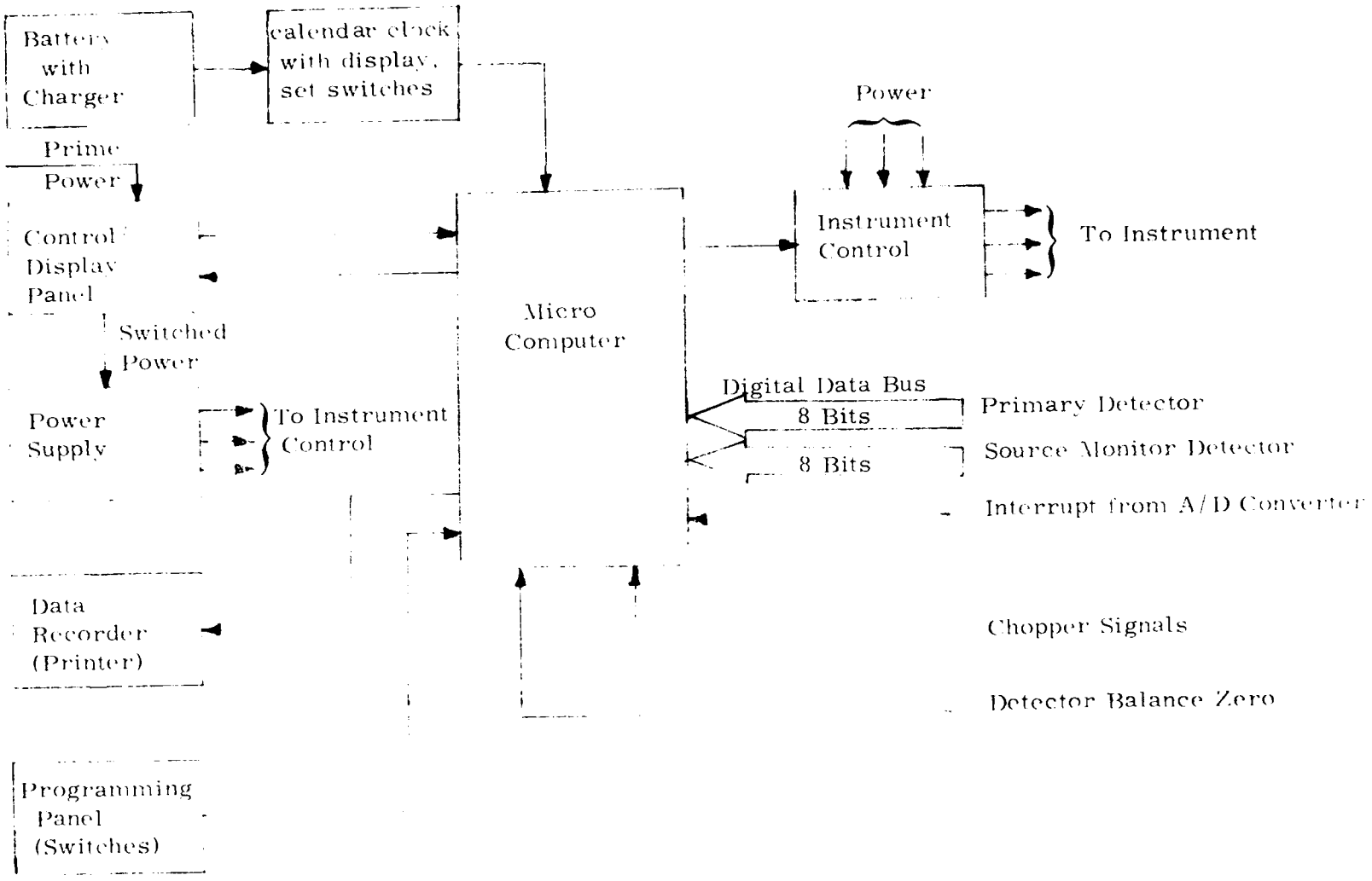

Figure B4.1. Block diagram of a possible configuration for the control and data processing function of the Aerosol Extinctiometer.

AUTOMATIC MODE OPERATION

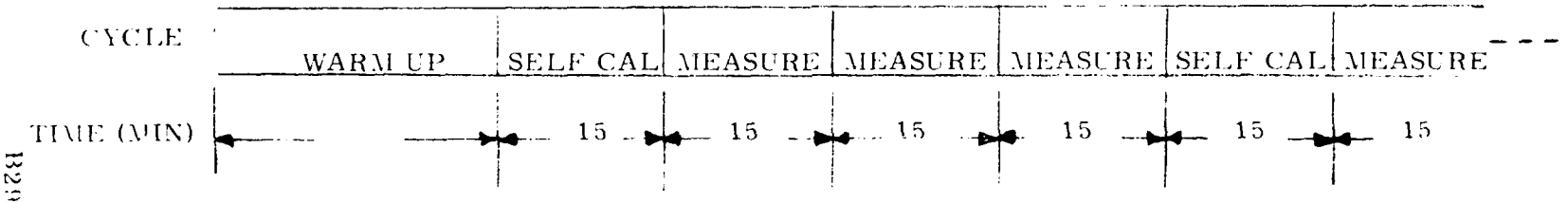

Figure B4.2. Sequence of Calibration and Measurement Cycles in the Automatic Mode of Operation.

In the automatic mode of operation the instrument will first perform a calibration cycle followed by N measurement cycles where N may be any number from 1 to 19 selected at the discretion of the operator. At the end of the N measurement cycles the instrument will perform another calibration cycle, and so on.

4.2 Instrument Functions and Displays

The master panel for Function Select and the Display appropriate to each function selected shall incorporate all features indicated in Table B4.1.

The manual mode of operation permits the individual powering of selected instrument components as indicated in the table. This feature is essential when instrument servicing and repair is required. The manual mode may also be used to perform a measurement at any one filter position. If commanded to switch to another filter while that measurement is in progress, or go to the automatic mode,the instrument will not do so until one of two steps in the microcomputer program is reached which specifically inquire into the status of the control panel. Once one of these program steps is reached it will proceed to implement the new instruction, which has been held in memory.

Table B4.2 gives the requirement for display of data in process at any given time. The particular wavelength channel is indicated by an illuminated numeral. Whichever signal, i.e. S_1 or S_2, is being accumulated in the ensemble averaging process is also displayed. The instantaneous value of the data sample is displayed for each blade of the chopper. This latter information is required as a diagnostic tool in gauging instrument performance and in making decisions regarding the use of data from either or both chopper blades. (In the manual mode this display can be utilized with the BEAM BALANCE FUNCTION to determine the amount of imbalance due to

TABLE B4.1. Control Panel Function Select and Display.

FUNCTION SELECT	DISPLAY
POWER: ON/OFF	Power: ON/OFF Warm-Up - ON
MODE	
MANUAL FUNCTION ENABLE AUTOMATIC	Manual Mode ON/OFF Automatic Mode ON/OFF
CYCLE	
DATA CYCLE CALIBRATE CYCLE	Data Cycle - ON Calibrate Cycle - ON
MANUAL COMMANDS	
CHOPPER POWER ON/OFF SOURCE POWER ON/OFF FENCE POWER A ON/OFF FENCE POWER B ON/OFF CHANNEL SELECT 1,2,3 BEAM BALANCE INC/DEC INSERT CALIBRATOR A INSERT CALIBRATOR B CHOPPER BLADE SELECT PRIMARY DETECTOR ON/OFF SOURCE MONITOR DETECTOR ON/OFF TAKE/PRINT DATA DATE/TIME SET	Chopper - ON Source - ON Fence A - ON Fence B - ON Channel Select 1,2,3 Beam Balance - INC/DEC Calibrator A - IN/OUT Calibrator B - IN/OUT Blade - 1,2, 1 + 2 Primary Detector ON/OFF Monitor Detector ON/OFF (See Data Display Table 4.2) Date/Time Display
AUTOMATIC CYCLE OPTIONS*	
CHANNEL 1,2,3 CYCLE CHOPPER BLADE SELECT 1,2,1+2 DATA CYCLES PER CAL CYCLE 1-19	Channel Position-1,2,3,Cycle Blade - 1,2, 1+2 Data Cycles Per Cal Cycle
*NOTE: See Figures 4.2, 4.3, and 4.4 for a description of automatic sequence functions.	

TABLE B4.2. Requirements for Display of Data in Process.

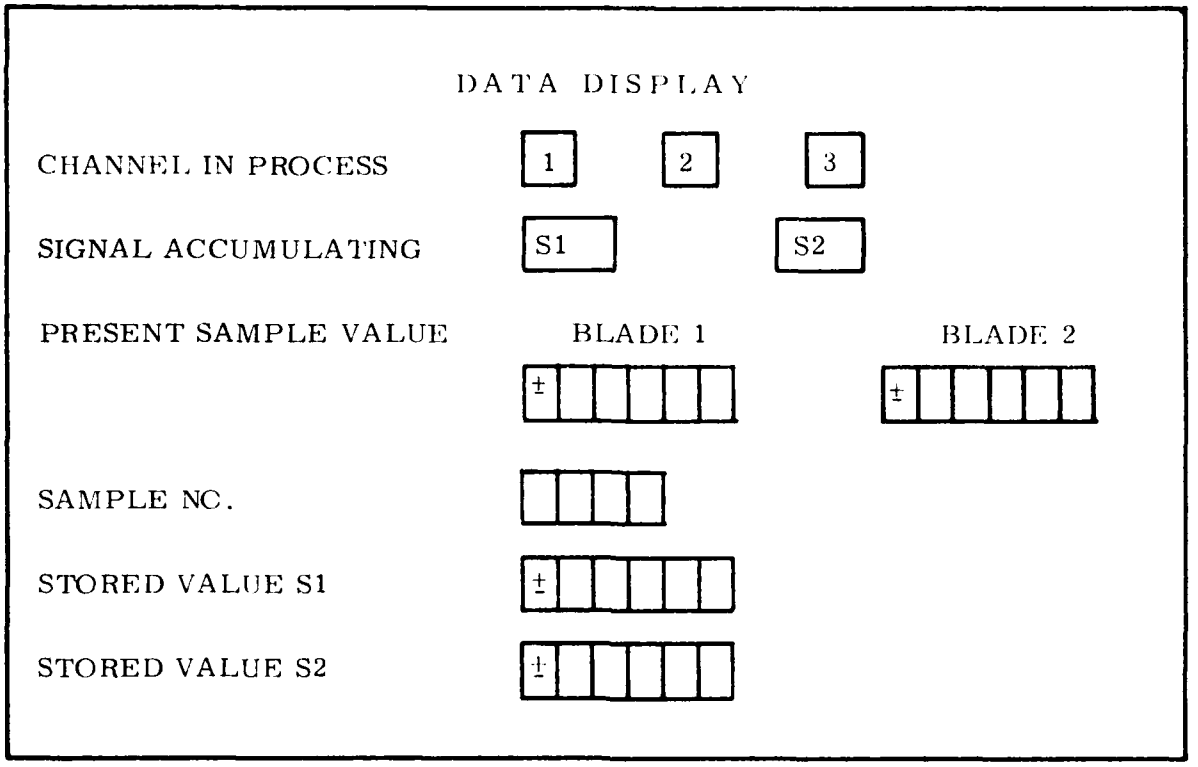

each chopper blade). Other display features include the total number of data samples which have been processed at that point in time for either S_1 or S_2. The stored value for the first of the two signals to be processed is displayed for the full time that the second signal is accumulating. The second signal is displayed for only a matter of seconds until the filter wheel is cycled.

Information to be recorded for each channel on a line printer is indicated in Table B4.3. The requirements here are self-explanatory and are not elaborated upon except in the case of the standard deviation. The standard deviation of the σ-measurements may be used as a diagnostic tool for gauging deteriorating instrument performance over a long period of time and for rejecting individual sets of measurements because of spurious signals (e.g. insects flying through one or the other of the two sample volumes).

4.3 Instrument Cycles

There are two types of instrument cycles, calibration and measurement. The first of these initiates a sequence of operations which performs a self calibration on both the A and B branch of the optical system for each of the three channels. This is accomplished by inserting a factory calibrated wire across the A or B beams, accumulating the necessary data and computing the new calibration factors. Figure B4.3 illustrates the sequence of events during this cycle. At the completion of the data processing for each channel the new calibration factor is placed in the microcomputer memory where it replaces the results of the previous calibration. The printed output includes both the new and previous calibration factor to assist in detecting instrument malfunction.

TABLE B4.3. Information to be printed for each channel during a measurement cycle or calibration cycle.

DATA CYCLE RECORD	CALIBRATION CYCLE RECORD
1. DATE	1. DATE
2. TIME	2. TIME
3. MODE	3. MODE
4. CYCLE	4. CYCLE
5. CHANNEL	5. CHANNEL
6. NO. DATA SAMPLES	6. NO. DATA SAMPLES
7. EXTINCTION COEFFICIENT	7. NEW CALIBRATION FACTOR
8. STANDARD DEVIATION ITEM 7	8. STANDARD DEVIATION ITEM 7
9. CHOPPER BLADE NO.	9. LAST CALIBRATION FACTOR
10. LAST CALIBRATION FACTOR	10. STANDARD DEVIATION ITEM 9
11. UNBALANCE FACTOR	11. CHOPPER BLADE NO.

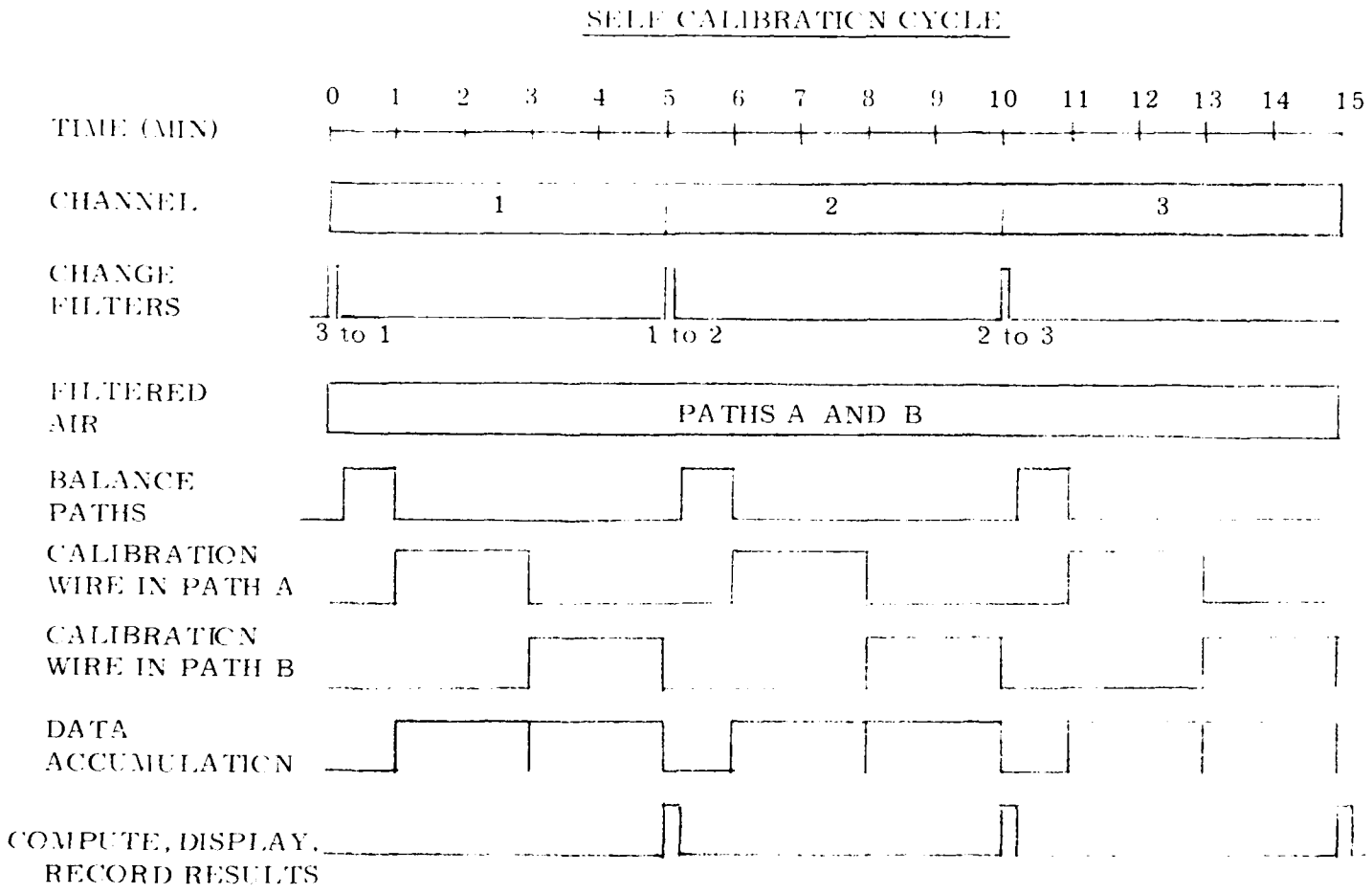

Figure B4.3. Sequence of events during each fifteen minute calibration cycle in the automatic mode of operation.

The measurement cycle initiates a sequence of operations which lead to the measurement of the atmospheric extinction coefficient for each of the three channels. Figure B4.4 illustrates the sequence of operations during this cycle. Each full 15 minute cycle is divided into three 5 minute periods, one for each channel. Each 5 minute period consists of two 100 second measurement periods, one with filtered air in the A beam and one with filtered air in the B beam. The remainder of each 5 minute period is devoted to housekeeping functions such as filter changing, beam balance, etc. During each 5 minute measurement period the DATA DISPLAY registers shown in Table B4.2 record the "in process" data. At the end of each 5 minute period the line printer records the data shown in Table B4.3.

The time sequences shown in both Figure B4.3 and B4.4 include a major fraction of a minute for changing the filter wheel followed by most of the remainder of the minute for acquiring beam balance. Although a filter change will probably be accomplished in a matter of seconds, the properties of pyroelectric detectors require a considerably larger period be devoted to permit recovery from a number of problems.

The noise power of pyroelectric detectors is seriously effected by microphonic and EMI pick-up. Suitable precautions can prevent degradation of detector performance by these two sources of extraneous noise. There are however two circumstances under which pyroelectric detectors are rendered inoperable; these two situations must be avoided in the instrument construction. The circumstance under which these two effects occur are not well documented or described in the literature but for purposes of this specification the effects are termed <u>thermal shock</u> and <u>thermal drift overload</u>.

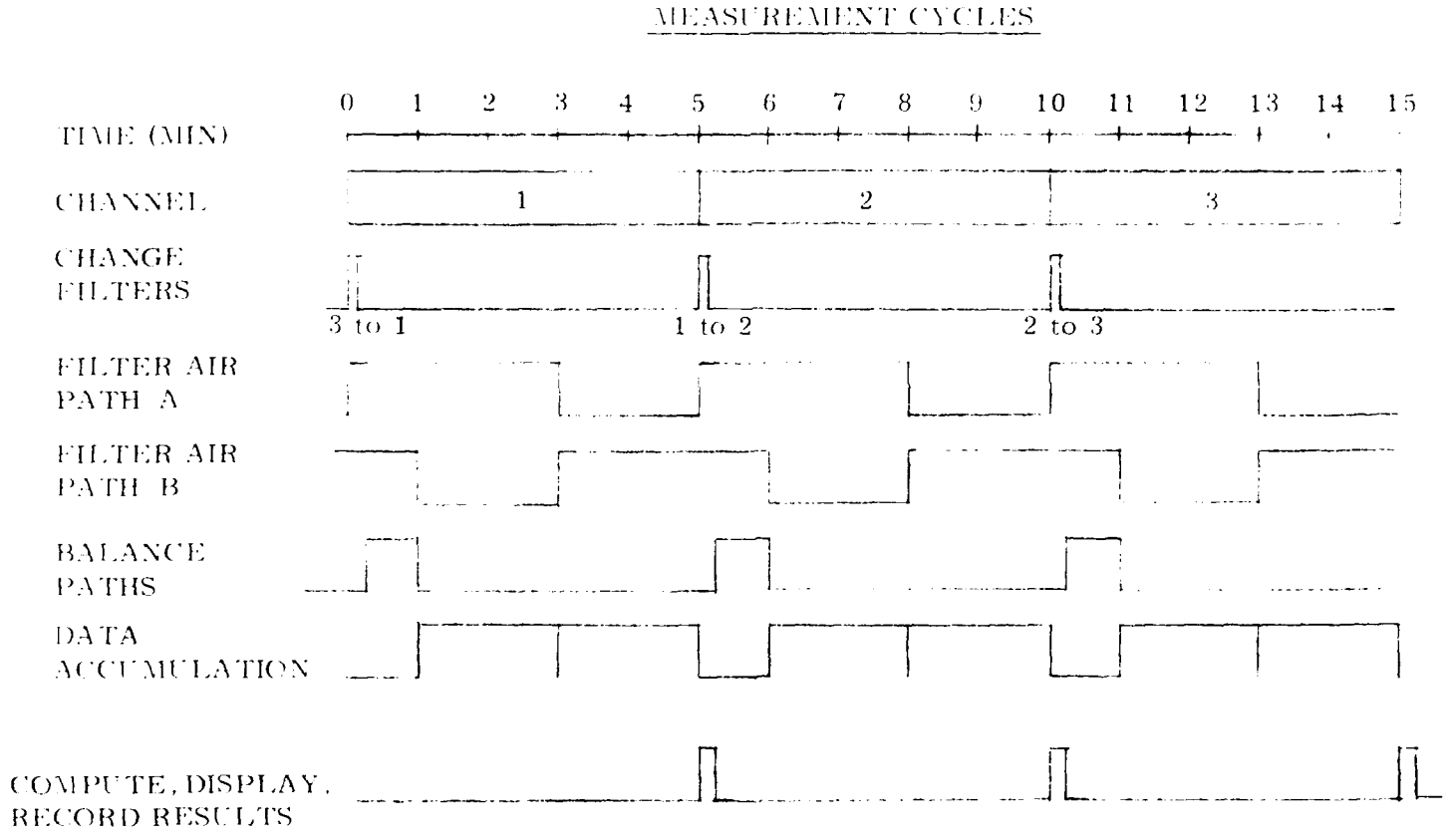

Figure B4.4. Sequence of events during each fifteen minute measurement cycle in the automatic mode of operation.

Thermal shock occurs when a sudden large change in thermal power level is delivered to the pyroelectric detector. The change can be either an increase or decrease. When thermal shock occurs the FET amplifier immediately following the detector is overloaded and the signal due to chopped radiation will disappear. Approximately four minutes is required for the detector to recover from thermal shock and perform in its normal manner.

Changing of filters in the aerosol extinctiometer is a situation which has the potential of inducing thermal shock because the thermal power level on the detector can be changed by large amounts when the filters are switched. The three sector filter wheel design incorporated into the optical system is intended to prevent thermal shock by allowing a smooth continuous transition from one filter to the next. Even with this precaution it may be necessary to allow some tens of seconds to elapse for a settling-down time for the primary pyroelectric detector after the filter wheel is turned and before data accumulation is initiated. The required amount of settling-down time must be determined during the construction phase of the instrument.

Thermal drift overload is another manifestation of the same phenomenom which produces thermal shock. Changes in the ambient temperature surrounding the detector generate low frequency currents in the pyroelectric detector which swamp the FET amplifier. Thermal drift overload is prevented by a carefully designed thermal enclosure for the detector.

4.4 Signal Sampling

The block diagrams of the electronics required for the primary detector and the source monitor detector are illustrated in Figure B4.5.

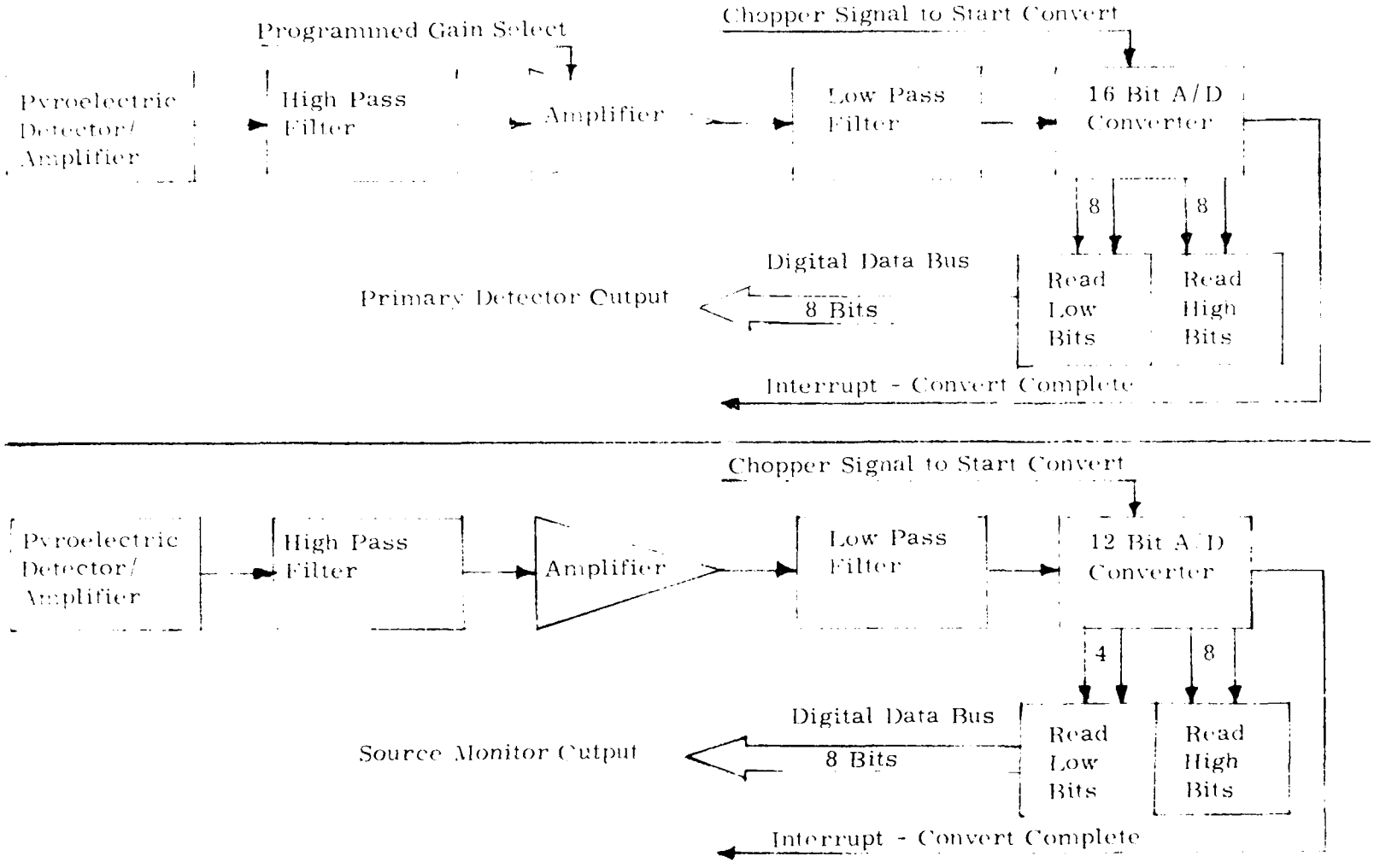

Figure B4.5. Block diagrams of primary detector and source monitor detector electronics.

The thermal time constant of the pyroelectric detectors is much larger than the period of the chopper wheel, hence the signal output from the detectors is an integral of the flux behavior during each opening or reflection associated with a given chopper blade. Maximum accuracy is obtained by choosing the time of sampling the signals to be near the end of the integral as shown in Figure B4.6. The signal is read into a sample and hold circuit just prior to a change in chopper blade status and the A/D conversion is started. The A/D conversion is completed a short time later and well before any change in blade status occurs.

4.5 Data Processing

A flow chart of the microcomputer program for the measuring sequence applicable to each of the three filters is given in Figure B4.7 (see also Figure B4.4). When the program reaches either of the blocks calling for data accumulation a condition exists to start responding to the program given in Figure B4.8. The data accumulation program initiallizes the data displays and sets the data counter to zero on the first pass through the program. During the data accumulation period this program continues to recycle until the 100 seconds of data have been accumulated. The interrupt program responds to the interrupt signal from the A/D converter which indicates completion of conversion of another data sample. This program senses first which chopper blade has produced the data sample and provides the option of either processing the data or going directly back to the data accumulation program if that particular chopper blade has not been selected. Options are provided to accept both chopper blades in which case each interrupt signal results in a data sample or to reject either chopper blade in which case every other interrupt signal results in a data sample. When the interrupt program accepts sufficient interrupt signals to complete a chopper cycle the program routes the data to update the data display and to perform

CHOPPER AND A/D CONVERTER OPERATION

PERFORMS NON-SYNCHRONOUSLY WITH COMPUTER PROGRAM

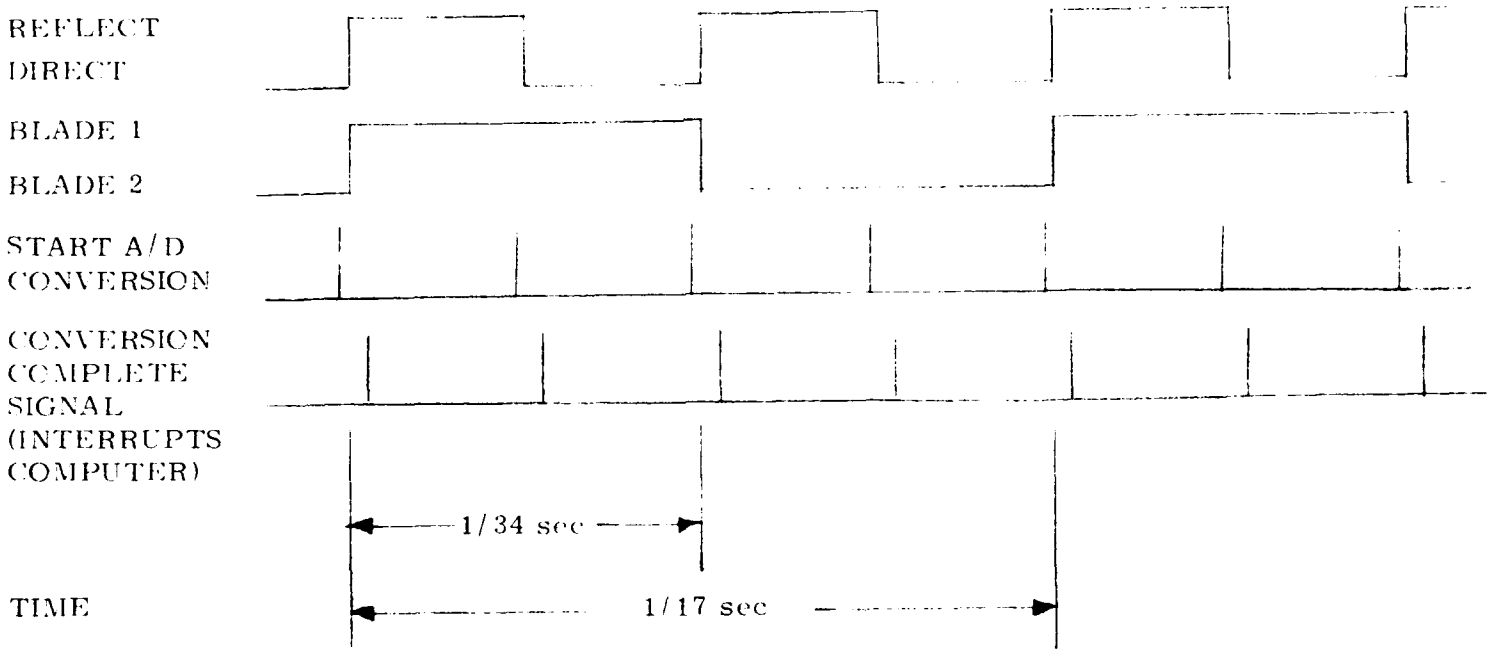

Figure B4.6. Relationship between chopper wheel status, the extraction of signals and the A/D conversion operation.

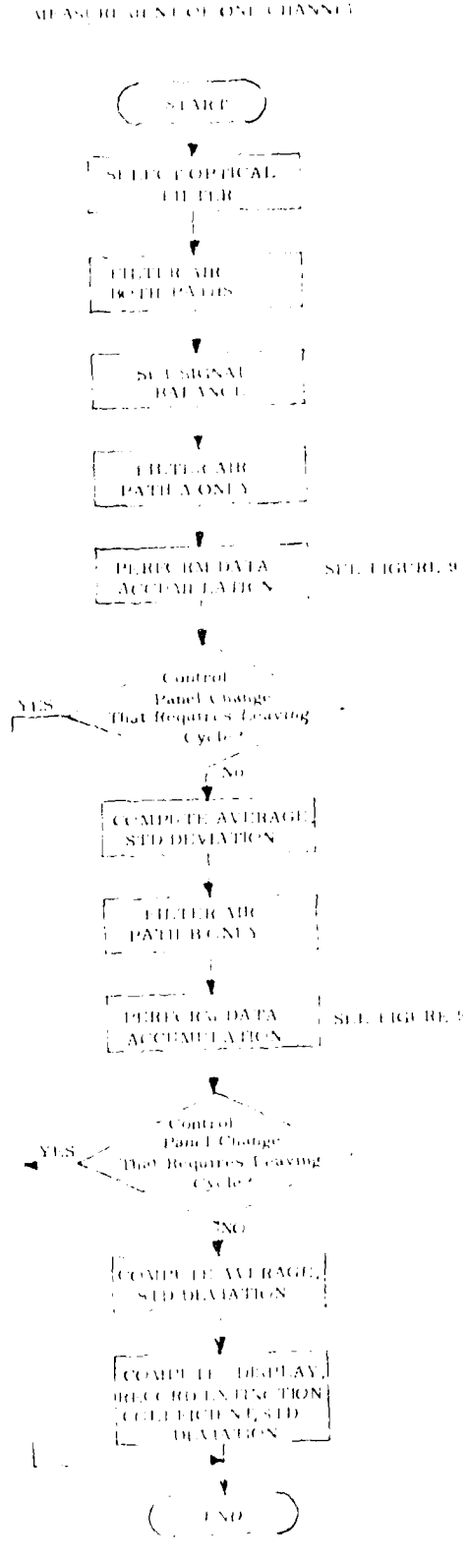

Figure B4.7. Flow chart of measurement sequence.

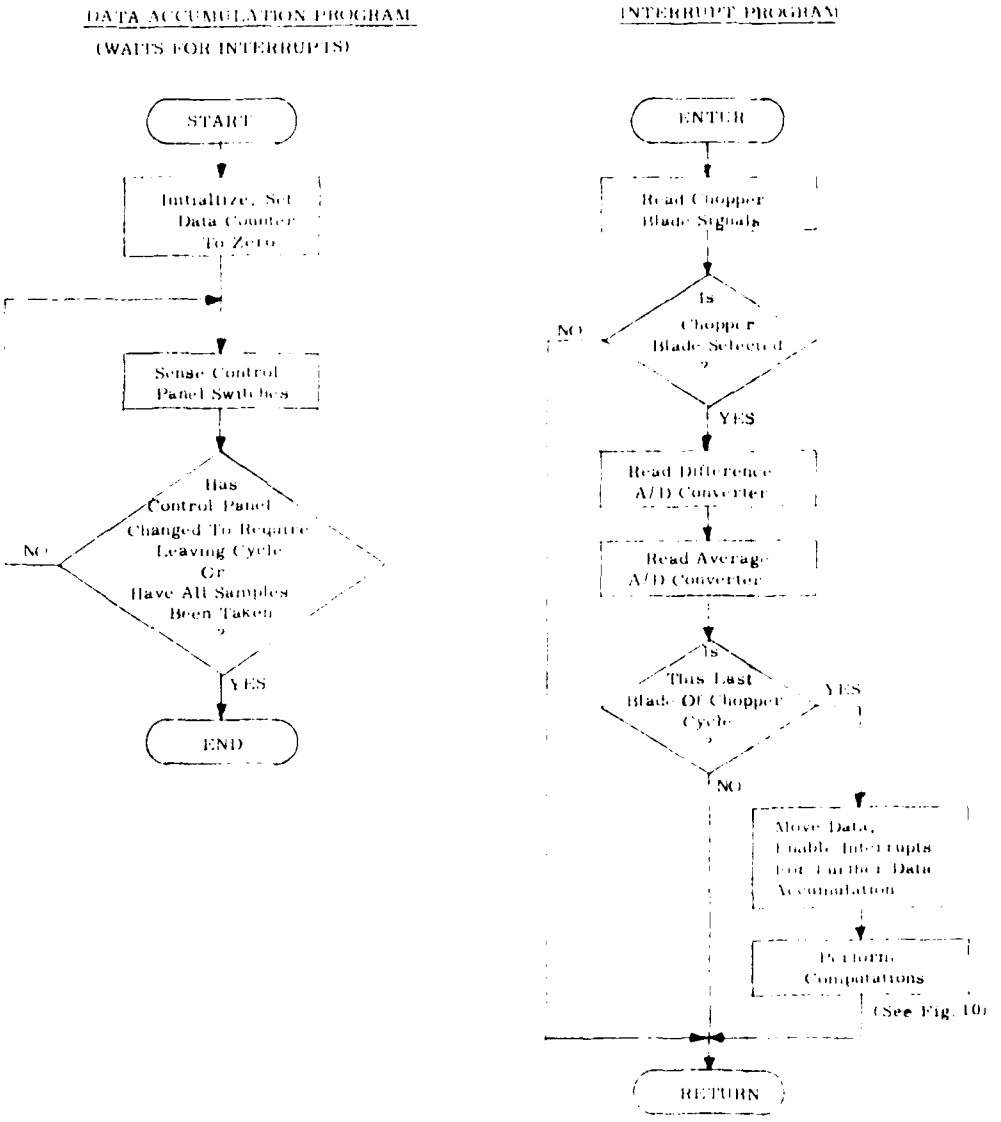

Figure B4.8. Flow chart of Data Accumulation Program.

the necessary calculations. The calculations are shown in Figure B4.9;one of the three options selected based on the chopper blades selected. At the completion of 100 seconds of data accumulation the program returns to the flow chart of Figure B4.7 and continues with the accumulation of the second set of data, S_2, by again implementing the programs shown in Figure B4.8 and B4.9. The final step in the measurement program is the computation and printing of the extinction coefficient and its standard deviation. To provide data for the standard deviation calculation the program accumulates the sum and the sum of the squares of the individual data values. The standard deviation is computed from the expression Std. Dev. $= (1/n \sum_{n} S_n^2 - \bar{S}^2)^{1/2}$ where the subscript n refers to either S_1 or S_2.

The microcomputer computational program requires the last calibration constant and the path length to be stored in memory.

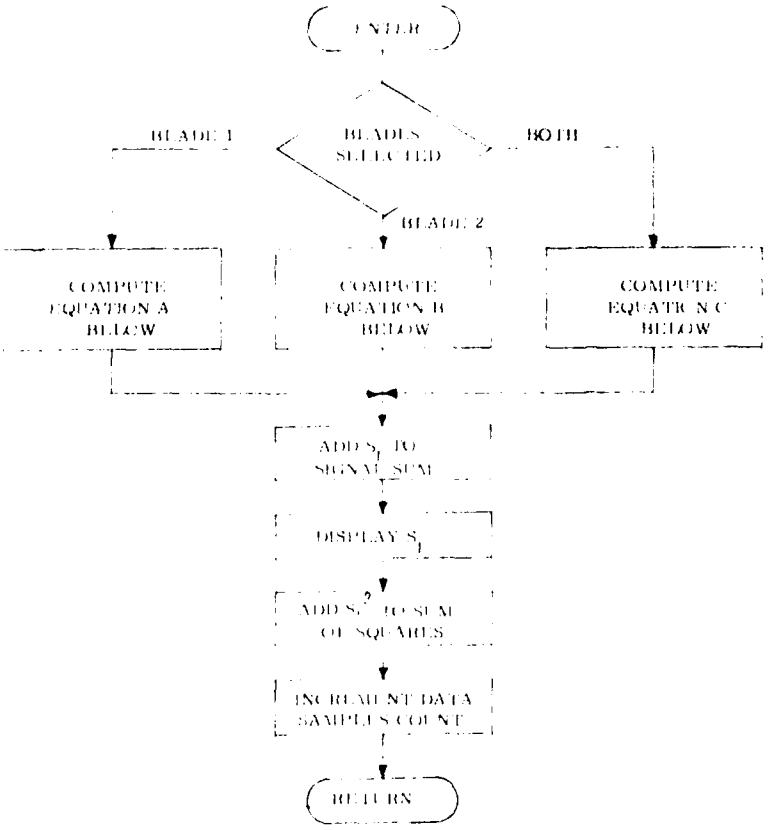

EQUATION A

$$S_1 = \frac{S_A - S_B}{S_{on} - S_{off}}$$

EQUATION B

$$S_1 = \frac{S'_A - S'_B}{S'_{on} - S'_{off}}$$

EQUATION C

$$S_1 = \left[\frac{S_A - S_B}{S_{on} - S_{off}} + \frac{S'_A - S'_B}{S'_{on} - S'_{off}}\right]$$

$$S_I = S_1 \text{ or } S_2$$

Figure B4.9. Flow Chart for the Computational Program of S_I and S_2

5. CRITICAL COMPONENT SPECIFICATIONS

5.1 Optical System

5.1.1 General Specifications

The optical system of the atmospheric aerosol extinctiometer is comprised of mirror optics except for an essential number of windows and the bandwidth selecting filters. A layout of the optical system is shown in Figure B5.1. There are five mirror flats, excluding the mirror chopper wheel, and seven concave aspheric mirrors in the system. Five of the aspherics are off-axis parabolas and two are off-axis ellipses.

Symmetries to the system permit parabolas P1 and P2 to be an identical pair of components as are parabolas P3 and P4. Cost savings are thus effected since these pairs of off-axis parabolas can be cut from the same parent parabola.

Elliptical mirrors E1 and E2 are the first and last imaging components of the system. Again the use of identical off-axis ellipsoidal mirrors is intended to reduce the costs in fabrication of these components.

A first-order optical design has arrived at the parameters and conjugate distance relationships for the uniaxial imaging components as given in Table B5.1. Consideration has been given to the manner in which parabolas are used with finite conjugate distances but no analysis of the aberrations of the system has been performed.

A design requirement of the optical system is that 90 percent of the radiation arriving at the primary detector fall within a circle 2.5 millimeters in diameter. The performance analysis (Section 3) assumed an effective detector diameter of 2 millimeters. An actual detector diameter of 3 millimeters will provide a comfortable boundary condition for the residual abberations and alignment of the optical system.

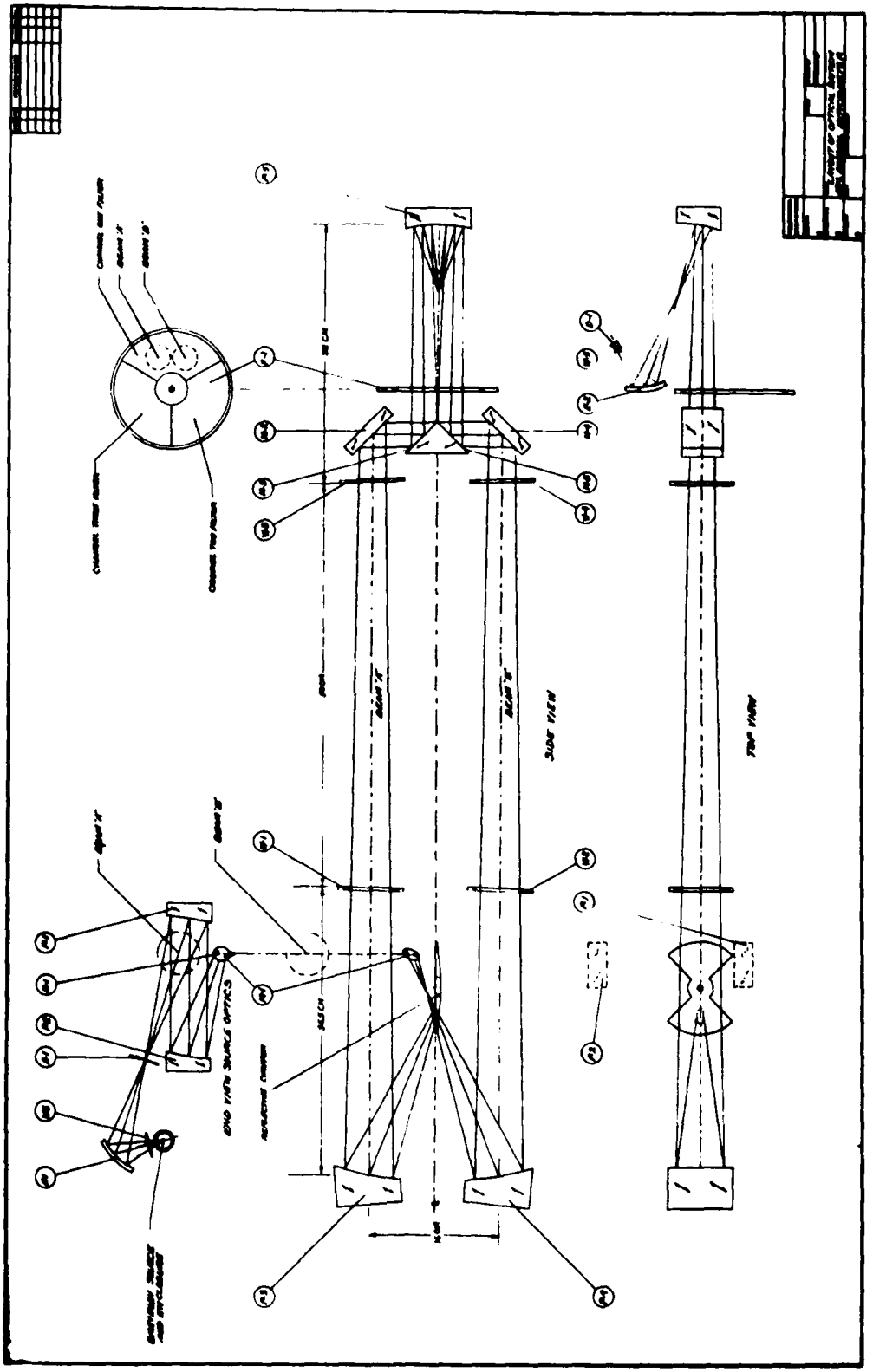

Figure B5.1. Layout of Optical System Atmospheric Aerosol Extinctiometer.

TABLE B5.1. Description of Aspheric Mirror Components and Conjugate Distance Relationships

Component	Conic Form	Conic Constant $(1-\epsilon^2)$	C.A. (cm)	Center C.A. to O.A. of Parent Mirror (cm)	Focal Length of Parent Mirror (cm)	OBJECT Dis. to C.A. (cm)	OBJECT Height (cm)	IMAGE Dis. FM C.A. (cm)	IMAGE Height (cm)	Magnification
E1	Ellipse	0.6914	20(1)	6.1(1)	f_1=4.06 f_2=14.22	6.1	0.2	12.2	0.4	2
P1	Parabola	0	6	10.0	18.0	18.25	0.4	∞	--	--
P2	Parabola	0	6	10.0	18.0	∞	--	18.25	0.4	--
P3	Parabola	0	8	10.8	19.5	24.0	0.4	127	21.2	5.29
P4	Parabola	0	8	10.8	19.5	24.0	0.4	127	21.2	5.29
P5	Parabola	0	11(2)	3.5(2)	8.0	127	6	8.5	0.4	.067
E2	Ellipse	0.6914	20(1)	6.1(1)	f_1=4.06 f_2=14.22	12.2	0.4	6.1	0.2	0.5

NOTE: (1) The off-axis ellipse is a portion of an ellipsoid with a 20 cm diameter aperture. The central ray of the radiation bundle is incident on the C.A. 6.1cm from the optical axis of the parent ellipse.

NOTE: (2) The off-axis parabola is one-half of a parent parabola having an 11cm diameter aperture. The central ray of the radiation bundle is incident on the C.A. 3.5 cm from the optic axis of the parent parabola.

5.1.2 Optimization of the Optical System Design

An optimization of the first-order optical system design using a computer optical design program is required. Merit function, spot diagram and knife edge analysis must be used to provide: (1) component focal lengths and tolerances (2) the surface accuracy (figure) of each component (3) optimum conjugate distance relationships (4) additive effects of tolerances and surface accuracies on the overall system performance, and (5) chief ray behavior to prescribe sufficient clear apertures for each component and thus avoid any vignetting in the system.

Optimization of the optical design must proceed in parallel with the mechanical design of the system. Trade-off exchanges must be made with due consideration given to mounting of the optical components, the elimination of potential interferences between mounts, minimization of stray light and the overall instrument configuration.

Consultation with an optical fabricator during the design phase is considered a desirable but not essential requirement. The generation of aspheric mirrors can be a costly process if unreasonable and/or unnecessarily difficult tolerancing is prescribed. The optical fabricator can also be consulted in cost/performance tradeoffs regarding specifications of: surface quality, thickness of mirrors, choice of materials for proper performance over the operating temperature range (-20°C to +50°C) and mounting techniques to prevent mirror distortion.

5.1.3 Transmittance of the Optical System

A design requirement of the optical system is that the transmittance of the system, including all mirrors, windows and the reflective chopper wheel, be 20 percent or better.

All mirrors should be gold coated. If a vapor deposition method

for coating is used, a protective overcoat must be provided. If hard electroplated gold coatings are used then the protective overcoat requirement may be dropped. In either case the reflectance requirement is 98 percent or better for each mirror surface.

The four windows that define the sample volumes and which are exposed to the ambient environment must be made of Raytran ZnSe (or equivalent) having a nominal (polished) thickness of 4 millimeters. The detector enclosure window and (if required) the source enclosure window must be made of BaF_2 having a nominal thickness of 1 millimeter. All windows should be sufficiently oversize to avoid vignetting and stray light effects and provide for ease of alignment of the optical system.

5.2 Graybody Source

The graybody source should be capable of sustained (very long life) operation at a temperature of 1400 K or higher. The emissivity must be 0.9 or better over the wavelength range from 1 to 12 microns. A specific source configuration is not defined here but the source must provide a circular area of at least 5 millimeters in diameter having a uniform temperature of 1400 K, or better, radiating into f/1.5 field-of-view.

The source size must be held to a minimum consistent with the above constraints. An oversize source will add unnecessarily to the electrical power demands of the instrument, create interference problems with adjacent optical components, and generate quantities of heated air which must be prevented from interfering with the internal function of the instrument and perturbing the sample volumes (either from heating of windows or modifying the ambient air by a venting system).

Candidate thermal sources to be investigated should include globars and resistance-wire heated ceramic rods.

A final requirement of the source is that it not add any noise power to the NEP of the primary pyroelectric detector when operated in conjunction with that detector.

5.3 Primary Detector and Associated Electronics

5.3.1 Detector

Type	Pyroelectric
Wavelength Range	0.9 to 12μ
Element Size	3 mm diameter
Permanent Window	BaF_2
NEP (0.9-12μ, 34 Hz; 1 Hz BW)	$\leq 10^{-9}$ W/Hz$^{1/2}$
Voltage Responsivity	43 V/W
Temperature Range	-20 to +85°C
Temperature Coefficient	< .2 percent/°C

5.3.2 Amplifier

Maximum Noise Voltage (RMS) (Referred to Input)	≤ 15 nV/Hz$^{1/2}$
Maximum Gain Nonlinearity	± .004 percent
Maximum Gain Change vs Temp.	±30ppm/°C
Minimum Bandwidth	10 KHz
Maximum Offset Voltage vs. Power Supply Variation	±6μV/V
Programmable Gain Range	4×10^4 to 5×10^5

5.3.3 Filter

Bandwidth	5 Hz to 170 Hz
Attenuation at Frequencies Higher than 30 KHz	80 db

5.3.4 A/D Converter

Relative Accuracy; Full Scale Reference	±.0015 percent at 25 C
Resolution	16 bits
Full Scale Temperature Coefficient	5ppm/ C
Quantizing Error	±1/2 LSB
Conversion Time	≤ 30 μsec
Monotonicity	Required
Missing Codes (0° to 70°C)	None Allowed

5.4 Source Monitor Detector and Associated Electronics

5.4.1 Detector

Type	Pyroelectric
Wavelength Range	0.9μ to 12μ
Element Size	2 mm diameter
Permanent Window	BaF_2
NEP (0.9-12μ; 34Hz; 1HzBW)	$\leq 10^{-9}$ w/Hz$^{1/2}$
Voltage Responsivity	98 V/W
Temperature Range	-20 to +85 C
Temperature Coefficient	<.2 percent/ C

5.4.2 Amplifier

Maximum Noise Voltage (RMS)	50 nV/Hz
Maximum Gain Nonlinearity	±0.02 percent
Maximum Gain Change vs Temp.	0.001 percent/°C
Minimum Bandwidth	10 KHz
Gain	5×10^4

5.4.3 Filter

Bandwidth	5 Hz to 170 Hz
Attenuation at Frequencies Higher than 30KHz	70 db

5.4.4 A/D Converter

Relative Accuracy; Full Scale Reference	±0.012 percent
Resolution	12 bits
Full Scale Temperature Coefficient	20ppm/°C
Quantizing Error	± 1/2LSB
Conversion Time	≤30μsec
Monotonicity	Required
Missing Codes (0° to 70°C)	None Allowed

5.5 Reflective Chopper Wheel

5.5.1 Assembly

The chopper wheel assembly shall provide a 34 Hz chopping frequency using a two-blade reflective chopper with a 50 percent duty factor. An interrupt or reflective sensor (or sensors) must be employed

to provide a reference signal (or signals) to the data processing system. Reference signals from the two blades shall be coded in a manner that will allow the data processing system to identify each blade.

5.5.2 Motor Drive

Frequency	17 Hz
Stability (over 4 minute period)	.01 percent
Stability (long term)	.1 percent
Temperature Coefficient	0.1 percent

5.5.3 Chopper Wheel Blades

Type	Reflective
No. of Slots	2
Blade Openings	90 $\pm$ 15 arc min.
Diameter	4.5 inches
Surface Flatness	one-wave vane-to-vane
Mirror Coating	Gold
Mirror Reflectance (1μ to 12μ)	$\geq$ 98 percent
Blade Edges	Knife Edge
Knife Edge Angle	$\leq$ 40 degrees
Knife Edge Quality	State-of-Art
Shaft/Hub Precession(includes Hub, Hub Seat, Shaft, Bearings)	Note (1)

Note (1) A HeNe laser beam reflected from the surface of the chopper blade when mounted to its shaft shall not precess in a circle greater than 1/8 inch in diameter at 20 feet when the blade is rotated through 360 degrees.

5.6 Wavelength Isolation Filters

5.6.1 Filter Wheel Assembly

The filter wheel is composed of three 120 degree segment filters forming a circular filter array. Metal webs at the junctions of the three filters are to be held to the minimum possible obscuration of the beam when the wheel is rotated from one filter position to the next.

Each of the three filters is to be fabricated by deposition coatings on a substrate material appropriate to its particular band pass requirements. The thickness of all filters is to be identical (for mounting purposes) and to be determined by consultation with the supplier of the filters, due consideration being given to mechanical strength, mounting technique and range of operating temperature of the instrument.

5.6.2 Channel 1 Filter Specification

Filter Type	Square Bandpass
Substrate Material	Vendor Selected
Coatings	A/R Coated
Center Wavelength	1.03μ to $\pm$2 percent
Band Pass (Half Peak Trans.)	0.98μ to 1.08μ $\pm$2 percent
Peak Transmittance (Ave.)	75 percent $\pm$5 percent
0.1 Percent Transmittance(Absolute)	
λ Short --(No less than)	0.89μ
λ Long --(No greater than)	1.20μ
Blocking (Outside Range; 0.1 percent or better)	Complete; UV to 20.5μ
Angle of Incident Radiation	Normal
Operating Temperature	-25°C to +50°C
Environmental Specifications:	
Humidity	per MIL-C-675A
Abrasion	per MIL-C-675A
Coating Adherence	per MIL-M-13508B

5.6.3 Channel 2 Filter Specification

Filter Type	Square Bandpass
Substrate Material	Vendor Selected
Coatings	A/R Coated
Center Wavelength	3.5μ $\pm$2 percent
Band Pass (Half Peak Trans.)	3.0μ to 4.0μ $\pm$2 percent
Peak Transmittance (Ave.)	75 percent $\pm$5 percent
0.1 Percent Transmittance (Absolute)	
λ Short -- (No less than)	2.7μ
λ Long -- (No greater than)	4.4μ
Blocking (Outside Range; 0.1 percent or better)	Complete; UV to 20.5μ
Angle of Incident Radiation	Normal
Operating Temperature	-25°C to +50°C
Environmental Specification:	
Humidity	per MIL-C-675A
Abrasion	per MIL-C-675A
Coating Adherence	per MIL-M-13508B

5.6.4 Channel 3 Filter Specification

Filter Type	Square Bandpass
Substrate Material	Vendor Selected
Coatings	A/R Coated
Center Wavelength	10.0μ $\pm$2 percent
Band Pass (Half Peak Trans.)	8.0 to 12.0μ $\pm$2 percent
Peak Transmittance (Ave.)	75 percent $\pm$5 percent
0.1 Percent Transmittance (Absolute)	
λ Short --(No less than)	7.3μ
λ Long --(No greater than)	13.3μ

Channel 3 Filter Specification (Cont.)

Blocking (Outside Range; 0.1 percent - - - Complete; UV to 20.5μ or better)

Angle of Incident Radiation - - - - - - - - Normal

Operating Temperature - - - - - - - - - - -25°C to +50°C

Environmental Specification

Humidity - - - - - - - - - - - - - - - - -per MIL-C-675A

Abrasion - - - - - - - - - - - - - - - - -per MIL-C-675A

Coating Adherence - - - - - - - - - - - -per MIL-M-13508B

5.7 Air Filtering System

An air filtering system must be provided which is capable of excluding all aerosols, dust and fog droplets greater than 0.1 micron in diameter from the volume of air containing the reference beam of radiation. (A system capable of simultaneously filtering the air in both beams is highly desirable for calibration purposes, but is not an essential requirement of this specification).

Because the reference volume of air must represent 100 percent transmission relative to the sample volume of air it is essential that no change occur, due to the filtering process, which will add or deplete molecules present in the ambient air which are capable of absorbing infrared radiation at 1 micron or in the 3 to 4 and 8 to 12 micron regions.

Continuum absorption by water vapor is a major contributor to atmospheric attenuation of IR radiation in the 10 micron spectral region. A difference in the amount of water vapor present in the reference beam as compared to the sample beam can result in a false measurement of the aerosol extinction coefficient in that wavelength region. It is thus necessary to put limits on those factors in a filtering process which would result in a perturbation of the measurement in the 8 to 12 micron channel. Those factors are pressure, temperature and the mixing ratio of water vapor to dry air. The limits imposed on changes of these quantities are prescribed in Section 2.2.6 of this specification.

Of the two possible approaches for filtering air the Alternating Cylinder approach is most susceptible to changes in the water vapor content of the filtered ambient air. The Electrostatic Fence approach is most susceptible to the production of other absorbing molecules which may perturb the measurement. An analysis is required which puts limits on the amount of these molecules which may be tolerated and a determination of the amounts of these molecules generated by an electrostatic fence is also required.

Further requirements on the filtering technique to be employed are:

(1) During normal operation of the instrument 15 seconds are allotted to the time gap between measurements of S_1 and S_2. In that time the reference volume of air is switched from one path to the other and sufficient time must elapse so that ambient air has occupied the sample path.

(2) The instrument will perform its measurement function at all wind speeds up to 30mph (Force 6 on the Beaufort Scale).

APPENDIX C

EFFECTS OF WATER VAPOR IMBALANCE ON EXTINCTIOMETER MEASUREMENTS

In the 8-14 micron wavelength region, the extinction coefficient can be considered to be made up of an aerosol component and a water vapor continuum component; that is

$$k_{ext} = k^{a}_{ext} + k^{v}_{ext}$$

In either of the two air filtering techniques under consideration, the aerosol component is measured by comparing two optical signals, one of which is a "reference" signal made when the aerosol has been removed from a portion of the air sample. It is assumed that the water vapor content in the air is identical in the two configurations. This appendix examines the sensitivity of the measurement to imbalances in the water vapor content of the sample and reference volumes of air. The error model for the measurement is

$$k^{a}_{ext} = \hat{k}^{a}_{ext} + \Delta k^{a}_{ext} + \Delta k^{v}_{ext}$$

where the caret denotes the true value and the delta quantities the error attributed to the aerosol and water vapor components. All of the measurement errors except for water vapor are lumped into the aerosol error component. The water vapor error component consists only of the systematic errors arising from imbalance. The extinction subscript ext is dropped from the remainder of the discussion.

The absolute error in the water vapor component must be much less than the remainder of the measurement error, $\Delta k^{v} << \Delta k^{a}$ This inequality can be manipulated in the following way to arrive at a more convenient formulation

$$\Delta k^v << \frac{\Delta k^a}{k^a} - \quad k^a = E\, k^a$$

$$\frac{\Delta k^v}{k^v} << E \quad \frac{k^a}{k^v}$$

where E is the desired relative error in the measurement of aerosol extinction coefficient. The relative error in the water vapor component is equal to the relative change in the water vapor density in the air. The meteorological expression for the water vapor density of moist air is

$$\rho_v = \frac{r}{1 + r/\epsilon} \quad \frac{p}{RT}$$

where r = mixing ratio of water vapor to dry air

ϵ = ratio of molecular weight of water vapor to that of dry air

= 0.622

p = barometric pressure

T = absolute temperature

R = gas constant for dry air

Then

$$\frac{dk^v}{k^v} = \frac{d\rho_v}{\rho_v} = \frac{dp}{p} - \frac{dT}{T} + \frac{1}{1 + r/\epsilon} \quad \frac{dr}{r}$$

The multiplying factor in front of the relative error in the mixing ratio can be ignored for this analysis since $r \sim 10^{-2}$.

Using these relations, a graph has been constructed which shows the value of aerosol extinction coefficient on the ordinate axis which can be measured to a relative error of E percent when the relative error in

water vapor imbalance is less than a given relative percent error shown on the abscissa axis. A model atmosphere for a midlatitude summer is used with T = 294 K, Rel. Humidity = 76 percent, barometric pressure = 1013 mb and the water vapor continuum extinction coefficient is 0.23 km^{-1} at a wavelength of 10.6 microns. The relative measurement error, E, is given values of 20, 50, and 100 percent.

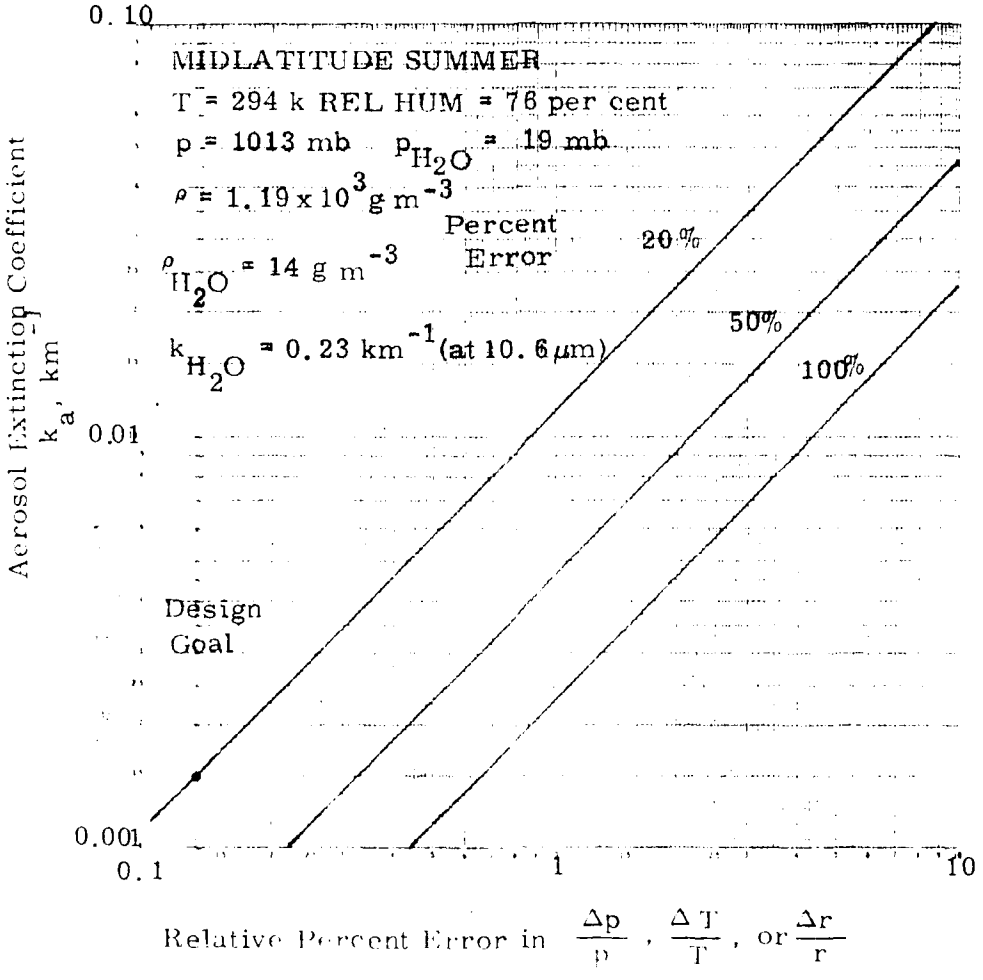

Figure C1. Results of an error analysis for one extinctiometer measurement situation in the 8-14 μ spectral region.

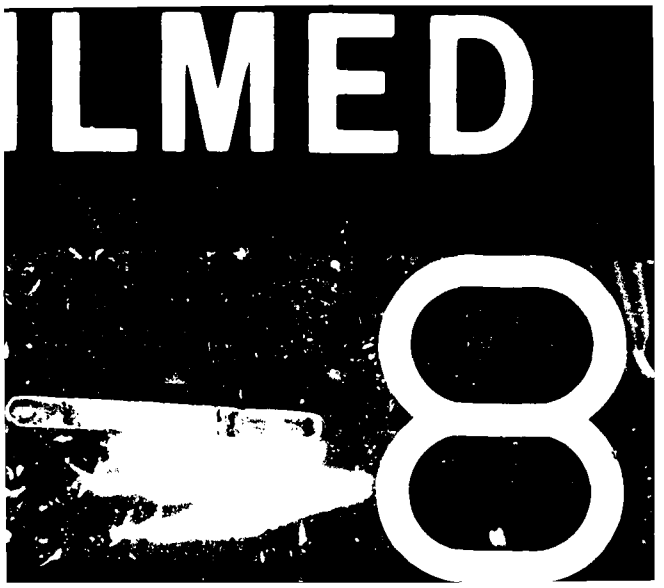
LMED
8